3.0 SUMMARY OF SURFACE WATER DATA IN THE LA CIENEGA AREA

By Laura Petronis and Jack Frost, NMOSE, and Jack Veenhuis, NM Hydrologic, LLC

3.1 General Description of Surface Waters in the Study Area

The surface-water and geographic features in the La Cienega Area are shown in Figure 3.1. Cienega Creek flows through the central part of the region. Tributaries that contribute flow to Cienega Creek include Arroyo Hondo, Canorita de las Bacas, Guicu Creek, and Alamo Creek. Upstream, towards the Sangre de Cristo Mountains, Arroyo Hondo is the larger tributary and valley, whereas Cienega Creek originates locally at a wetland, or "cienega". Where Cienega Creek and Arroyo Hondo converge, the larger valley becomes Cienega Creek.

Most of the channels associated with these drainages are generally dry but conduct storm and snowmelt runoff as they cross the alluvial slope surface overlying the buried Española Basin. As the creeks and arroyos approach the La Cienega Area, a diffuse area of springs and seeps emerge from the stream beds and hillsides and are channeled into acequias and the tributaries and Cienega Creek. The Cienega Creek channel has become entrenched below the surrounding floodplain for the last approximately 1¼ miles, before entering the Santa Fe River. The river flows through the northern and western sides of the La Cienega Area, and joins with Cienega Creek in the southwestern corner of the study area.

Most of the surface water in the La Cienega valley is captured by the acequia system for irrigation during the farming season from roughly April through October. In addition to the diversion into the ditches, there are also ponds and sumps (excavated areas that collect water) that have been created along areas of the La Cienega and lower Santa Fe River valleys that collect and distribute water for irrigation.

The lower Santa Fe River, defined here as the river downstream of the WWTP, west of SR 599, has also been used for irrigation in the area of Cieneguilla, in areas along the Santa Fe Canyon, and downstream in the La Bajada area. In the area of Cieneguilla, springs are reported by Spiegel and Baldwin (1963) to have emerged from a wide

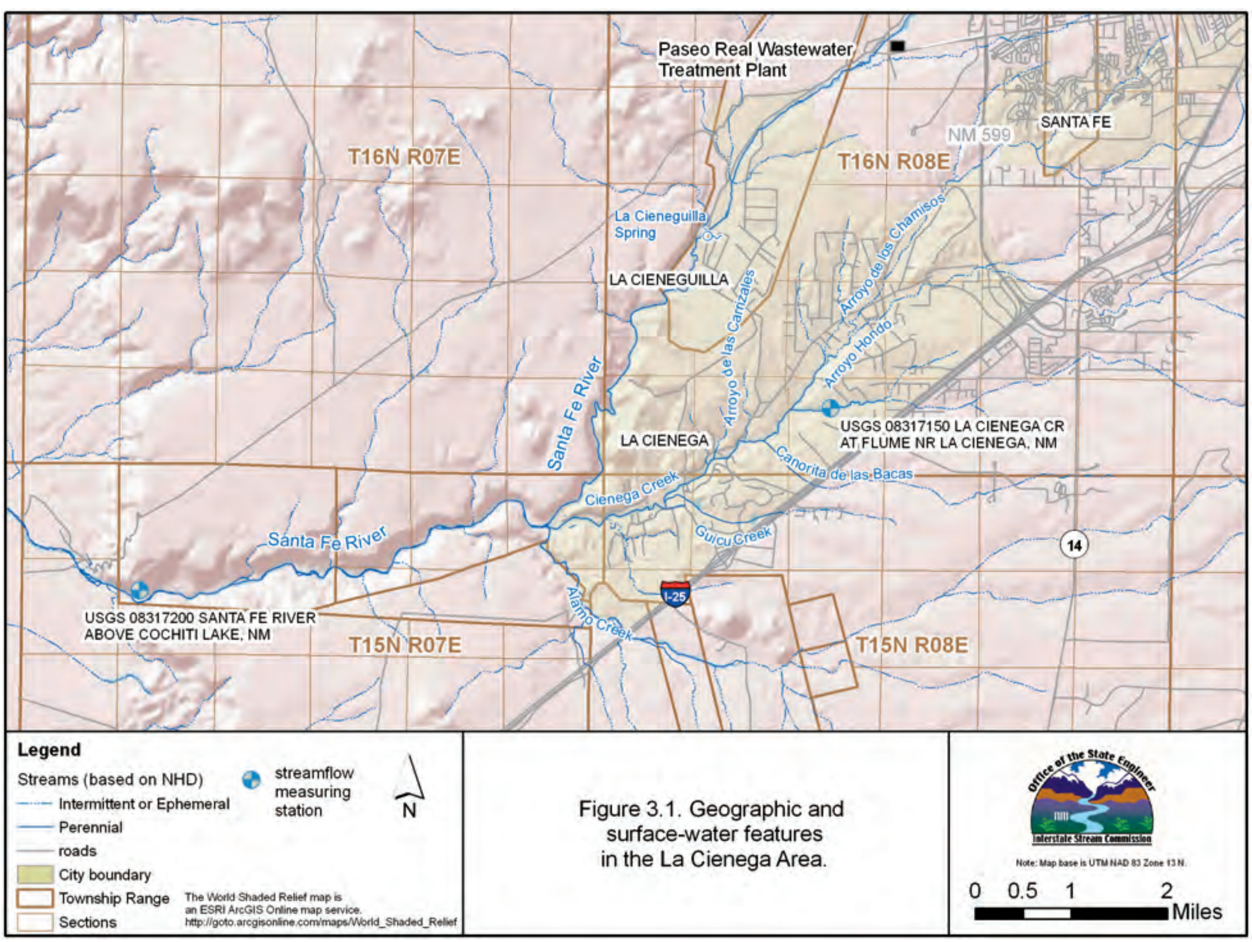

Figure 3.1: Geographic and surface-water features in the La Cienega Area.

sandy area of the Santa Fe River channel at 16N.8E.20.312 and those springs were diverted for irrigation on a 30-acre area on the northwest side of the Santa Fe River in the Cieneguilla area. Presently, there are some diversions from the Santa Fe River to lands in the Cieneguilla area. From the 1960's to the present, the WWTP has been discharging treated effluent to the lower Santa Fe River, which has substantially augmented and varied the flow. In addition, much of the floodplain has been fenced to exclude livestock, and native cottonwoods, willows, and wetland plants and animals have become established.

3.2 Streamflow Measurements

Streamflow measurements have been made in several locations in the La Cienega Area during the last 60 years or so. Generally, springs and seeps have not been directly measured; their contributions have typically been accounted for by stream reach. Most of the historical measurements have been made near the Acequia de la Cienega headgate, along Cienega Creek near the confluence with the Santa Fe River, or at multiple locations along the lower Santa Fe River. The NMOSE recently funded a streamflow study to better understand current gains and losses to reaches along the lower Santa Fe River. Additionally, the NMOSE conducted a study (funded in part by EPA WPDG) to measure streamflow at multiple locations along Cienega Creek and its tributaries. This study assessed gains and losses to streamflow in the lower Cienega Creek watershed.

Surface water features in the greater La Cienega Area have a long history of human modification. Flows in the springs, streams, and waterworks vary seasonally and based on water use. It is difficult to measure and characterize the workings of the system. There are daily fluctuations and it is difficult to resolve small gains and losses attributable to groundwater interactions.

The following sections present the available historical streamflow data, along with the more recent data collection (directed by the NMOSE), for three different areas: the Acequia de la Cienega headgate, Cienega Creek and its tributaries, and the lower Santa Fe River.

Acequia de la Cienega Headgate. The USGS periodically measures Cienega Creek streamflow near the Acequia de la Cienega headgate and those data are available on the USGS National Water Information System (NWIS) website (USGS 08317150 LA CIENEGA CR AT FLUME NR LA CIENEGA, NM) (see Figure 3.1 for location). Hydroscience Associates, Inc. (2004) reports that additional streamflow data at this location have also been reported by the United States Department of Agriculture Natural Resources Conservation Service (formerly the Soil Conservation Service (SCS)), the USGS and Ditch operators. Table 3.1 lists those data that have been collected at this site.

Table 3.1: Streamflow data reported by the USGS and others at or near the USGS measuring site Cienega Creek at Flume near La Cienega, NM (USGS 08317150).

Date	Flow (ft^3/s)	Source
3/17/1966	1.55	HAI-SCS
5/13/1971	0.76	HAI-SCS
1975	0.56	HAI-SCS
6/19/1986	0.55	HAI-USGS
5/19/1989	0.62	HAI-USGS
7/17/1990	0.48	HAI-USGS
10/18/1990	0.58	HAI-USGS
3/25/1991	0.64	HAI-USGS
6/17/1991	0.56	HAI-USGS
8/28/1991	0.32	HAI-USGS
11/26/1991	0.66	HAI-USGS
7/8/1992	0.37	HAI-USGS
11/19/1992	0.61	HAI-USGS
2/21/1997	0.56	USGS
5/20/1997	0.56	USGS
6/23/1997	0.57	USGS
8/22/1997	0.46	USGS

Date	Flow (ft^3/s)	Source
7/2/2004	0.65	HAI-Tom Simons
7/2/2004	0.39	USGS NWIS
7/19/2004	0.48	USGS NWIS
3/30/2005	0.53	USGS NWIS
7/11/2005	0.53	USGS NWIS
7/15/2005	0.34	USGS NWIS
3/27/2007	0.55	USGS NWIS
5/1/2007	0.62	USGS NWIS
9/4/2007	0.5	USGS NWIS
6/30/2008	0.37	USGS NWIS
7/8/2008	0.43	USGS NWIS
3/25/2009	0.5	USGS NWIS
4/1/2009	0.54	USGS NWIS
7/6/2009	0.49	USGS NWIS
7/7/2009	0.49	USGS NWIS
9/10/2009	0.37	USGS NWIS
5/6/2010	0.55	USGS NWIS

Date	Flow (ft^3/s)	Source
6/14/2001	0.36	USGS
3/26/2002	0.53	USGS
7/19/2002	0.38	USGS
12/23/2003	0.56	HAI-HAI
3/26/2003	0.54	USGS
7/11/2003	0.5	USGS
4/8/2004	0.64	USGS

Date	Flow (ft^3/s)	Source
8/12/2010	0.47	USGS NWIS
9/22/2010	0.47	USGS NWIS
4/5/2011	0.63	USGS NWIS
5/13/2011	0.6	USGS NWIS
5/17/2011	0.66	USGS NWIS
8/17/2011	0.45	USGS NWIS
5/22/2012	0.42	USGS NWIS

HAI-USGS = data from USGS cited by Hydroscience Associates, Inc. (2004) HAI-SCS = data from SCS cited by Hydroscience Associates, Inc. (2004)
HAI-HAI = data from Hydroscience Associates, Inc. cited by Hydroscience Associates, Inc. (2004) HAI-Tom Simons = data from Tom Simons cited by Hydroscience Associates, Inc. (2004)
USGS-NWIS = data from the USGS NWIS database
(note that some data from the USGS NWIS was also cited by Hydroscience Associates, Inc. (2004))

Cienega Creek and Tributaries. Although measurements have been made near the Acequia de la Cienega headgate, and there have been other sporadic streamflow measurements within the Cienega Creek watershed, no previous studies were identified in the literature that have estimated gains and losses by stream reach along Cienega Creek and its tributaries using streamflow data. The SWQB Wetlands Program agreed to fund a streamflow study of this area (EPA WPDG) to improve the understanding of where and how much spring and seep discharge is occurring to streams in the lower Cienega Creek watershed. The NM Hydrologic, LLC, and NMOSE (2012b) report, *Streamflow Measurement Study of the Cienega Creek and tributaries and the lower Santa Fe River, Santa Fe County, NM,* describes the detailed streamflow investigation. A summary from that study is presented below.

Streamflow measurements were made at multiple locations on Cienega Creek, Arroyo Hondo, Canorita de Las Bacas, Guicu Creek, and Alamo Creek in February 2012. For many reasons, flow can be variable in the system and can be difficult to measure. The study was conducted in the winter during a period with minimal evapotranspiration, no irrigation diversions and minimal precipitation so that baseflow gains and losses could be estimated from the streamflow measurements. Flows in Cienega Creek were also monitored periodically to ensure that data were collected during periods of minimal flow variation; if large variations in flow were observed during the measurement period, the data collected were not used in the evaluation of gains and losses.[1] Additionally, a few streamflow measurements were determined to be poor and were not used.

Figure 3.2 shows the locations and values of each of the measurements. The streamflow measurements show that in the late winter, prior to the irrigation season in 2012, Cienega Creek streamflow increased in a downstream direction. Arroyo Hondo was measured to contribute about 0.4 ft^3/s to Cienega Creek, Cienega Creek above Arroyo Hondo contributed 0.6 ft^3/s, the Canorita de las Bacas ditch[2] above Mill Pond (which flows through the Leonora Curtin Wetland Preserve and El Rancho de las Golondrinas) contributed about 0.1 to 0.2 ft^3/s, Guicu Creek may have contributed from 0.2 to 0.5 ft^3/s and Alamo Creek added about 0.2 ft^3/s. In late February, 2012, the total flow in Cienega Creek just above the confluence with the Santa Fe River (when adding the streamflow measurement from Alamo Creek) was 1.9 to 2.0 ft^3/s. A cubic foot per second is about two acre-feet of passing flow per day.

1 Flows on Cienega Creek were monitored periodically by observing the gage height on a staff gage installed at Cienega Creek above Canorita de Las Bacas. Generally the gage height at that location during the study ranged within 0.02 ft, but one measurement was made on Cienega Creek that was outside of that range and was not used in the evaluation of gains and losses on Cienega Creek.

2 The Canorita de Las Bacas ditch above Mill Pond was measured because no flow was observed in the main channel in the vicinity of the measurement location.

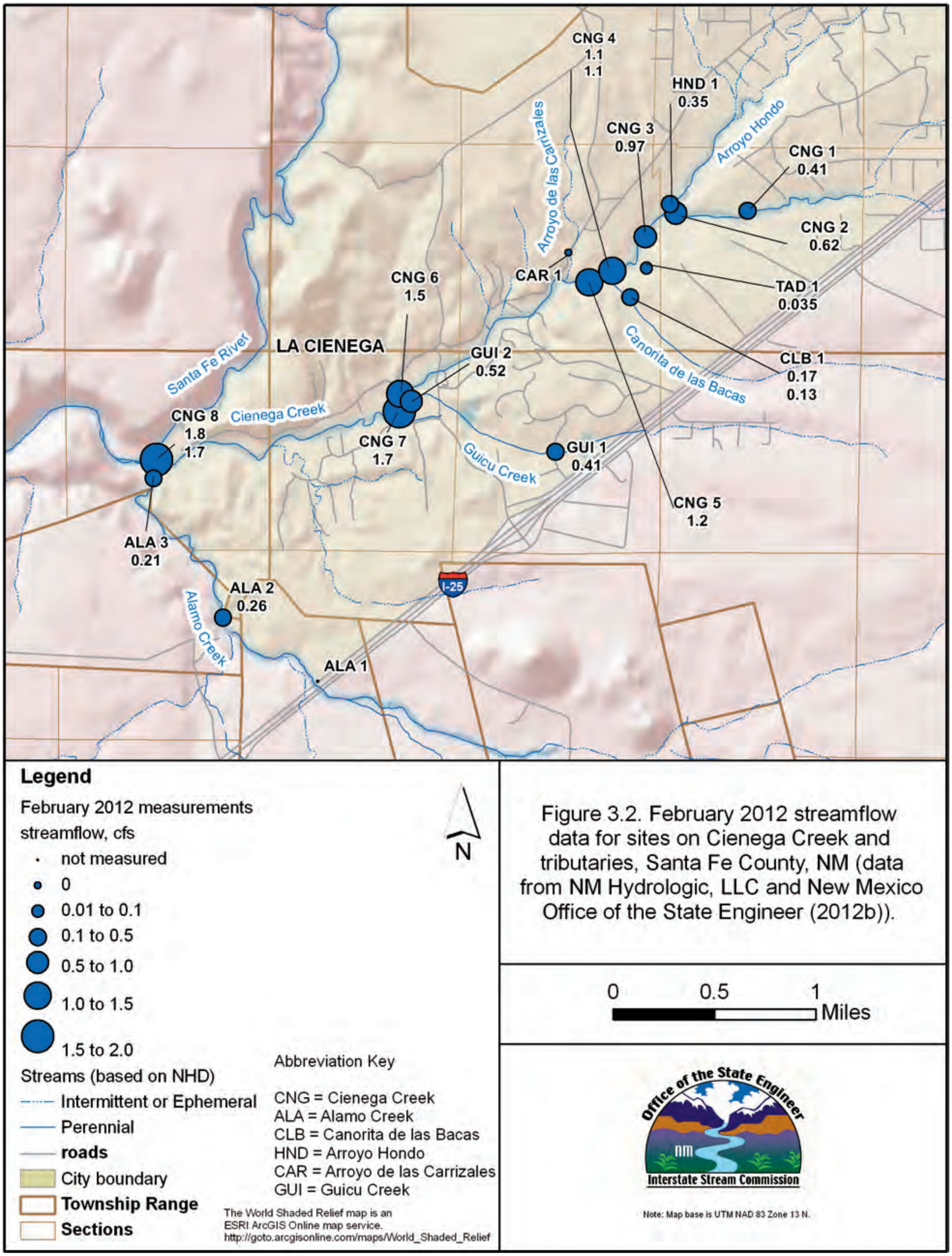

Figure 3.2. February 2012 streamflow data for sites on Cienega Creek and tributaries, Santa Fe County, NM (data from NM Hydrologic, LLC and New Mexico Office of the State Engineer (2012b)).

Figure 3.2: February 2012 streamflow data for sites on Cienega Creek and tributaries, Santa Fe County, NM (data from NM Hydrologic, LLC and NMOSE (2012b)).

Figure 3.3 depicts Cienega Creek streamflow versus distance upstream from the confluence with the Santa Fe River. Measured flow increases in a downstream direction and, generally, bigger gains are attributed to the tributaries. Between the tributaries, there was some additional gain in the streamflow as well, particularly in the stretch of Cienega Creek between Canorita de las Bacas and Guicu Creek, where a gain of about 0.3 ft^3/s was estimated.

For the Canorita de las Bacas and Guicu Creek, the measured tributary flows were greater than the difference between the Cienega Creek measurements made on either side of the tributary (i.e. the upstream and downstream measurements). Both the tributary from the Canorita de las Bacas and Guicu Creek enter Cienega Creek as several dispersed channels which may cause some flow into the subsurface that was not captured by the difference in the upstream and downstream measurements. When estimating gains and losses within Cienega Creek, the measurements made in Cienega Creek are probably more representative of changes in surface flow as one proceeds to the confluence with the Santa Fe River.

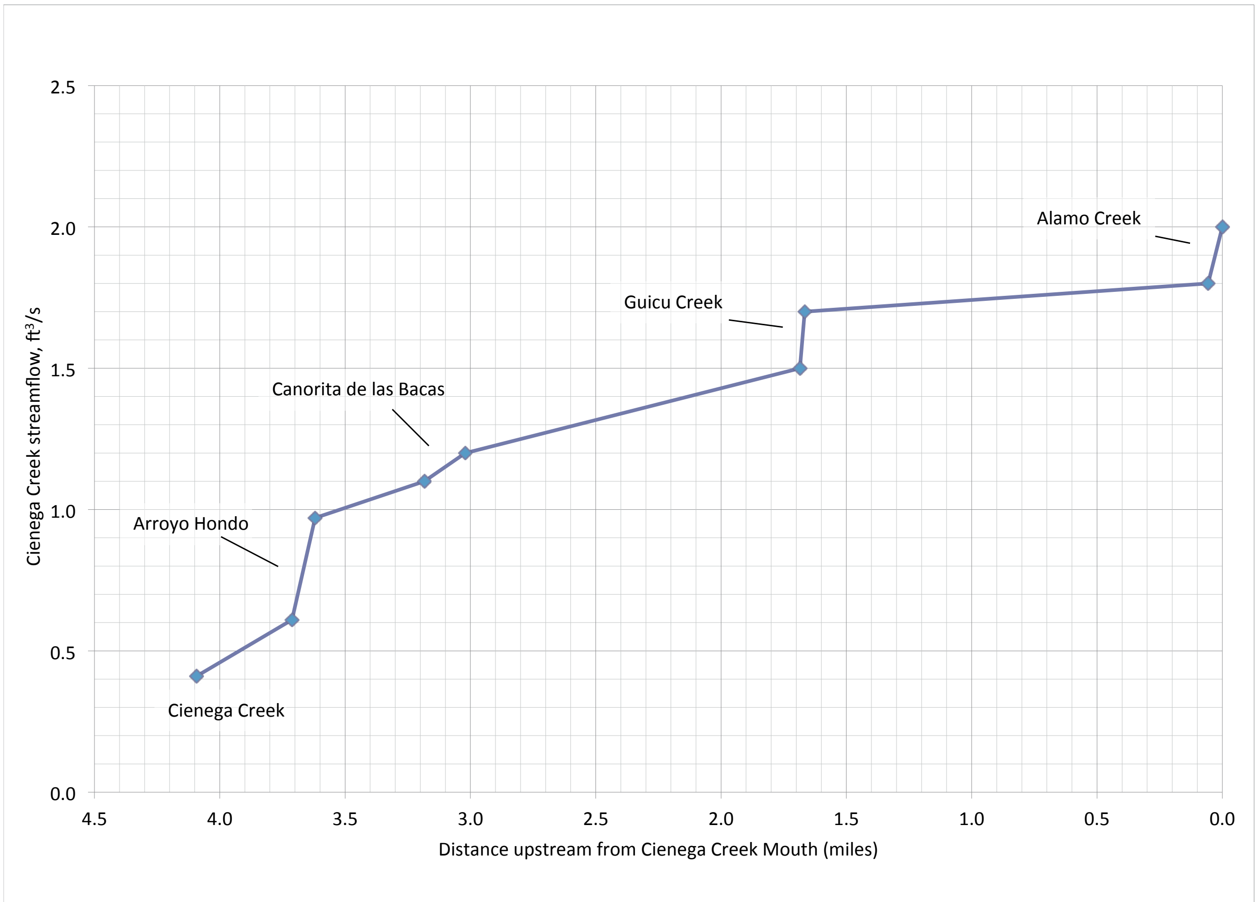

Figure 3.3: Cienega Creek streamflow versus distance downstream, based on streamflow measurements made between February 17, 2012 and February 22, 2012 (0 miles represents the Cienega Creek confluence with the Santa Fe River) (data from NM Hydrologic, LLC and NMOSE (2012b)). Note that Cienega Creek flow at mile 0.1 measured 1.7 ft3/s on February 29, 2012 (not shown on figure).

Lower Santa Fe River: Streamflow measurements. A few studies have measured streamflow in the Lower Santa Fe River. It is difficult to confirm the methodologies used and locations occupied between some of the older studies. Complicating comparisons to the present, those streamflow data may be influenced by recent precipitation, antecedent soil moisture, bank storage, and evapotranspiration. Major irrigation diversions do not appear to have occurred during the winter studies. Many of the reported gains and losses are quite small.

The following summarizes those studies.

Spiegel and Baldwin (1963): The earliest reported measurements on the Lower Santa Fe River were made by Spiegel and Baldwin (1963) in the early 1950's at two locations (see Figure 3.6 for estimated locations). One site was in the narrow canyon on the Santa Fe River near Cieneguilla about 0.1 mile below the then reported Cieneguilla springs and irrigated areas. The other measurement site was on the Santa Fe River near the Gallegos Ranch below the confluence with Cienega Creek.

At the Santa Fe River near Cieneguilla site, measured streamflow was variable and was periodically affected by irrigation activities, as well as runoff and seasonal changes in evapotranspiration. Figure 3.4 shows a plot of the streamflows that were measured (based on Spiegel and Baldwin (1963)'s Figure 48, p. 190). Based on the assumption that the January 1952 measurement was representative of groundwater discharge (because it was made in the winter measurements during periods of minimal evapotranspiration, no irrigation diversions, and no runoff), Spiegel and Baldwin (1963) estimated that the baseflow discharge to springs in the La Cieneguilla area was 0.92 ft^3/s (roughly two acre-feet per day).

At the Santa Fe River near Gallegos Ranch site, the measured streamflow was variable and was periodically affected by upstream irrigation activities along both the Lower Santa Fe River and Cienega Creek and tributaries, as well as runoff and seasonal changes in evapotranspiration.[3] Figure 3.5 shows a plot

3 Spiegel and Baldwin (1963, pp.175-176) note that the sewage from the Siler Road wastewater treatment plant was conveyed to the southwest for irrigation and of the water that does return to the Santa Fe River "at maximum flow it is completely absorbed within 1½ miles of the point of entry into the channel." This return flow is not thought to have directly affected the streamflow measurements made by Spiegel and Baldwin in the early 1950s as the point of entry was several miles upstream from La Cieneguilla.

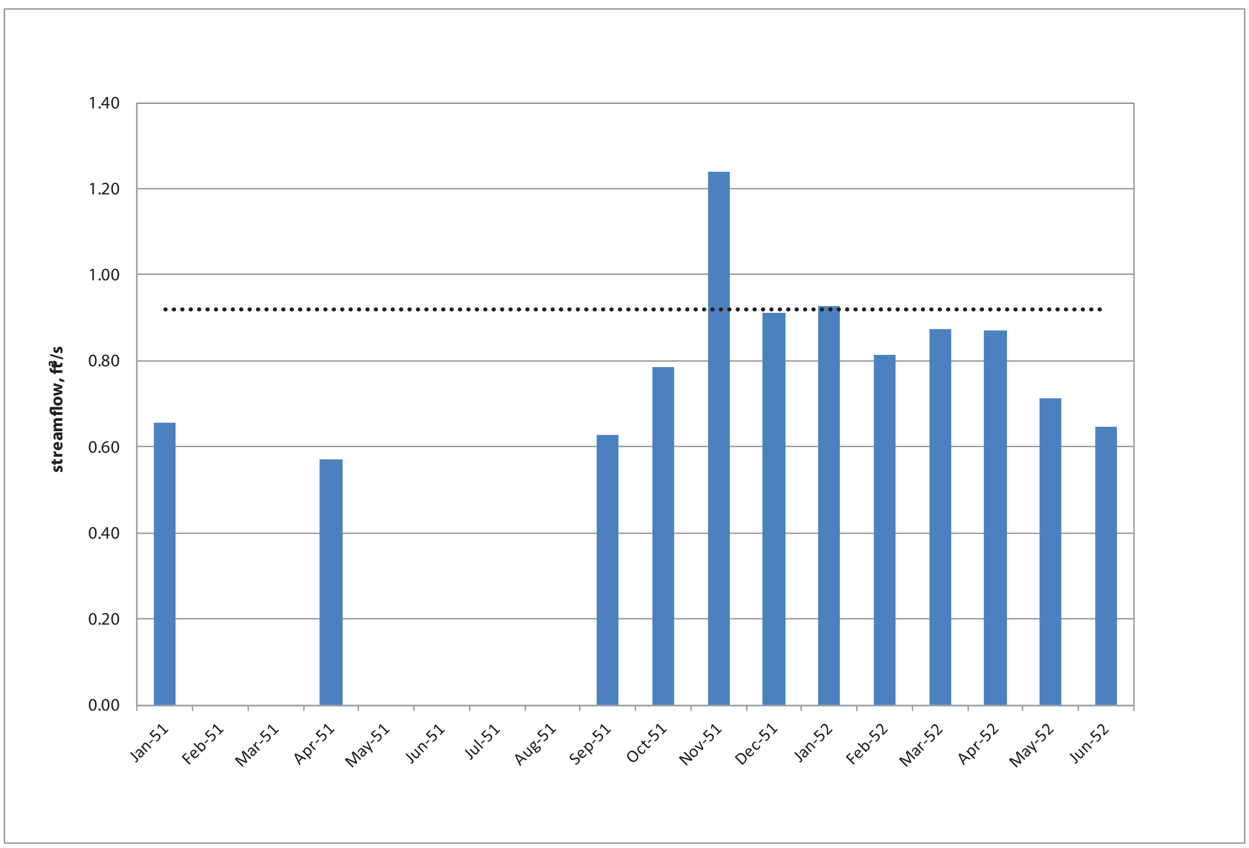

Figure 3.4: Measured streamflow by Spiegel and Baldwin (1963) at the Santa Fe River near Cieneguilla site (see Figure 3.6 for estimated location). Measured streamflow was periodically affected by irrigation activities, as well as runoff and seasonal changes in evapotranspiration. Spiegel and Baldwin estimated the total groundwater discharge contributing to flow at this site to be 0.92 ft^3/s based on the January 1952 measurement.

of the streamflow measured at this site (based on Spiegel and Baldwin (1963)'s Figure 48, p. 190). Based on a December 1952 measurement, Spiegel and Baldwin (1963) estimated that the baseflow discharge to all of the springs and streams in the La Cienega area from the Santa Fe River, Cienega Creek, and tributaries, was 6.5 ft^3/s (about 13 acre-feet per day). By inspection of Figures 3.4 and 3.5, other estimates are possible. Spiegel and Baldwin (1963) acknowledged that the data collected were not conclusive and that more work was needed to better quantify groundwater discharge to the area.

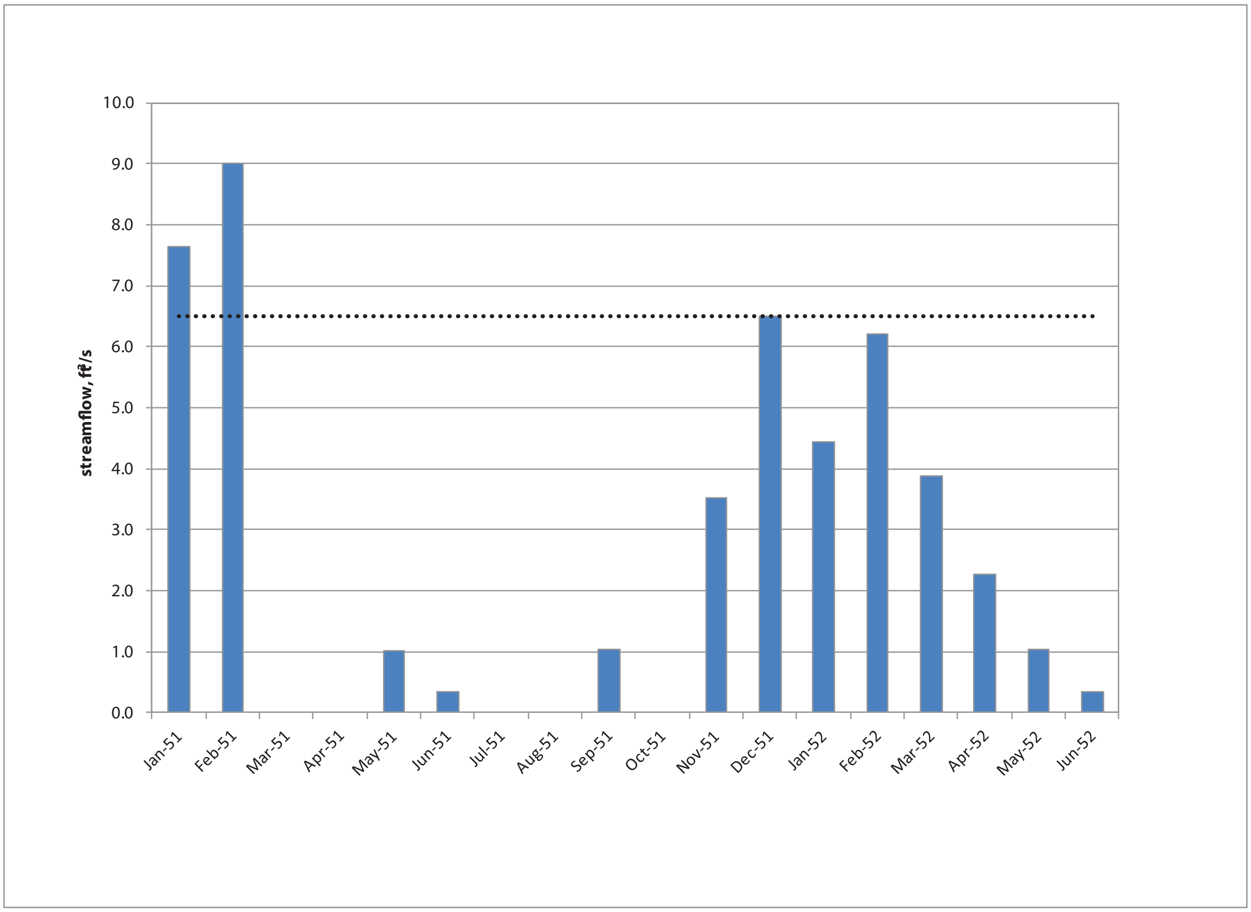

Figure 3.5: Measured streamflow by Spiegel and Baldwin (1963) at the Santa Fe River near Gallegos Ranch site (see Figure 3.6 for estimated location). Measured streamflow was periodically affected by runoff, seasonal changes in evapotranspiration, and upstream irrigation activities along both the Lower Santa Fe River and Cienega Creek and tributaries. Spiegel and Baldwin estimated the total groundwater discharge contributing flow at this site to be about 6.5 ft^3/s based on the assumption that the December 1952 measurement represented the flow of groundwater discharge. They acknowledged that the data collected were not conclusive and that more work was needed to determine the accurate amount of groundwater discharge to the area.

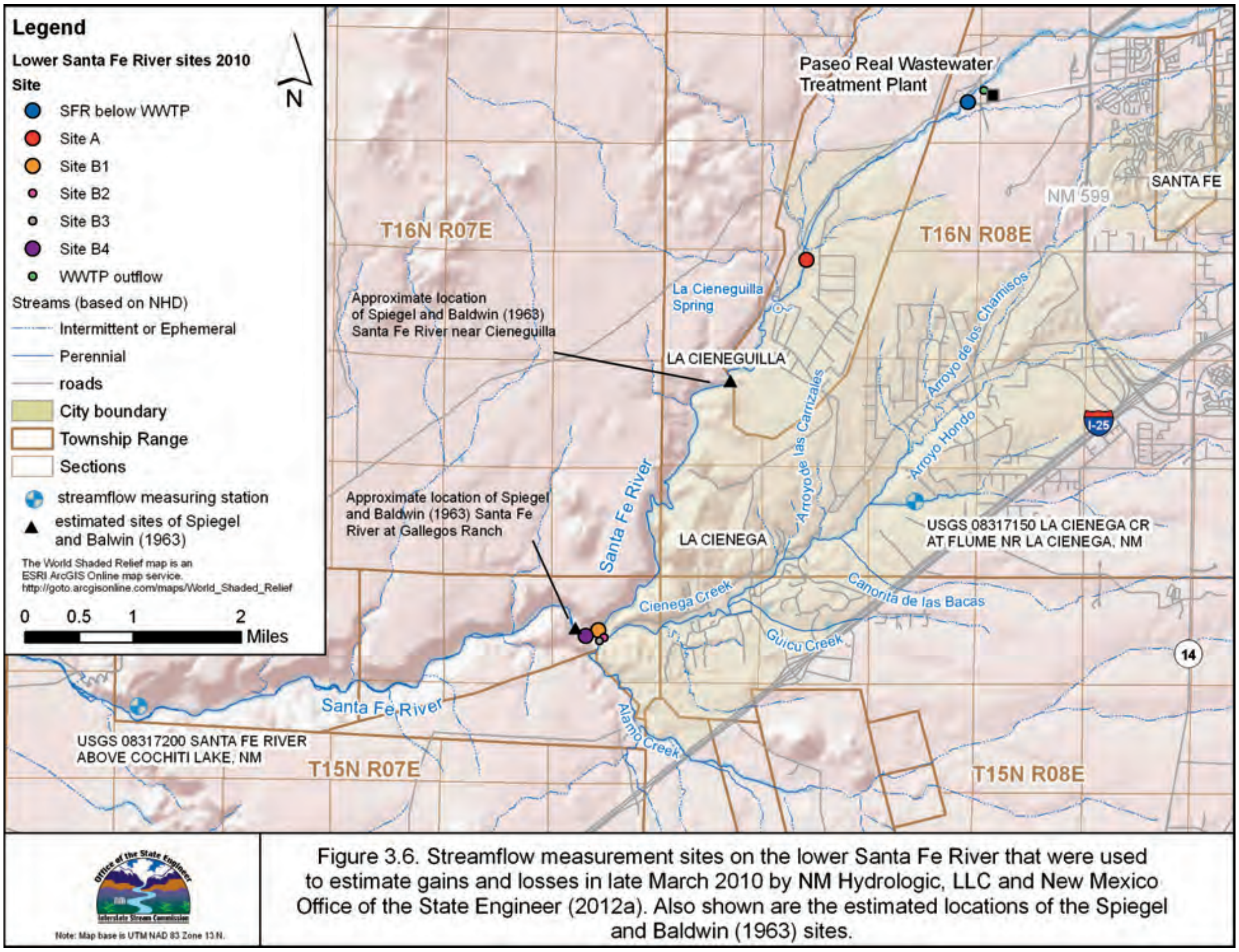

Figure 3.6: Streamflow measurement sites on the lower Santa Fe River that were used to estimate gains and losses in late March 2010 by NM Hydrologic, LLC and NMOSE (2012a). Also shown are the estimated locations of the Spiegel and Baldwin (1963) sites.

USGS seepage investigations: The USGS has also made measurements along the Santa Fe River during seepage investigations conducted during June and July in 1973, 1979 and 1980 (USGS, 1975; USGS, 1980; USGS, 1981). Because these measurements were made in the summer during times of higher evapotranspiration and irrigation, and because the WWTP quantity of discharge was variable, the information is not comparable to wintertime baseflow gains and losses in the Lower Santa Fe River.

Peery et al (2007): Peery and others (2007) prepared a hydrogeologic assessment of the Three Rivers Ranch (formerly the Gallegos Ranch, located at the confluence of the Santa Fe River, Cienega Creek, and Alamo Creek) for the owner, the Cohiba Club. For their study, they collected new streamflow data for Cienega and Alamo Creeks. Although their investigation did not provide new measurements for the lower Santa Fe River, their Cienega and Alamo Creek data are useful because they provide information concerning the tributary discharge to the Santa Fe River.

In their study, they made measurements during January 2007. Heavy snowfalls occurred in late December. Streamflow measured in a 90 degree v-notch weir on Cienega Creek (likely above the confluence with Alamo Creek) was computed to range from 2.6 to 3.3 ft^3/s. Streamflow measured in a 90 degree v-notch weir on Alamo Creek ranged from 0.2 to 0.3 ft^3/s. Because these were winter measurements, it is thought that evapotranspiration rates were minimal and it is unlikely that irrigation diversions were occurring upstream. It is uncertain how much snowmelt might have contributed to the measurements.

NM Hydrologic, LLC and NMOSE (2012a): The NMOSE worked with NM Hydrologic, LLC to compute streamflow in the Lower Santa Fe River, so that gains and losses could be estimated for several reaches of the river between the WWTP and the USGS gage, Santa Fe River above Cochiti Lake, NM (Figure 3.6). A detailed description of this streamflow measurement project is provided in a report by NM Hydrologic, LLC and the New Mexico Office of the State Engineer (2012a) titled, *Streamflow Measurement Study of the Lower Santa Fe River, Santa Fe County, NM: City of Santa Fe Wastewater Treatment Plant to the USGS Gage, Santa Fe River above Cochiti Lake, NM.* A summary of this report follows.

The project to estimate gains and losses along the lower Santa Fe River was conducted in the early spring of 2010.[4] Because flow from the WWTP varied considerably during the day, it was necessary to acquire Santa Fe River streamflow data continuously for several days at selected sites. During the study, streamflows at the downstream end of the tributary creeks, Cienega and Alamo, were also monitored. The sites for which streamflow data were acquired for the study are shown on Figure 3.6 and are listed below:

- The City of Santa Fe's WWTP
- Site A: Santa Fe River, about 4,000 ft downstream from Calle Debra Bridge, in the La Cieneguilla area
- Site B (consisting of several sub-sites)
    - B1: Santa Fe River, upstream of the confluence with Cienega Creek
    - B2: Cienega Creek, upstream of the confluence with Alamo Creek
    - B3: Alamo Creek, upstream of the confluence with Cienega Creek
    - B4: Santa Fe River, downstream of the confluence with Cienega Creek
- Santa Fe River above Cochiti Lake, NM, USGS Gage (08317200)

Streamflow data from the WWTP[5] and the USGS gage were acquired from the City of Santa Fe and the USGS, respectively. Streamflow was computed at Sites A and B1 using pressure transducer/datalogger units to record gage height and a rating curve that was developed at each site. Streamflow at Sites B2 and B3 was computed using 90 degree V-Notch weirs, and Site B4 was calculated by summing B1, B2, and B3. To estimate the gains and losses between the sites, several 24-hour periods were established for each site (after accounting for travel time between the sites) and the differences between the average flows for the 24-hour periods at each site were taken. Most of the data used to estimate gains and losses were collected between March 26 and March 31, 2010.

Figures 3.7, 3.8, and 3.9 show hydrographs plotted for adjacent upstream and downstream sites on the Santa Fe River. In each figure, the upstream site hydrograph is time-shifted to account for the travel time to allow for easier visual comparison of the upstream and downstream site flows (e.g. Figure 3.8 shows the computed streamflow at Site B1 and the flow at Site A shifted by +7.0 hours). All streamflow hydrographs exhibited a somewhat regular diurnal pattern, which corresponded to WWTP outfalls, corresponding to water use in the City of Santa Fe: a period of low flow was followed by a rapid rise to high flow, and then a gradual decline in flow. The diurnal pattern occurred later at the downstream sites due to the longer travel time.

4 This project was also attempted in 2012; however, there were equipment-related complications.

5 An adjustment was made to the WWTP reported streamflow values based on independent measurements which are described in NM Hydrologic, LLC and NMOSE (2012a)

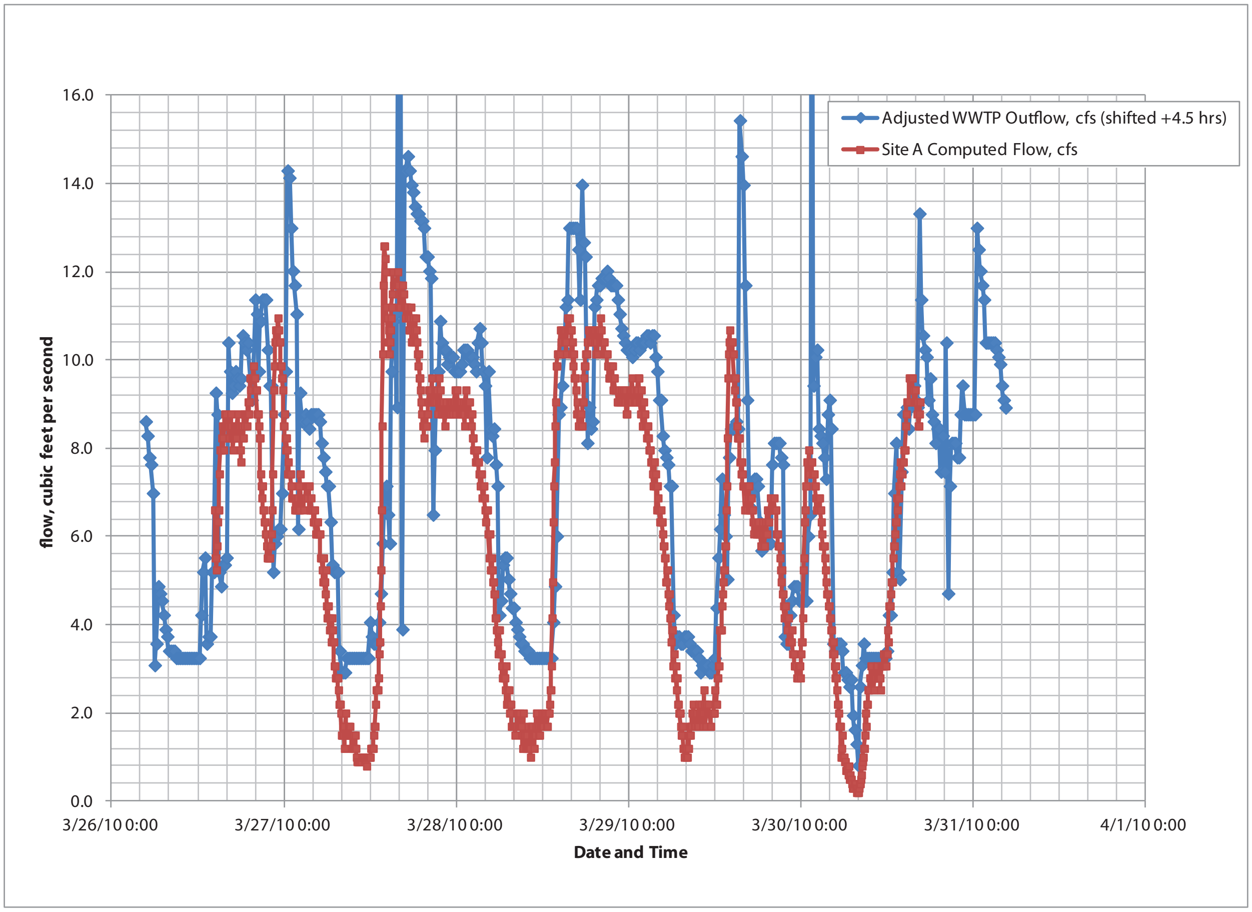

Figure 3.7: Hydrographs of the adjusted WWTP outflow, time shifted by +4.5 hours, and computed streamflow at Site A (from NM Hydrologic, LLC and NMOSE (2012a)).

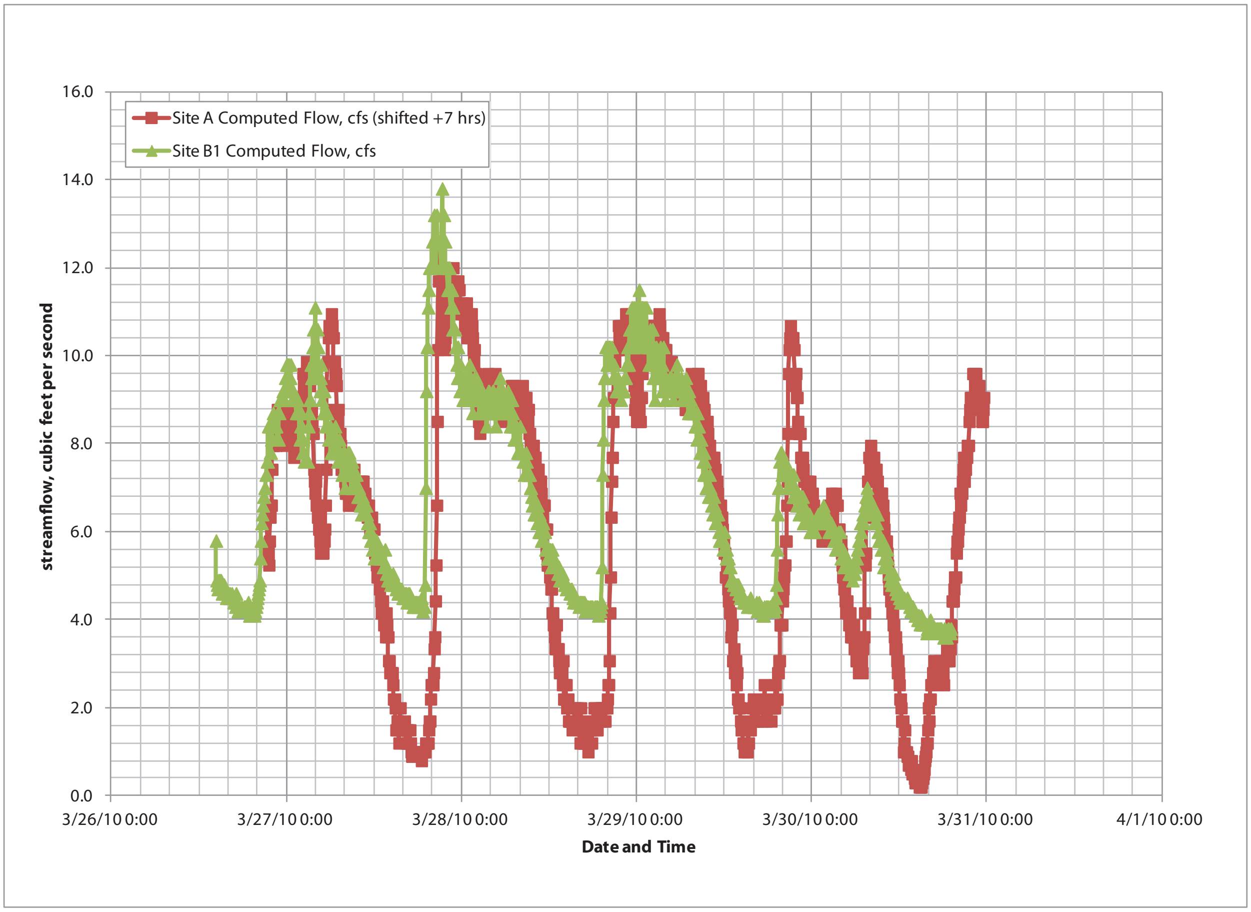

Figure 3.8: Hydrographs of the computed streamflow at Site A, time shifted by +7 hours, and computed streamflow at Site B1(from NM Hydrologic, LLC and NMOSE (2012a)).

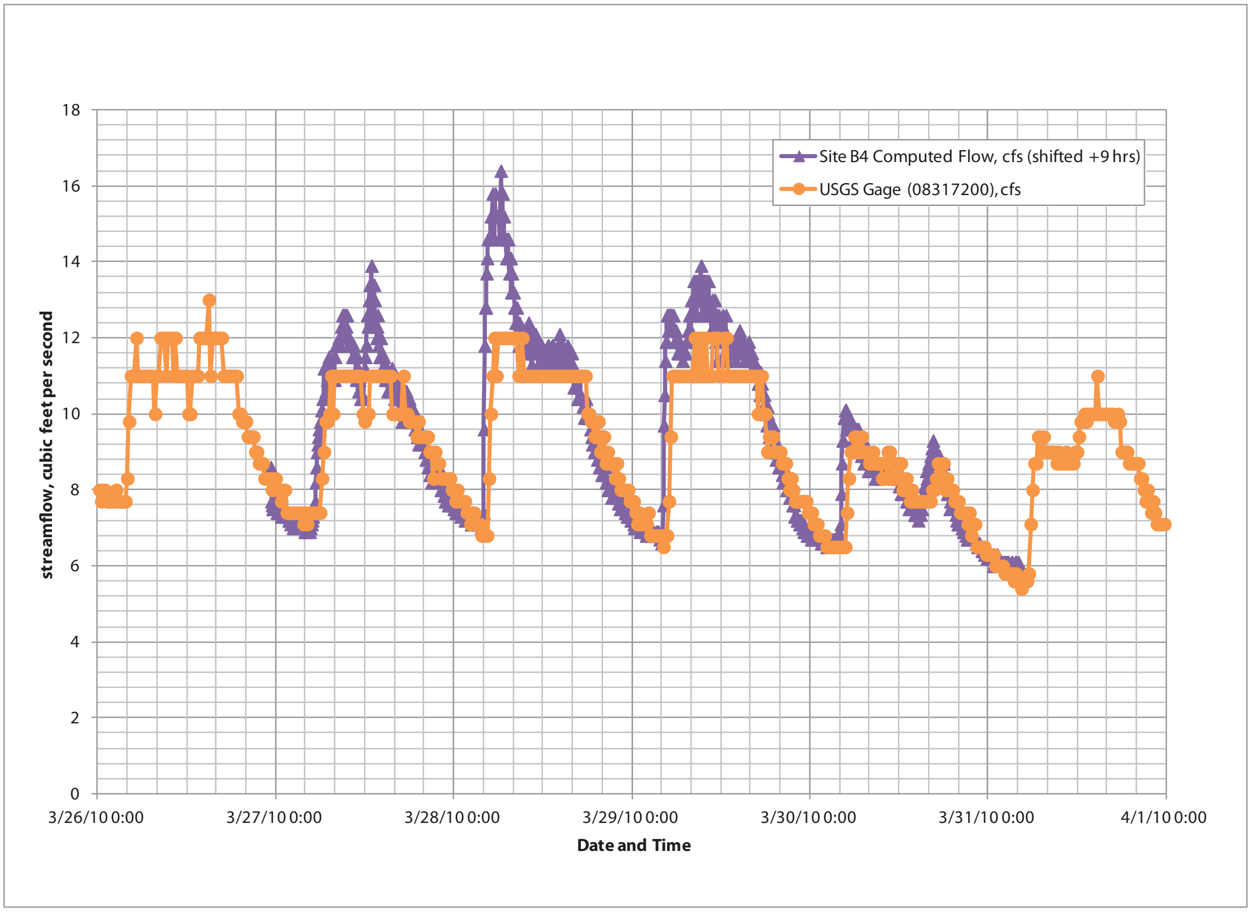

Figure 3.9: Hydrographs of the computed streamflow at Site B4, time shifted by +9 hours, and computed streamflow at the USGS Gage, Santa Fe River above Cochiti Lake, NM (08317200) (from NM Hydrologic, LLC and NMOSE (2012a)).

For each site, several 24-hour periods of flow were defined over the multiple day investigation; each started at the approximate end of a low flow interval, just prior to the rapid rise in flow. In the graphs, because the WWTP pulse arrived at later times farther downstream, the defined 24-hour periods lagged at sites farther downstream and were shifted in time for comparison purposes. The resulting average 24-hour flows were calculated, and were compared to determine the potential gain or loss that occurred between each of the sites. Table 3.2 shows the estimated gains and losses for each reach and 24-hour period between March 26 and 31, 2010. The results are summarized below:

- Between the WWTP and Site A (which is located just upstream of the estimated zone of discharge for the La Cieneguilla springs), the estimated loss in streamflow for three 24-hour periods ranged from 1.4 to 1.6 ft^3/s.
- Between Site A and B1, the estimated gain in streamflow for three 24-hour periods ranged from 0.9 to 1.0 ft^3/s. This represents the area between La Cieneguilla and the former Gallegos Ranch (now the Three Rivers Ranch), above the confluence with Cienega Creek (i.e. does not include flow from Cienega Creek). It includes the estimated area of La Cieneguilla Springs.
- Between Site A and B4 (just below the Cienega Creek confluence with the Santa Fe River), the estimated gain in streamflow for three 24-hour periods ranged from 3.2 to 3.6 ft^3/s, which included 2.3 to 2.6 ft^3/s inflow from Cienega and Alamo Creeks. Streamflow on Cienega Creek and Alamo Creek just above their confluence was measured periodically throughout the latter half of the month of March 2010, and measurements made earlier showed that combined flow from these two creeks was as high as 3.0 ft^3/s.
- Between Site B4 and the USGS gage Santa Fe River above Cochiti Lake, NM (08317200), the estimated loss in streamflow for four 24-hour periods ranged from 0.2 to 0.6 ft^3/s.

Table 3.2: Estimated average streamflow gains or losses for each reach based on data collected between 3/26/2010 and 3/31/2010 (a negative number indicates a loss in streamflow) (data from NM Hydrologic, LLC and NMOSE (2012b))

Date*	adjusted WWTP to Site A, ft^3/s	Site A to Site B1, ft^3/s	Site A to Site B4**, ft^3/s	Site B4 to USGS Gage, ft^3/s
3/26/2010	insufficient data	insufficient data	insufficient data	-0.4
3/27/2010	-1.6	1.0	3.6	-0.6
3/28/2010	-1.4	0.9	3.3	-0.6
3/29/2010	-1.4	0.9	3.2	-0.2

* represents the start date of the 24-hour period for all sites but the USGS Gage which started on the following day due to longer travel time.
** Site B4 is below the confluence with Cienega Creek. Tributary inflow from Cienega Creek and Alamo Creek was determined to be 2.3 to 2.6 ft^3/s between 3/27/2010 and 3/29/2010.

There was no recorded precipitation during the March 26-31, 2010 investigation and temperatures increased during the day over the course of the 5-day period. Streamflow at Cienega and Alamo Creek decreased from mid- March to the end of March by a combined 0.9 ft^3/s, which could suggest that streamflow was responding to snowmelt and runoff that winter, increased evapotranspiration due to the temperature increase, or both. Although there was no precipitation during the study, there was a series of precipitation events that delayed the study and which also led to runoff in the Santa Fe River that was observed near the SR 599 bridge upstream of the WWTP during the beginning of the March 26-31, 2010 study. If these unmeasured flows reached the WWTP, because they represent a gain to the river, it would lead to an underestimation of streamflow losses in the reach between the WWTP and Site A for those days.[6]

The differences in streamflow between the selected sites probably are characteristic of those reaches during this early spring season and, based on previous observations and results may vary during years or seasons with more or less seasonal precipitation.

6 It is thought that flows in the Santa Fe River upstream of the WWTP may have stopped by March 27, 2010, but certainly by March 28, 2010, based on an observation made that day. Flow upstream of the WWTP did not resume until March 31, 2010.

3.3 Discussion

As has been discussed in the previous sections, there are three general locations in the La Cienega area where historical and recent streamflow data are available. One is in Cienega Creek near the Acequia de la Cienega headgate; another is just downstream of Cieneguilla, and a third area is Cienega Creek and the Santa Fe River just downstream of Cienega Creek.

The data that have been reported for Cienega Creek near the Acequia de la Cienega headgate are plotted in Figure 3.10. The plot shows that there were two measurements that were higher than 0.7 ft^3/s (3/17/1966, 1.55 ft^3/s and 5/13/1971, 0.76 ft^3/s). Since about 1975, there is considerable scatter in the data, and flows appear to fluctuate between about 0.3 and 0.7 ft^3/s. Some of the fluctuations may be related to seasonal changes in evapotranspiration and periodic storm or snowmelt runoff. It is uncertain what the conditions were like at the time of the first two measurements prior to 1975 that recorded higher flows. If the conditions during the first two reported measurements were representative of groundwater discharge to the creek (and not influenced by storm or snowmelt runoff or measurement error), then it may indicate that there was a decline in streamflow at this location of Cienega Creek in the late 1960's and early 1970's.

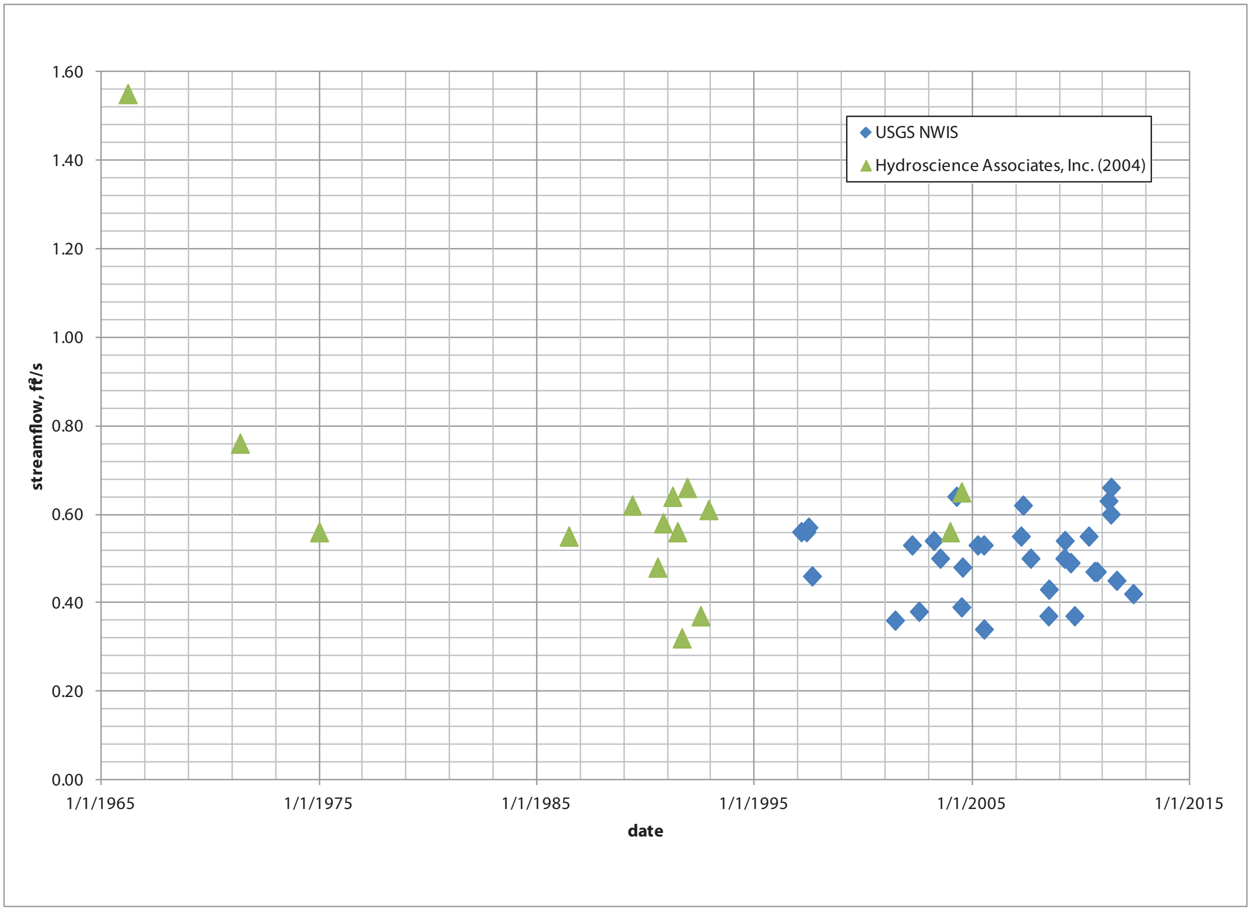

Figure 3.10: Streamflow measurements in Cienega Creek near the Acequia de la Cienega headgate. Data are plotted according to source.

At Cieneguilla, Spiegel and Baldwin (1963) estimated that 0.92 ft^3/s of spring flow was discharging to the Santa Fe River based on a measurement made in January 1952. Discharge occurred as water rising in the streambed. The more recent estimate by NM Hydrologic, LLC and the NMOSE (2012a), was based on late March 2010 streamflows. In the recent study, a 0.9 to 1.0 ft^3/s gain was estimated between a site just above Cieneguilla and a site just above the Santa Fe River confluence with Cienega Creek. In Spiegel and Baldwin's earlier study, they also made a measurement in March, which was almost 0.9 ft^3/s. It is reasonable to say that in 1952, the Cieneguilla spring was flowing about 0.9 ft^3/s in months with minimal evapotranspiration, diversions and surface runoff. The channel of the river has changed in since 1952, and the spring may be obscured by WWTP flows presently. In the NM Hydrologic, LLC and the NMOSE (2012a) study, if it is assumed that the major area of gain is associated with the spring in the Cieneguilla area, then there has not been a decline in flow. More investigation would be needed along the Santa Fe Canyon to understand if there is an important contribution of groundwater discharging to the Santa Fe River below the spring at Cieneguilla.

At the site below the confluence with the Santa Fe River and Cienega Creek, Spiegel and Baldwin (1963) estimated the component of groundwater discharge to streamflow in the Santa Fe River (which included flow from both the Cieneguilla area and Cienega Creek) to be 6.5 ft^3/s, based on a December 1952 streamflow measurement. As discussed previously, winter time measurements during periods of no precipitation or runoff, minimal evapotranspiration, and no irrigation diversions, represent the best periods to estimate groundwater discharge leaving the La Cienega area. In 2010, NM Hydrologic, LLC and the NMOSE (2012a) were unable to conduct their study in the winter due to precipitation and snowmelt, so the study was delayed until late March. In late March 2010, the groundwater discharge to streamflow estimated at the Santa Fe River below the confluence with Cienega Creek ranged from 3.2 to 3.6 ft^3/s. A comparison of the December 1952 estimate with the March 2010 estimate suggests that there may have been a decline between the early 1950's, when Spiegel and Baldwin (1963) made their measurements, and 2010. However, there are a number of factors that should be considered. One, Spiegel and Baldwin (1963) measured 4.4, 6.2, and 3.9 ft^3/s in the months of January, February, and March 1953, respectively, which represents a variation in streamflow from month to month of up to 2.3 ft^3/s. If just the March 1953 measurement (3.9 ft^3/s) is compared to the late March 2010 measurement (3.2 to 3.6 ft^3/s), there is not much difference between the two time periods. Of course, it is uncertain why the March 1953 flows were lower than the December 1952 flows, or how the December 2009 flows would have compared to the March 2010 flows. It is a hydrologic premise that the baseflows in the winters reflect the steady groundwater discharges continuing throughout the year, but that has not been demonstrated here. Additional study of seasonal changes in the present day flows along the Santa Fe River and Cienega Creek is needed to better understand how flows may have changed with time.

Although the late March 2010 NM Hydrologic, LLC and the NMOSE (2012a) gains and losses investigation did not include measurements in the depth of winter, this study did include measurements of Cienega and Alamo Creek flows near the confluence with the Santa Fe River, which can be compared to other recent measurements made in January 2007 (Peery et al., 2007) and February 2012 (NM Hydrologic, LLC and the NMOSE, 2012b) at the same locations. Unusually heavy snowfalls occurred in December preceding the Peery et al., 2007 measurements. Table 3.3 lists the reported Cienega and Alamo Creek streamflow for each study. Note that during the NM Hydrologic, LLC and the NMOSE (2012a) study, although the main part of the investigation was conducted between March 26 and March 31, 2010, Cienega and Alamo Creek streamflows were monitored from the middle to the end of March 2010. Flows from those creeks decreased near the end of the month and the range of measurements is presented in the table below. Of the three studies, the lowest combined flows were measured in February 2012 (2.0 to 2.1 ft^3/s), and the highest combined flows were measured in January 2007 (2.8 to 3.6 ft^3/s). The months preceding the measurements in February 2012 received less precipitation than the months preceding the measurements in January 2007 (Table 3.3). Finch and Peery (1995) suggested that La Cienega springs flow was related in part to precipitation. It is possible that streamflow variability occurs not only month to month, but year to year, depending on whether it was a wetter or drier year.

Table 3.3: A comparison of recent measurements of streamflow in Cienega and Alamo Creeks during the non-irrigation season.

Study	**Peery et al., 2007**	**NM Hydrologic, LLC and NMOSE, 2012a**	**NM Hydrologic, LLC and NMOSE, 2012b**
Date of measurement	January 2007	March 2010	February 2012
Total Precip for month, in.	0.5	1.5	0.1
Total Precip for month of measurement and previous two months, in.	2.0	3.2	1.8
Total Precip for month of measurement and previous eleven months, in.	14.6	12.2	8.9
Cienega Creek	2.6 to 3.3 ft^3/s	1.9 to 2.6 ft^3/s	1.7 to 1.8 ft^3/s
Alamo Creek	0.2 to 0.3 ft^3/s	0.3 to 0.4 ft^3/s	0.3 ft^3/s
Combined Cienega and Alamo Creek	2.8 to 3.6 ft^3/s	2.2 to 3.0 ft^3/s	2.0 to 2.1 ft^3/s

(Precipitation reported at the Santa Fe County Municipal Airport and provided by the NCDC)

In conclusion, within the last few years, the combined Cienega and Alamo Creek flows measured in January through March have generally ranged from 2.0 to 3.6 ft^3/s. If we assume the 0.9 to 1.0 ft^3/s estimate of gains from below Cieneguilla spring that was measured in March 2010 is representative of the baseflow gain in that reach, then the approximate range in baseflow contribution at the Santa Fe River below the confluence with Cienega Creek can be estimated to range from 2.9 to 4.6 ft^3/s for a January through March period in the last few years. While there is some overlap with the range of values reported by Spiegel and Baldwin (1963) for the December 1952 to March 1953 period (3.9 to 6.5 ft^3/s), the flows for that earlier period are somewhat higher than the estimates for more recent years.

3.4 Recommendations for Monitoring

Measuring streamflow on the Santa Fe River is challenging because of the daily variations in flow. To more accurately assess gains and losses along the river below the WWTP, recording streamflow gages would need to be established at key locations, so that streamflow could be better computed. Because of WWTP releases, the Santa Fe River has more water and is totally changed from the pre development condition.

During the winter months, flows in Cienega Creek and tributaries are likely to be fairly representative of the natural system. Continued winter monitoring of streamflow on Cienega and Alamo Creeks upstream of the confluence with the Santa Fe River (during periods with no irrigation diversions) would be useful data to collect to improve our understanding of the variability of Cienega and Alamo Creek flow not only during the winter months but over longer periods of time. Continued streamflow measurements at the Acequia de la Cienega headgate would also be useful, particularly if additional measurements were made during the winter months.

4.0 GEOLOGY AND HYDROGEOLOGY OF WETLANDS AND SPRINGS

By Peggy Johnson, Daniel Koning and Stacy Timmons, NMBGMR

4.1 Geologic, Hydrologic and Geochemical Methods

The geologic map used in this study is a digital ArcGIS combination of the 7.5-minute Turquoise Hill quadrangle map (1:24,000) (Koning and Hallett, 2001) and more detailed 1:12,000 mapping completed by Daniel Koning for this study during the summer and fall of 2011. Four new geologic cross sections were constructed that incorporated the subsurface locations of a monoclinal hinge, called the Rancho Viejo hinge zone, and the base of the Santa Fe Group (SFG) from Grauch et al. (2009). Aeromagnetic maps (USGS et al., 1999; Grauch and Bankey, 2003; Grauch et al., 2009) were used to delineate certain buried rocks, especially the Cieneguilla basanite. The base of the Ancha Formation was mapped using lithologic interpretations from cores, cuttings, geophysical logs, exploration and water well logs, and outcrop exposures. Saturated thickness estimates for the Ancha Formation were calculated from a subset of wells used to map the formation base and additional well records that met the following requirements: a shallow well just penetrating or nearly penetrating the base of the formation, a known location, an interpretable lithologic record, and a measured or otherwise reliable water level.

Water levels were measured between March 2011 and May 2012 in 45 wells in the shallow aquifer up-gradient of springs and wetlands using a graduated steel tape or an electric meter. Measurements were made to a repeatable accuracy of 0.02 ft. The major springs (22 in total) located at the head of emergent wetlands were inventoried and described. All sites were field located with a handheld GPS. Site elevations were calculated in ArcGIS using the 10–meter DEM and GPS-derived coordinates. Site information for wells and springs is presented in Tables 4.1 and 4.2; locations are shown on Figure 4.1. Groundwater elevation data were contoured by hand on a large- scale topographic base at 20-foot intervals, and digitized to create a water-table map for the study area. Groundwater flow lines, which approximate horizontal flow, were constructed normal to equipotential lines. Repeat measurements were made in several wells to evaluate seasonal and long-term water level changes. Water-level data are presented in Table 4.3.

Table 4.1: Well inventory.

	Well Location Information			Site Information Available					Well Construction					
Site ID	UTM Easting NAD83	UTM Northing NAD83	Elevation (ft asl)	NMOSE well record	Water sample	Water level	Site visit	Water bearing formation	Well depth (ft bgs)	Screen top (ft bgs)	Screen bottom (ft bgs)	Drill date	Driller static water level (ft bgs)	Static Water Elevation (ft asl)
EB-001	398529	3935208	6065	RG-39419	x	x	x	QTaas/Tg	221	47	221	3/15/1983	32	6033
EB-002	399070	3935822	6073	RG-61825		x	x	QTa/Tti	380	90	370	3/3/1995		
EB-019	400304	3935932	6144	RG-27637S	x	x	x	QTa	80	50	80	3/1/1979	37	6108
EB-102	402734	3934466	6199	Unknown		x	x	QTa						
EB-130	404633	3939633	6325	Unknown		x	x	Tts	225			1/1/1951	180	6146
EB-131	403262	3939063	6276	RG-29416Ex	x			QTa/Tts	222	180	220	10/1/1977	142	6134
EB-132	400609	3936794	6180	RG-08223		x	x	QTaas	135	60	90	12/2/1962	60	6113
EB-134	401980	3938280	6190	RG-32553	x			QTaas	137	90	134	6/1/1979	61	6129
EB-135	401760	3938450	6212	RG-32554Ex	x			QTaas	116	73	112	6/20/1979	70	6142
EB-172	405330	3943594	6462	RG-24042		x	x	Tts	493	353	470	10/13/1973	307	6156
EB-219	399267	3942749	6218	RG-00590	x	x	x	Ttsf	244	76	237	8/24/1956	76	6143
EB-220	403153	3938661	6260	RG-03824T		x	x	QTa	161	125	161	5/10/1971	125	6138
EB-221	404187	3937969	6243	RG-22251X7		x	x	QTa/Tts	220	160	220	1/20/1974	130	6115
EB-222	404457	3937957	6269	RG-22251X8		x	x	QTa/Tts	220	160	220	1/19/1974	130	6141
EB-223	399840	3938918	6165	RG-25952	x	x	x	QTa	100	40	95	5/8/1975	42	6123
EB-293	402450	3939520	6199	RG-11826S	x			Tts	340	102	340	9/5/1970	60	6139
EB-301	396972	3935730	5889	RG-32228		x	x	Tg	30			6/1/1951	24	5867
EB-303	400274	3937732	6123	RG-80582	x	x	x	QTa	62			1/1/1942	31	6085
EB-304	400149	3937292	6103	RG-21300	x	x	x	QTa	60	20	40	7/20/1978	14	6090
EB-305	400377	3937211	6127	RG-21301		x	x	QTa	75	20	75	7/24/1978		
EB-306	399495	3937699	6102	Unknown		x	x	QTa	43					
EB-309	399896	3939990	6231	RG-23683x2		x	x	Tts	300	120	280	5/1/1992	107	6125

	Well Location Information			Site Information Available					Well Construction					
Site ID	UTM Easting NAD83	UTM Northing NAD83	Elevation (ft asl)	NMOSE well record	Water sample	Water level	Site visit	Water bearing formation	Well depth (ft bgs)	Screen top (ft bgs)	Screen bottom (ft bgs)	Drill date	Driller static water level (ft bgs)	Static Water Elevation (ft asl)
EB-310	402100	3939571	6180	RG-56355		x	x	QTa/Tts	307	47	267	7/1/1998	43	6140
EB-312	400935	3936570	6179	RG-08823		x	x	QTa	135			12/2/1962	60	6112
EB-313	399260	3937304	6075	RG-14450	x	x	x	QTa/Tte	100			3/20/1967	85	5993
EB-314	399155	3937207	6060	RG-14450X		x	x	QTa	12			1/1/1986		
EB-315	400028	3937110	6113	RG-11278	x	x	x	QTa/Tte				1/1/1962		
EB-316	399790	3937163	6086	None		x	x	QTa/Tte	8			10/4/2007		
EB-319	404105	3938254	6274	RG-22251x4	x		x	Tts	200	160	200	1/22/1974	125	6151
EB-321	403986	3938251	6263	RG-22251x2		x	x	QTa/Tts	180	140	180	1/20/1974	130	6134
EB-323	397066	3937953	6041	RG-58916	x	x	x	Tg	220	160	220	2/1/1994	60	5974
EB-324	398590	3941443	6170	RG-65490		x	x	Tts	300	200	280	5/21/1997	40	6130
EB-325	398586	3940948	6149	RG-65564		x	x	Tts	300	200	280	5/18/1997	35	6114
EB-326	399072	3942360	6201	RG-65488		x	x	Tts	300	200	280	5/18/1997	50	6151
EB-327	398568	3942028	6188	RG-65489		x	x	Tts	300	200	280	5/23/1997	50	6139
EB-328	397578	3942243	6374	RG-75421	x	x	x	Tts	510	410	510	3/9/2001	285	6090
EB-329	399211	3940177	6212	RG-29536	x	x	x	Tts	132	100	132	8/1/1978	80	6133
EB-330	399133	3935759	6068	RG-34701S		x	x	QTa	100			5/28/1982	10	6061
EB-331	398988	3936088	6104	RG-61494		x	x	QTa/Tt/Tcb	400	70	390	1/25/1995	50	6057
EB-332	399720	3935678	6099	RG-74595	x	x	x	QTa	160	80	140	8/30/2000	18	6081
EB-333	399807	3935592	6120	RG-55622		x	x	QTa	140	80	120	6/26/1992	16	6098
EB-334	401921	3937456	6143	RG-74594		x	x	QTa	140	60	120	9/5/2000	58	6086
EB-335	402763	3937837	6212	RG-73995		x	x	QTa	160	100	160	6/28/2000	65	6142
EB-336	403199	3944575	6366	Exempt	x		x	Tts	1900	1880	1900	3/29/2004	212	6155
EB-337	403199	3944575	6366	Exempt	x		x	Tts	1065	1045	1065	3/29/2004	206	6161
EB-338	403199	3944575	6366	Unknown	x	x	x	Tts	600	580	600	3/29/2004	190	6177
EB-339	403035	3938347	6259	RG-44219	x	x	x	QTa	200	160	200	8/20/1985	135	6126
EB-340	399686	3936057	6126	RG-05530X		x	x	QTa	155			11/17/1956		
EB-361	405210	3944796	6446	RG-75063		x	x	Tts	500	460	500	2/2/2004	280	6167
EB-362	401318	3943215	6283	RG-45867		x	x	QTa	150	130	150	6/25/1986	131	6155
EB-363	401833	3943342	6300	RG-45867	x	x	x	QTa	170	145	160	5/8/1990	148	6157
EB-364	402532	3943573	6335	RG-45867	x	x	x	Tts	214	194	214	4/12/1990	185	6152
EB-365	401354	3943580	6277	RG-54182		x	x	QTa	125	105	125	11/1/1991	119	6160
EB-366	401829	3943023	6348	Exempt	x	x	x	QTa	204	184	204	8/5/1995	189	6161
EB-370	401630	3937747	6159	RG-48749	x			QTaas	90	24	61	12/23/1987	27	6132
EB-373	401729	3941231	6273	RG-29860	x	x	x	Tts	300			1/1/1940	80	6194
EB-377	399150	3933319	6047	RG-45727		x	x	QTt	65			7/22/1986	23	6026
EB-378	400477	3933822	6124	RG-51797		x	x	QTt	110	60	109	1/24/1990	18	6107
EB-379	401253	3934512	6206	RG-45723		x	x	QTa/Tte	227	137	227	7/25/1986	108	6099
EB-382	404931	3939843	6335	RG-54184		x	x	Tts	252	231	252	8/10/1991	180	6155
EB-383	404020	3936245	6289	RG-03824	x		x	Tteas	715			10/1/1954	125	6164
EB-387	403690	3937134	6242	Exempt		x	x	QTa	115					
EB-388	403442	3937136	6224	Exempt		x	x	QTa	91					
EB-389	403458	3936959	6241	Exempt		x	x	QTa	121					
EB-391	404639	3939485	6306	RG-75255	x	x	x	TTs	300	200	300	6/14/2001	159	6148
EB-392	404853	3938331	6270	RG-73973		x	x	QTa/Tts	220	160	200	5/17/2000	152	6119
EB-407	405069	3941697	6365	RG-26718		x	x	QTa	247			1/1/1953		
EB-459	401778	3942035	6311	RG-29860S	x		x	Tts	470	360	470	10/29/1980	175	6136
EB-509	396936	3933700	5955	RG-24679		x		Tg	272	20	271	9/4/1974	12	5945
EB-569	402917	3939407	6246	Unknown	x			Tts						
EB-579	398379	3942119	6197	RG-55884	x	x	x	Tts	240	180	220	8/5/1992	35	6162
EB-607	405006	3936039	6341	Exempt	x	x	x	QTa/Tta	340	230	330	5/13/2005	198	6143
EB-671	403283	3944985	6393	RG-89039		x		Tts	700	380	680	3/29/2007	175	6218
EB-672	401499	3939441	6160	RG-79212		x		Tts	500	460	480	9/10/2005	35	6125
EB-691	400249	3937717	6118	RG-92758		x	x	QTa/Tte/Tcb	180			9/23/2011	37	6082
LC-006	397628	3939546	6112	RG-90070	x	x	x	QTa/Tcb	86			1/1/1988	3	6104
LC-009	399771	3936914	6079	RG-34497 CLW		x	x	QTa/Tcb	180			10/1/2007		
LC-010	399811	3937131	6105	RG-34500POD2		x	x	QTa/Tcb	180	60	180	10/4/2007	22	6084

	Well Location Information			Site Information Available					Well Construction					
Site ID	UTM Easting NAD83	UTM Northing NAD83	Elevation (ft asl)	NMOSE well record	Water sample	Water level	Site visit	Water bearing formation	Well depth (ft bgs)	Screen top (ft bgs)	Screen bottom (ft bgs)	Drill date	Driller static water level (ft bgs)	Static Water Elevation (ft asl)
LC-011	399265	3937311	6075	RG-14450POD3		x	x	Tcb/Tte	340	240	320	2/15/2007	61	6016
LC-025	400000	3936280	6084	None		x	x	Qva/QTa	18			1/1/2002		
LC-026	399995	3936316	6087	None	x	x	x	QTa	8			1/1/2002		
LC-027	401705	3937727	6163	RG-60798		x	x	QTa/Tts	102			11/14/1994	37	6118
LC-028	399769	3936918	6079	RG-34497		x	x	QTa/Tcb						
LC-029	400290	3935932	6145	None		x	x	QTa						
LC-030	398982	3935662	6044	None		x	x	QTa	13					

Table 4.2: Spring and surface water inventory.

	Well Location Information			Site Information Available			
Site ID	UTM easting NAD83	UTM northing NAD83	Elevation (ft asl)	Site type	Water bearing formation	Water sample	Site visit
EB-302	397006	3936374	6002	Spring	Tg		x
EB-595	401950	3944200	6301	Stream	NA	x	x
EB-624	400057	3933375	6099	Spring	Tti	x	
EB-654	401005	3937572	6120	Spring	Qva/QTa		x
LC-001	399265	3935671	6036	Spring	Qva/QTa	x	x
LC-002	398603	3935594	6004	Spring	Qva/QTa		x
LC-003	398346	3935963	6020	Spring	QTa/Tg	x	x
LC-004	398481	3935768	6027	Spring	QTa/Tg		x
LC-005	400922	3937561	6119	Spring	Qva/QTa	x	x
LC-007	399439	3937177	6039	Spring	QTasr/Tcb	x	x
LC-008	399472	3936672	6050	Spring	QTaas/Te	x	x
LC-012	399793	3936418	6076	Spring	Qva/QTa/Tte		x
LC-015	399009	3937651	6115	Spring	QTasr/Tcb		x
LC-016	399824	3937994	6095	Spring	QTa	x	x
LC-017	399197	3935742	6052	Spring	QTa	x	x
LC-018	399212	3935682	6036	Spring	QTa	x	x
LC-019	399212	3935699	6036	Spring	QTa	x	x
LC-020	398652	3935424	6034	Spring	QTa	x	x
LC-021	400462	3937369	6088	Spring	QTaas/Tcb	x	x
LC-022	397721	3939493	6088	Spring	Qva/QTa/Tcb	x	x
LC-023	400085	3938409	6105	Spring	QTa	x	x
LC-024	398982	3937584	6101	Spring	QTasr/Tte		x
LC-031	396201	3934130	5917	Spring	Not examined		
LC-032	396176	3933800	5922	Spring	Not examined		
LC-033	401185	3943424	6260	Effluent	Not examined	x	x

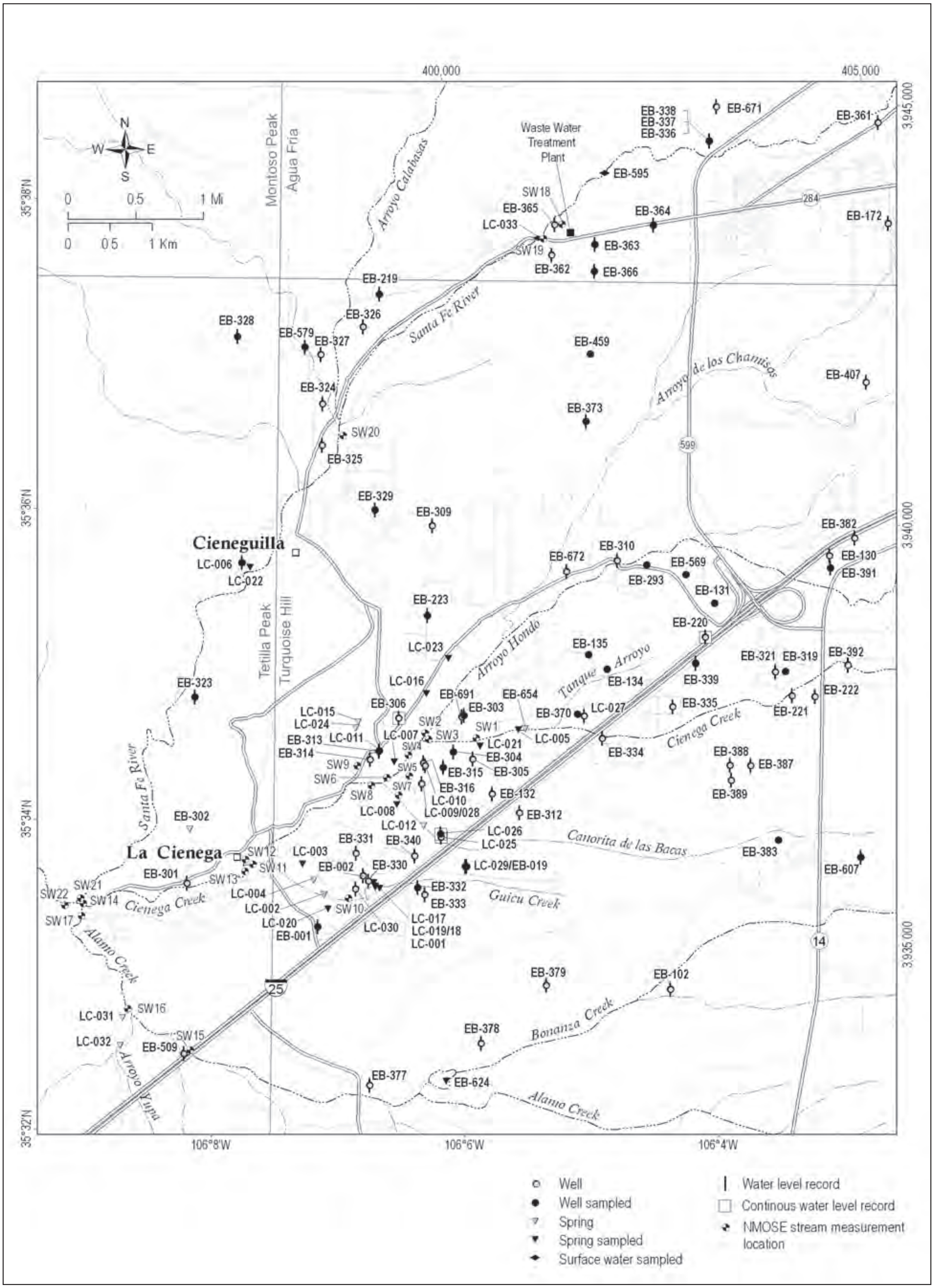

Figure 4.1: Inventory of wells and springs in the La Cienega Area with water level and chemistry data.

Table 4.3: Water-level data for 2012 groundwater conditions near La Cienega (Figure 4.13) and water-level changes over time (Figures 4.14 through 4.16).

		Most recent water level			Seasonal (summer/fall 2011 to winter 2012)				Historic (approx. 2004 to approx. 2012)			
Site ID	Site type	Date measured	Water depth (ft below TOC*)	Water depth elevation (ft asl)**	Date measured	Water depth (ft below TOC)	Water depth elevation (ft asl)	Change in depth (ft) from 2011 to 2012	Date measured	Water depth (ft below TOC)	Water depth elevation (ft asl)	Change in depth (ft) from 2004 to 2012
EB-001	controlwell	1/9/2004	48.91	6016.58								
EB-002	controlwell	2/27/2004	27.95	6045.80								
EB-019	well	2/14/2012	45.20	6100.24	10/5/2011	45.85	6099.59	-0.86	3/23/2004	44.34	6101.10	-0.86
EB-102	well	3/16/2011	62.05	6136.91					3/31/2004	60.35	6134.90	-1.70
EB-130	controlwell	3/24/2004	182.41	6143.21								
EB-132	well	2/15/2012	62.08	6111.33	10/5/2011	62.50	6110.91	0.42	2/10/2004	61.36	6112.05	-0.72
EB-172	controlwell	5/18/2007	304.80	6158.57								
EB-219	controlwell	5/30/2005	67.00	6152.00								
EB-220	well	2/14/2012	136.43	6126.58	6/21/2011	136.19	6126.82	-0.24	2/18/2004	131.40	6131.61	-5.03
EB-221	controlwell	5/18/2007	105.25	6139.43								
EB-222	well	3/9/2011	134.65	6136.70								
EB-223	well	2/15/2012	46.21	6118.61	7/21/2011	46.65	6118.17	0.44	2/11/2004	46.31	6118.51	0.10
EB-301	controlwell	1/9/2004	22.93	5868.12								
EB-302	spring	2/11/2004		6002.42								
EB-303	well	2/14/2012	16.29	6099.52	10/6/2011	17.03	6098.78	0.74				
EB-304	well	2/14/2012	15.68	6088.57	10/6/2011	16.47	6087.78	0.79	1/9/2004	15.16	6089.09	-0.52
EB-305	well	2/14/2012	24.65	6104.74	6/2/2011	24.79	6104.60	0.14	1/9/2004	24.17	6105.22	-0.48
EB-306	well	2/14/2012	21.03	6082.35	6/2/2011	21.18	6082.20	0.15	2/10/2004	21.20	6082.18	0.17
EB-309	controlwell	2/11/2004	107.50	6124.11								
EB-310	controlwell	2/11/2004	40.27	6142.31								
EB-312	well	2/15/2012	54.45	6118.02	10/5/2011	54.71	6117.76	0.26	2/10/2004	53.25	6119.22	-1.20
EB-313	well	2/15/2012	23.93	6054.08	10/5/2011	24.74	6053.27	0.81	2/10/2004	23.83	6054.18	-0.10
EB-314	well	2/15/2012	6.60	6056.50	10/5/2011	6.70	6056.40	0.10	2/10/2004	5.34	6057.76	-1.26
EB-315	well	2/15/2012	14.36	6092.19	10/5/2011	15.26	6091.29	0.90	2/10/2004	13.91	6092.64	-0.45
EB-316	well	2/15/2012	5.02	6079.75	6/22/2011	6.10	6078.67	1.08	2/10/2004	4.50	6080.27	-0.52
EB-321	well	2/15/2012	132.50	6131.09	10/5/2011	132.14	6131.45	-0.36	2/20/2004	133.39	6130.20	0.89
EB-323	controlwell	2/21/2004	23.00	6010.66								
EB-324	controlwell	5/21/1997	40.00	6130.14								
EB-325	controlwell	5/18/1997	35.00	6114.37								
EB-326	controlwell	6/28/2005	49.81	6151.25								
EB-327	controlwell	3/26/2004	49.75	6139.02								
EB-328	controlwell	6/7/2005	287.86	6087.36								
EB-329	controlwell	5/11/2005	92.23	6121.11								
EB-330	well	10/5/2011	11.63	6059.68								
EB-331	controlwell	2/27/2004	55.06	6052.22								
EB-332	well	2/14/2012	8.92	6090.10	7/21/2011	10.17	6088.85	1.25	2/27/2004	8.05	6090.97	-0.87
EB-333	well	2/14/2012	19.44	6094.19	10/5/2011	20.22	6093.41	0.78				
EB-334	well	2/15/2012	40.97	6103.28	10/5/2011	41.24	6103.01	0.27	2/27/2004	39.92	6104.33	-1.05
EB-335	well	2/14/2012	81.41	6125.42	7/21/2011	81.45	6125.38	0.04	2/27/2004	79.50	6127.33	-1.91
EB-338	well	3/29/2012	186.44	6180.03					1/20/2005	185.41	6177.59	-0.88
EB-339	well	2/15/2012	139.64	6121.63	6/2/2011	139.37	6121.90	-0.27	4/29/2004	138.53	6122.74	-1.11
EB-340	well	2/15/2012	53.02	6073.88	10/5/2011	53.72	6073.18	0.70	4/29/2004	52.33	6074.57	-0.69
EB-361	controlwell	6/8/2005	288.80	6158.51								
EB-362	well	2/14/2012	131.80	6153.85	10/20/2011	132.30	6153.35	0.50	6/10/2004	133.71	6151.94	1.91
EB-363	well	2/14/2012	149.35	6155.32	10/20/2011	149.80	6154.87	0.45	6/10/2004	149.99	6154.68	0.64
EB-364	well	2/14/2012	180.45	6156.06	10/20/2011	180.90	6155.61	0.45	6/10/2004	180.53	6155.98	0.08
EB-365	well	2/14/2012	120.80	6158.10	10/20/2011	121.30	6157.60	0.50	6/10/2004	123.64	6155.26	2.84
EB-366	well	2/14/2012	190.75	6158.94	10/20/2011	191.20	6158.49	0.45	6/10/2004	189.90	6159.79	-0.85
EB-373	well	2/14/2012	119.10	6154.94	10/20/2011	118.60	6155.44	-0.50				
EB-377	controlwell	6/24/2004	14.15	6034.81								
EB-378	controlwell	6/24/2004	26.15	6098.95								
EB-379	controlwell	6/24/2004	102.44	6104.70								
EB-382	controlwell	6/24/2004	186.98	6148.28								
EB-387	well	3/17/2012	100.23	6142.04	8/26/2011	100.09	6142.18	-0.14	1/1/2003	99.08	6143.19	-1.15

		Most recent water level			Seasonal (summer/fall 2011 to winter 2012)				Historic (approx. 2004 to approx. 2012)			
Site ID	Site type	Date measured	Water depth (ft below TOC*)	Water depth elevation (ft asl)**	Date measured	Water depth (ft below TOC)	Water depth elevation (ft asl)	Change in depth (ft) from 2011 to 2012	Date measured	Water depth (ft below TOC)	Water depth elevation (ft asl)	Change in depth (ft) from 2004 to 2012
EB-388	well	3/17/2012	90.14	6134.10	8/26/2011	90.25	6133.99	0.11	1/1/2003	89.17	6135.07	-0.97
EB-389	well	3/17/2012	110.40	6130.87	8/26/2011	110.27	6131.00	-0.13	1/1/2003	109.25	6132.02	-1.15
EB-391	controlwell	7/1/2004	159.70	6147.68								
EB-392	controlwell	7/15/2004	126.11	6144.79								
EB-407	controlwell	3/23/2004	218.10	6147.29								
EB-509	controlwell	3/24/2005	49.29	5907.90								
EB-579	controlwell	5/30/2005	57.00	6140.24								
EB-607	well	1/5/2012	199.68	6141.32	8/19/2011	199.80	6141.20	0.12	5/23/2005	197.83	6143.17	-2.07
EB-624	spring			6099.48								
EB-671	controlwell	5/1/2007	195.00	6197.79								
EB-672	controlwell	9/10/2005	34.70	6125.21								
EB-691	well	5/24/2012	25.23	6094.37								
LC-001	spring			6036.27								
LC-002	spring			6004.07								
LC-003	spring			6020.22								
LC-004	spring			6027.17								
LC-005	spring			6119.45								
LC-006	well	2/14/2012	2.54	6104.17	7/8/2011	3.79	6102.92	1.25				
LC-007	spring			6039.02								
LC-008	spring			6050.49								
LC-009	well	2/15/2012	15.48	6064.48	10/5/2011	18.06	6061.90	2.58				
LC-010	well	2/15/2012	16.73	6089.31	10/5/2011	17.40	6088.64	0.67				
LC-011	well	2/15/2012	26.31	6050.25	10/5/2011	32.91	6043.65	6.60				
LC-012	spring			6076.34								
LC-015	spring			6115.17								
LC-016	spring			6095.31								
LC-017	spring			6052.11								
LC-018	spring			6036.27								
LC-019	spring			6036.27								
LC-020	spring			6033.75								
LC-021	spring			6087.95								
LC-022	spring			6087.97								
LC-023	spring			6104.59								
LC-024	spring			6100.77								
LC-025	well	2/16/2012	8.05	6076.79	10/4/2011	12.45	6072.39	4.40				
LC-026	well	2/15/2012	6.66	6080.46	10/4/2011	7.00	6080.12	0.34				
LC-027	well	2/14/2012	32.64	6122.75	10/4/2011	33.20	6122.19	0.56				
LC-028	well	2/15/2012	7.47	6066.74	10/5/2011	9.89	6064.32	2.42				
LC-029	well	10/5/2011	45.74	6100.31								
LC-030	well	2/15/2012	10.41	6034.37								
LC-031	spring			5917.00								
LC-032	spring			5922.00								

*Water level measured from Top of Casing (TOC)

**Water elevation used for water table map (Figure 4.13)

Between March and October 2011, groundwater samples were collected by NMBGMR from 9 wells, 13 springs, and the discharge outflow from the Santa Fe WWTP. Samples were collected from domestic wells and springs using either dedicated submersible pumps or a peristaltic pump. Waters were analyzed for major and minor ion and trace element chemistry, oxygen and hydrogen isotopes, and field measurements of specific conductance, dissolved oxygen, pH and temperature. Thirteen samples were also analyzed for carbon isotopes (^{4}C and $^{13}C/^{12}C$ ratio) and tritium (^{3}H). Seven samples were analyzed for chlorofluorocarbon (CFC) recharge ages. Existing geochemical data, including combinations of ion, trace element, and stable isotope chemistry, from 21 sites in the study area were incorporated from an existing NMBGMR database of 2005 and historical sampling events (Johnson et al., 2008). Published carbon isotope (^{14}C and $^{13}C/^{12}C$ ratio) and ^{14}C age data from Manning (2009) were also incorporated into the data set for La Cienega. Sample information and geochemical data are provided in Tables 4.4, 4.5 and 4.6. Details about site characteristics, sample collection, and sample analysis are discussed in Appendix D: Methods.

Table 4.4: Chemistry data for well, spring, and stream waters.

Table 4.4A		Field Parameters					General Chemistry*							
Site ID	Site type	Temp (°C)	Temp (°F)	Specific conductivity (µS/cm)	DO*	Field pH	Specific conductivity (µS/cm)	Lab pH	Total dissolved solids	Hardness	Total anions (meq/L)	Total cations (meq/L)	Charge balance (% diff)	Water type
EB-001	well								355	212			4.49	Ca-Na-Mg-HC03-S04
EB-019	well						354	8.4	188	125			-1.07	Ca-Na-HC03
EB-131	well						230	7.0	92	152.1			-11.55	Ca-Na-HC03
EB-134	well						230	7.3	150	112.8			10.68	Ca-Na-HC03
EB-135	well						225	8.2	166	96.8			3.24	Ca-Na-HC03
EB-219	well	17	62.6	133		6.8			125				3.51	Ca-Mg-HC03
EB-223	well	15.6	60.1	146	8.7	8.0	255	7.9	163	80	2.56	2.62	1.12	Ca-Na-HC03
EB-293	well							8.2	144	81			-2.99	Ca-Na-HC03
EB-303	well	16.5	61.7	594	8.9	7.6	565	7.8	391	256	6.36	6.25	-0.89	Ca-HC03-S04-Cl
EB-304	well							7.8	141	77				Ca-Na-HC03
EB-313	well	16.2	61.2	266	0.5	7.2	255	7.4	180	80	2.95	2.79	-2.64	Ca-Na-HC03-S04
EB-315	well	15.3	59.5	259	4.8	8	240	8.2	160	97			0.40	Ca-Na-HC03
EB-319	well						324	8.0	182	111			4.00	Ca-Na-HC03
EB-323	well	20.6	69.1	415		6.9			350				5.02	Na-Ca-Mg-HC03
EB-328	well	18	64.4	253	2.6	8.3	235	8.3	155	53			1.78	Na-Ca-HC03
EB-329	well	16.4	61.5	234	4.7	7.9	220	8.1	152	73			-2.47	Ca-Na-HC03
EB-332	well	15.6	60.0	265	8.2	7.9	260	7.4	180	95	2.89	2.9	0.24	Ca-Na-HC03
EB-336	well	19.6	67.3	551	0.6	8.5	550	8.5	316	5			-0.75	Na-HC03
EB-337	well	18	64.4	288	7.3	8.1	270	8.2	191	27			-1.68	Na-HC03
EB-338	well	16.3	61.3	159		8.0	150	8	108	65			-2.07	Ca-HC03
EB-339	well						239	7.8	128	47			-2.98	Na-Ca-HC03-S04
EB-363	well	14	57.2	135		6.7			130				-13.28	Ca-HC03
EB-364	well	16.4	61.5	176	7.5	7.8	185	7.9	125	82	1.92	2.06	3.50	Ca-HC03
EB-366	well	16.1	60.9	210	8.3	7.7	220	7.9	140	93	2.29	2.25	-1.04	Ca-HC03
EB-370	well						440	7.9	252	221.97			13.10	Ca-Na-HC03-S04
EB-373	well	17.5	63.5	247	6.4	7.5	265	7.9	164	106	2.68	2.73	0.84	Ca-Na-HC03
EB-383	well												1.09	Na-Ca-HC03
EB-391	well							8	177	114			2.19	Ca-HC03
EB-459	well	18	64.4	250		7.3			162				-6.55	Na-HC03-S04
EB-569	well						254	7.0		106			2.22	Ca-HC03
EB-579	well							6.9	135	88			3.22	Ca-Na-HC03
EB-595	stream	23.2	73.8	251	4.7	8.3	230	8.4	141	98			0.73	Ca-HC03
EB-607	well	18.7	65.7	216	3.5	8		8.1	227	44.1				Na-Ca-HC03
EB-624	spring						322	7.6	274	171			3.54	Ca-Na-Mg-HC03
LC-001	spring	21.6	70.9	278	3.6	7.9	275	7.7	175	94	2.88	2.82	-1.03	Ca-Na-HC03
LC-003	spring	13.6	56.4	457	1.6	7.4	470	7.3	296	189	4.8	4.95	1.57	Ca-Na-Mg-HC03-S04
LC-005	spring	14	57.2	367	6.7	7.6	380	7.6	236	147	3.97	3.8	-2.18	Ca-Na-HC03
LC-006	well	15.1	59.2	279	10.6	7.2	275	7.5	189	117	2.96	2.89	-1.23	Ca-HC03
LC-007	spring	12.1	53.7	567	3	7.2	440	7.6	305	136	4.92	4.78	-1.43	Ca-Na-HC03-S04
LC-008	spring	15.0	59.1	405	3.6	7.3	390	7.5	263	152	4.39	4.28	-1.18	Ca-Na-HC03
LC-016	spring	15.5	59.9	307	6.8	7.4	2290	7.6	206	88	3.34	3.26	-1.20	Na-Ca-HC03
LC-017	spring	12.9	55.3	397	6.1	7.8								
LC-018	spring	10	50.0	271	5.3	7.7								
LC-019	spring	12.0	53.5	218	7.1	7.9								
LC-020	spring	7.5	45.5	809	5.2	7.3								
LC-021	spring	11	51.8	349	7.3	7.7								
LC-022	spring	9.1	48.4	667	7.5	6.9								
LC-023	spring	18.5	65.3	375	5.7	7.7	305	7.4	212	70	3.32	3.42	1.44	Na-Ca-HC03
LC-026	well	14.9	58.8	358	1.4	7.6	565	7.4	344	218	5.55	5.7	1.35	Ca-Na-HC03-Cl-S04
LC-033	effluent	25.8	78.4	703	5.9	7.6	736	7.8	454	142	7.61	7.32	-1.94	Na-Ca-HC03-Cl

*Units are mg/L (ppm)

Table 4.4B	Major and minor ions*															
Site ID	**Ca**	**Mg**	**Na**	**Ca:Na Ratio**	**K**	**HCO3**	**CO3**	**SO4**	**Cl**	**Br**	**F**	**Fe**	**Mn**	**NO3**	**Chemistry laboratory name**	**Sample date**
EB-001	61	15	41	1.7		197	5	59	26		2	0.03	<0.03	2.9	Unknown	4/1/1995
EB-019	39	7	20	2.2	1.7	149		16	19		0.21	<0.05		12.7	Hall Environmental	3/1/1996
EB-131	23	4	21	1.3		142	0	15	4		0.04	0	0	19.5	Environmental Biochemists	11/9/1977
EB-134	37	5	36	1.2		152	<1	8	6		0.21	<0.1	<0.02	19.9	Albuchemist, Inc.	9/24/1979
EB-135	34	3	27	1.4		150	<1	11	4		0.2	<0.1	<0.02	6.9	Albuchemist, Inc.	9/24/1979
EB-219	27	8	9	3.4	1.2	113		9	7		0.23				Scientific Lab. Div. of NM	9/13/1984
EB-223	26	3	23	1.3	1.2	120		19	5	0.12	0.28	<0.02	<0.001	2.6	NMBGMR	10/4/2011
EB-293	32		13	2.9		119		11	5			<0.02	<0.01		Inter Mountain Laboratories Inc.	1/30/2001
EB-303	86	10	25	3.9	2.4	170		97	47	0.64	0.17	<0.02	<0.001	14	NMBGMR	6/22/2011
EB-304	24	4	14	2.0		116		12	8		<0.05	4.36	0.19	5.1	Assaigai Analytical Laboratories	5/18/2004
EB-313	25	4	27	1.1	1.3	130		32	5	0.1	0.29	1.6	0.52	0.1	NMBGMR	6/22/2011
EB-315	31	5	13	2.7	1.6	120		15	8	0.12	0.24	0.23	<0.001	4	NMBGMR	5/11/2005
EB-319	32	8	30	1.2	5	167		16	10			<0.1	<0.05		NMDWB	9/25/1997
EB-323	54	17	67	0.9	4.3	314		18	32		0.51				Scientific Lab. Div. of NM	9/13/1984
EB-328	16	3	33	0.6	1.8	110	4	14	6	<0.1	0.57	0.04	<0.001	4.8	NMBGMR	6/7/2005
EB-329	24	3	19	1.4	1.2	120		11	6	<0.1	0.26	0.17	<0.001	6.4	NMBGMR	5/11/2005
EB-332	28	7	22	1.5	2.2	140		11	8	0.11	0.34	<0.02	0.001	7.1	NMBGMR	7/21/2011
EB-336	2	<1	125	0.0	1	275	12	22	6	0.14	1.6	0.02	0.009	1.3	NMBGMR	4/8/2005
EB-337	11	<1	54	0.2	1.8	150		21	3	0.11	0.4	0.04	0.002	3.8	NMBGMR	4/8/2005
EB-338	22	3	7	3.7	0.9	95		4	2	<0.1	0.29	0.10	<0.001	1.4	NMBGMR	4/9/2005
EB-339	15	1	39	0.4		122	0	28	1		0.27	0.09	<0.01		Controls for Environmental Pollution, Inc.	10/2/1987
EB-363	24	0	7	3.9	1.6	102		10	4		0.26				Scientific Lab. Div. of NM	12/27/1984
EB-364	27	4	9	3.4	1	105		4	3	0.04	0.22	<0.02	<0.001	1.5	NMBGMR	10/20/2011
EB-366	31	4	8	4.2	1.0	115		7	7	0.08	0.23	<0.02	<0.001	4.3	NMBGMR	10/20/2011
EB-370	79	6	23	4.0		144	<5	62	14		0.24	0.15	0.019	8.7	Assaigai Analytical Laboratories	1/13/1988
EB-373	35	5	13	3.1	1.4	125		17	8	0.09	0.24	<0.02	<0.001	4.1	NMBGMR	10/20/2011
EB-383	21	2	34	0.7	1.8	130	0	18	4						NMDWB	4/1/1997
EB-391	38	4	11	4.2		144		7	3		<0.05	<0.07	<0.02	4.4	Assaigai Analytical Laboratories	5/5/2004
EB-459	11	0	58	0.2	0	155		32	9		0.48				Scientific Lab. Div. of NM	12/27/1984
EB-569	36	4	9	4.6	2.6	142	<1	<2	5		0.3				NMDWB	3/17/1997
EB-579	30	4	14	2.5		115		6	5		<0.5	<0.01	<0.01	3.1	Assagai Analytical Laboratories	6/21/2000
EB-595	31	5	10	3.7	1.6	87	4	23	12	<0.1	0.27	0.24	0.02	0.2	NMBGMR	5/12/2005
EB-607	16	1	32	0.6	1.4	134	0	15	2	0.02	0.4	<0.01	<0.001	0.8	LANL	9/26/2006
EB-624	47	12	27	2.0	3.5	231	<1	16	7						Unknown	9/8/1998
LC-001	28	6	20	1.6	2.4	145		14	6	0.07	0.35	0.11	0.004	3.1	NMBGMR	6/1/2011
LC-003	56	12	25	2.6	2.6	155		54	34	0.33	0.25	<0.02	0.005	9.2	NMBGMR	6/1/2011
LC-005	49	6	19	3.0	1.1	175		23	15	0.13	0.25	<0.02	0.001	10	NMBGMR	6/1/2011
LC-006	35	7	12	3.3	1.7	115		10	17	0.13	0.21	<0.02	<0.001	22	NMBGMR	6/21/2011
LC-007	43	7	46	1.1	2.2	180		65	15	0.16	0.29	0.02	0.056	12	NMBGMR	6/22/2011
LC-008	45	10	26	2.0	3.8	180		32	25	0.21	0.31	0.03	0.016	2.9	NMBGMR	6/22/2011
LC-016	29	4	34	1.0	1.9	155		24	8	0.11	0.36	<0.02	0.005	3.6	NMBGMR	6/22/2011
LC-017															NMBGMR	3/25/2011
LC-018															NMBGMR	3/25/2011
LC-019															NMBGMR	3/25/2011
LC-020															NMBGMR	3/25/2011
LC-021															NMBGMR	3/25/2011
LC-022															NMBGMR	3/25/2011
LC-023	23	3.2	45	0.59	2.6	145		29	10	0.38	0.4	0.29	0.033	1.4	NMBGMR	7/20/2011
LC-026	69	11	28	2.83	4.6	155		63	57	0.62	0.22	<0.02	0.002	4.9	NMBGMR	10/4/2011
LC-033	45.3	7	90.5	0.57	21.5	239	<5	48	75.3	0.17	0.34	0.10	0.02	9.01	NMBGMR	8/30/2012

*Units are mg/L (ppm)

Table 4.4C	Trace Elements*													
Site ID	Ag	Al	As	B	Ba	Be	Cd	Co	Cr	Cu	Hg	Li	Mo	Ni
EB-001	<0.03		<0.01		0.17		<0.002		<0.03	<0.03	<0.0004			
EB-019														
EB-131														
EB-134														
EB-135														
EB-219														
EB-223	<0.0005	0.001	0.004	0.037	0.089	<0.0005	<0.0005	<0.0005	0.002	<0.0005		0.012	0.001	<0.0005
EB-293	<0.01	<0.05								<0.01				
EB-303	<0.0005	<0.0005	0.002	0.025	0.22	<0.0005	<0.0005	<0.0005	0.002	0.001		0.015	<0.001	0.001
EB-304	<0.01	<0.8	0.004		0.12	<0.002	<0.001		<0.15	<0.17				<0.09
EB-313	<0.0005	0.001	0.008	0.041	0.13	<0.0005	<0.0005	<0.0005	<0.0005	<0.0005		0.012	0.002	0.001
EB-315	<0.001	0.001	0.003	0.02	0.12	<0.001	<0.001	<0.001	0.001	0.003		0.009	0.001	<0.001
EB-319														
EB-323														
EB-328	<0.001	0.001	0.004	0.071	0.055	<0.001	<0.001	<0.001	0.013	0.001		0.015	0.002	<0.001
EB-329	<0.001	<0.001	0.004	0.028	0.11	<0.001	<0.001	<0.001	0.001	0.001		0.008	0.001	<0.001
EB-332	<0.0005	0.003	0.004	0.027	0.11	<0.0005	<0.0005	<0.0005	0.002	0.001		0.013	0.001	0.001
EB-336	<0.001	0.016	0.042	0.17	0.029	<0.001	<0.001	<0.001	0.006	0.005		0.069	0.002	<0.001
EB-337	<0.001	0.002	0.018	0.061	0.11	<0.001	<0.001	<0.001	0.005	0.003		0.03	0.002	<0.001
EB-338	<0.001	0.001	0.001	0.009	0.17	<0.001	<0.001	<0.001	<0.001	0.001		0.004	<0.001	<0.001
EB-339	<0.01		<0.01		<0.1		<0.001		<0.01	<0.01	<0.0004			
EB-363														
EB-364	<0.0005	0.009	0.002	0.011	0.13	<0.0005	<0.0005	<0.0005	0.001	0.004		0.005	<0.001	0.001
EB-366	<0.0005	0.006	0.001	0.013	0.13	<0.0005	<0.0005	<0.0005	<0.0005	<0.0005		0.005	<0.001	0.001
EB-370														
EB-373	<0.0005	0.002	0.001	0.026	0.11	<0.0005	<0.0005	<0.0005	0.001	<0.0005		0.007	<0.001	<0.0005
EB-383														
EB-391	<0.01	<0.2	0.002		0.15	<0.002	<0.0005		<0.15	0.26	<0.0002			<0.09
EB-459														
EB-569			0.002		0.195	<0.0002	<0.0001		0.001		<0.0002			0.001
EB-579	<0.01	<0.1	<0.001		0.13	<0.002	<0.001		<0.01	<0.02	0.001			<0.02
EB-595	<0.001	0.013	0.001	0.017	0.055	<0.001	<0.001	<0.001	0.001	0.003		0.006	0.001	0.001
EB-607	<0.001	0.006	0.005	<0.002	0.12	<0.001	<0.001	<0.001	0.002	<0.001	<0.0025	0.013	<0.05	<0.001
EB-624														
LC-001	<0.0005	0.078	0.002	0.026	0.1	<0.0005	<0.0005	<0.0005	0.001	<0.0005		0.013	0.003	0.001
LC-003	<0.0005	0.005	0.003	0.027	0.17	<0.0005	<0.0005	<0.0005	0.001	0.003		0.016	0.002	0.001
LC-005	<0.0005	0.001	0.003	0.024	0.19	<0.0005	<0.0005	<0.0005	0.001	<0.0005		0.012	<0.001	0.001
LC-006	<0.0005	<0.0005	0.001	0.012	0.11	<0.0005	<0.0005	<0.0005	0.001	0.003		0.008	<0.001	<0.0005
LC-007	<0.0005	0.24	0.004	0.056	0.11	<0.0005	<0.0005	0.001	0.002	0.004		0.016	0.001	0.002
LC-008	<0.0005	0.32	0.009	0.028	0.16	<0.0005	<0.0005	0.005	0.002	0.007		0.016	0.002	0.002
LC-016	<0.0005	0.005	0.005	0.056	0.11	<0.0005	<0.0005	0.001	0.002	0.001		0.016	0.001	0.001
LC-017														
LC-018														
LC-019														
LC-020														
LC-021														
LC-022														
LC-023	<0.0005	0.35	0.013	0.059	0.099	<0.0005	<0.0005	0.005	0.002	0.005		0.018	<0.001	0.002
LC-026	<0.0005	0.009	0.002	0.023	0.24	<0.0005	<0.0005	0.001	0.001	0.001		0.017	<0.001	0.001
LC-033	<0.0005	0.013	0.002	0.237	0.062	<0.0005	<0.0005	0.005	0.002	0.011		0.03	0.004	0.002

*Units are mg/L (ppm)

Table 4.4D	Trace Elements*													
Site ID	Pb	P04	Sb	Se	Si	Si02	Sn	Sr	Th	Ti	Tl	U	V	Zn
EB-001	<0.003			<0.01										
EB-019														
EB-131														
EB-134														
EB-135														
EB-219		0.03				21.4		0.18						0.21
EB-223	<0.0005	<0.5	<0.0005	0.001	10	22	<0.0005	0.13	<0.0005	<0.001	<0.0005	0.003	0.007	0.024
EB-293														<0.025
EB-303	<0.0005	<0.5	<0.0005	0.005	11	24	<0.0005	0.47	<0.0005	0.001	<0.0005	0.005	0.007	0.005
EB-304	<0.001		<0.005	<0.005							<0.001			0.3
EB-313	<0.0005	<0.5	<0.0005	<0.001	8.7	19	<0.0005	0.17	<0.0005	0.001	<0.0005	0.001	0.001	0.007
EB-315	<0.001	<0.5	<0.001	0.001	10	21	<0.001	0.21	<0.001	0.001	<0.001	0.002	0.009	0.01
EB-319														
EB-323		0.69				34.2								
EB-328	<0.001	<0.5	<0.001	0.002	10	21	<0.001	0.27	<0.001	<0.001	<0.001	0.004	0.021	0.008
EB-329	<0.001	<0.5	<0.001	<0.001	9	20	<0.001	0.16	<0.001	0.001	<0.001	0.002	0.006	0.021
EB-332	<0.0005	<0.5	<0.0005	<0.001	12	25	<0.0005	0.23	<0.0005	0.002	<0.0005	0.002	0.013	0.003
EB-336	<0.001	<0.5	<0.001	0.002	9.1	20	<0.001	0.049	<0.001	0.002	<0.001	0.013	0.045	0.003
EB-337	<0.001	<0.5	<0.001	<0.001	10	21	<0.001	0.2	<0.001	0.001	<0.001	0.005	0.019	0.008
EB-338	<0.001	<0.5	<0.001	<0.001	10	21	<0.001	0.083	<0.001	0.001	<0.001	<0.001	0.004	0.001
EB-339	<0.001			<0.01										<0.1
EB-363						21.4								
EB-364	<0.0005	<0.5	<0.0005	<0.001	11	23	<0.0005	0.13	<0.0005	0.001	<0.0005	0.001	0.006	0.005
EB-366	<0.0005	<0.5	<0.0005	<0.001	9.7	21	<0.0005	0.14	<0.0005	0.001	<0.0005	0.001	0.003	0.004
EB-370														
EB-373	<0.0005	<0.5	<0.0005	<0.001	9	19	<0.0005	0.15	<0.0005	0.001	<0.0005	0.003	0.005	0.002
EB-383														
EB-391	<0.0005		<0.005	<0.005							<0.0005			<0.02
EB-459		0.01				19								
EB-569			<0.0004	0.001										
EB-579	<0.001		<0.001	<0.001							<0.001			0.02
EB-595	<0.001	<0.5	<0.001	<0.001	6.3	14	<0.001	0.11	<0.001	0.002	<0.001	0.004	0.002	0.001
EB-607	<0.0002	<0.01	<0.05	<0.001	11.9	25.4	<0.05	0.16	<0.05	<0.002	<0.001	0.002	0.009	<0.001
EB-624														
LC-001	<0.0005	<0.5	<0.0005	0.001	11	23	<0.0005	0.23	<0.0005	0.005	<0.0005	0.004	0.014	0.003
LC-003	<0.0005	<0.5	<0.0005	0.002	11	24	<0.0005	0.48	<0.0005	0.001	<0.0005	0.004	0.012	0.016
LC-005	<0.0005	<0.5	<0.0005	0.001	11	23	<0.0005	0.27	<0.0005	<0.001	<0.0005	0.003	0.008	0.003
LC-006	<0.0005	<0.5	<0.0005	<0.001	12	26	<0.0005	0.24	<0.0005	0.002	<0.0005	0.001	0.004	0.029
LC-007	<0.0005	<0.5	<0.0005	0.002	12	25	<0.0005	0.26	<0.0005	0.019	<0.0005	0.009	0.009	0.013
LC-008	<0.0005	<0.5	<0.0005	0.001	13	27	<0.0005	0.34	<0.0005	0.014	<0.0005	0.01	0.022	0.009
LC-016	<0.0005	<0.5	<0.0005	<0.001	11	25	<0.0005	0.16	<0.0005	0.001	<0.0005	0.004	0.009	0.004
LC-017														
LC-018														
LC-019														
LC-020														
LC-021														
LC-022														
LC-023	0.001	<0.5	<0.0005	0.002	11	24	<0.0005	0.14	<0.0005	0.004	<0.0005	0.004	0.016	0.016
LC-026	<0.0005	<0.5	<0.0005	0.004	13	27	<0.0005	0.39	<0.0005	0.001	<0.0005	0.002	0.008	0.005
LC-033	0.001	12.1	<0.0005	0.001	11.1	23.8	<0.0005	0.424	<0.0005	0.004	<0.0005	0.001	0.003	0.093

*Units are mg/L (ppm)

Table 4.5: Isotopic data for well, spring, and stream waters.

Site ID	Site type	Sample date	$\delta^{2}H$ (‰)	$\delta^{18}O$ (‰)	^{3}H (TU)*	$\delta^{13}C$ (‰)	^{14}C activity (pmC)	^{14}C error (pmC)	^{14}C apparent age (RCYBP)	^{14}C apparent age error (RCYBP)	Adjusted ^{14}C age (RCYBP)**	Minimum-maximum adjusted ^{14}C age (RCYBP)**
EB-223	well	10/4/2011	-80.1	-12.17	0.03	-9.9	26.13	0.16	10780	50		
EB-303	well	6/22/2011	-74.68	-10.33	0.9	-14.5	58.7	0.21	4280	30		
EB-313	well	6/22/2011	-86.54	-12.06	0.01	-10.1	40.6	0.2	7240	40		
EB-315	well	5/11/2005	-83.4	-12.01								
EB-328	well	6/7/2005	-94.12	-12.89								
EB-332	well	7/21/2011	-79.98	-11.53	0.04	-10.6	43.37	0.21	6710	40		
EB-336	well	4/8/2005	-103.58	-14.27		-5.53			36,800**		35,400**	29,900-37,300**
EB-337	well	4/8/2005	-113.33	-15.65		-8.16			38,400**		33,700**	32,800-39,000**
EB-338	well	4/9/2005	-83.23	-12.34	<0.02	-11.6			5,300**		1,800**	400-4,700**
EB-364	well	10/20/2011	-77.13	-11.66	-0.01	-14.1	47.03	0.23	6060	40		
EB-366	well	10/20/2011	-78.14	-11.72								
EB-373	well	10/20/2011	-77.53	-11.75	-0.05	-13.2	34.03	0.17	8660	40		
EB-607	well	9/26/2006	-81.18	-11.49								
LC-001	spring	6/1/2011	-80.98	-11.41	0.04	-11.2	49.06	0.18	5720	30		
LC-003	spring	6/1/2011	-80.52	-11.24	0.42	-11.6	65.41	0.24	3410	30		
LC-005	spring	6/1/2011	-80.7	-11.37	0.11	-16.1	65.57	0.24	3390	30		
LC-006	well	6/21/2011	-79.47	-11.1	1.73	-10.6	82.45	0.3	1550	30		
LC-007	spring	6/22/2011	-84.83	-11.89								
LC-008	spring	6/22/2011	-79.36	-11.13	0.41	-14.2	73.44	0.27	2480	30		
LC-016	spring	6/22/2011	-84.93	-11.89	0.05	-12.1	50.93	0.19	5420	30		
LC-017	spring	3/25/2011	-79.43	-10.87								
LC-018	spring	3/25/2011	-81.36	-11.27								
LC-019	spring	3/25/2011	-80.77	-11.15								
LC-020	spring	3/25/2011	-80.77	-11.07								
LC-021	spring	3/25/2011	-80.26	-11.11								
LC-022	spring	3/25/2011	-77.49	-10.43								
LC-023	spring	7/20/2011	-83.47	-11.62	0.13	-12.6	54.61	0.2	4860	30		
LC-026	well	10/4/2011	-77.36	-11.6								
LC-033	effluent	8/30/2012	-86.53	-12.12								

* Standard analytical error for ^{3}H in all samples is 0.09 TU

pmC = percent modern carbon

RCYBP = radiocarbon years before present (1950), Cambridge half-life 5,730 +/-40 yr

** Manning (2009), ages calculated using Libby half-life, 5568 +/-30 yr

Table 4.6: CFC data and recharge ages.

			Water Concentration Corrected for Stripping Efficiency				Equivalent Atmospheric Concentration				CFC-Derived Recharge Age in years before sampling date			
			SF6	CFC12	CFC11	CFC113	SF6	CFC12	CFC11	CFC113	SF6	CFC12	CFC11	CFC113
Site ID	Lab ID	Date	pmol/Kg	pmol/Kg	pmol/Kg	pmol/Kg	pmol/mol	pmol/mol	pmol/mol	pmol/mol				
EB-223	108.01	10/4/2011	0.002	2.295	2.830	0.220	6.7	573.1	184.5	46.8	3	Supersaturated	30	26
EB-223	0108.01D	10/4/2011	0.002	2.436	2.988	0.243	8.2	608.4	194.8	51.6	Supersaturated	Supersaturated	29	25
EB-223	0108.01D2	10/4/2011	0.002	2.395	3.003	0.242	5.6	598.1	195.8	51.4	7	Supersaturated	29	25
EB-303	108.03	6/22/2011	0.010	208.845	48.345	2.214	32.6	52154.8	3152.0	470.2	Supersaturated	Supersaturated	Supersaturated	Supersaturated
EB-303	0108.03D	6/22/2011	0.007	241.219	50.619	2.335	23.3	60239.6	3300.3	495.9	Supersaturated	Supersaturated	Supersaturated	Supersaturated
EB-303	0108.03D2	6/22/2011	0.007	239.816	50.594	2.304	22.4	59889.4	3298.7	489.3	Supersaturated	Supersaturated	Supersaturated	Supersaturated
EB-313	108.02	6/22/2011	0.002	8.919	0.239	0.524	6.5	2227.4	15.6	111.2	3	Supersaturated	49	Supersaturated
EB-313	0108.02D	6/22/2011	0.004	9.039	0.310	0.584	12.7	2257.4	20.2	124.1	Supersaturated	Supersaturated	48	Supersaturated
EB-313	0108.02D2	6/22/2011	0.005	9.599	0.334	0.724	18.5	2397.2	21.8	153.8	Supersaturated	Supersaturated	48	Supersaturated
EB-332	108.04	7/21/2011	0.006	2.762	2.953	0.300	21.6	689.7	192.5	63.8	Supersaturated	Supersaturated	29	23
EB-332	0108.04D	7/21/2011	0.007	2.583	2.802	0.308	23.1	645.0	182.7	65.4	Supersaturated	Supersaturated	30	23
EB-332	0108.04D2	7/21/2011	0.007	2.637	2.645	0.305	22.4	658.5	172.5	64.8	Supersaturated	Supersaturated	32	23
EB-373	108.06	10/20/2011	0.003	26.746	14.646	2.045	10.8	6679.2	954.9	434.3	Supersaturated	Supersaturated	Supersaturated	Supersaturated
EB-373	0108.06D	10/20/2011	0.002	27.267	14.996	2.107	5.7	6809.3	977.7	447.5	7	Supersaturated	Supersaturated	Supersaturated
EB-373	0108.06D2	10/20/2011	0.003	26.975	14.957	2.116	9.0	6736.6	975.2	449.4	Supersaturated	Supersaturated	Supersaturated	Supersaturated
LC-006	108.05	6/21/2011	0.004	0.482	0.789	0.084	12.1	120.3	51.5	17.9	Supersaturated	42	42	33
LC-006	0108.05D	6/21/2011	0.004	0.776	0.967	0.106	12.7	193.7	63.1	22.5	Supersaturated	38	41	31
LC-006	0108.05D2	6/21/2011	0.004	0.496	0.796	0.036	13.0	124.0	51.9	7.6	Supersaturated	42	42	38
LC-008	108.07	6/22/2011	0.005	5.323	0.071	0.111	18.1	1329.4	4.6	23.5	Supersaturated	Supersaturated	56	31
LC-008	0108.07D	6/22/2011	0.003	4.610	0.052	0.019	10.7	1151.3	3.4	4.0	Supersaturated	Supersaturated	57	41
LC-008	0108.07D2	6/22/2011	0.005	2.879	0.123	0.011	15.4	719.0	8.0	2.3	Supersaturated	Supersaturated	53	44

Input data:
Recharge temperature: 11°C
Recharge elevation: 2100 m

"Supersaturated" means there are additional non-atmospheric sources of the CFC or SF6.

4.2 Results of Geologic and Hydrologic Studies

Geologic Setting. La Cienega lies along the southwest margin of the Española Basin (Figure 4.2), one of a series of structural basins in the Rio Grande rift. The Española Basin is bordered by the Sangre de Cristo Mountains on the east and the Jemez Mountains on the west. The thick section of sediments that fills the basin, collectively called the Santa Fe Group, was derived from erosion of surrounding highlands as the basins tectonically subsided over the past 28 million years. These sediments consist of sand, silt, clay, and gravel, and are locally interbedded with minor volcanic flows and ashes. In the Santa Fe area as well as the study area, Santa Fe Group sediments form the primary aquifers (Spiegel and Baldwin, 1963).

The Española Basin is asymmetric and takes the form of a west-tilted half-graben that is structurally bounded by major fault systems to the northwest and southwest (Biehler et al., 1999; Koning et al., *in press*). On the east, the basin boundary consists of a system of discontinuous, small-displacement faults and monoclines along the base of the Sangre de Cristo Mountains. In the study area, mapped faults are small and have low displacements (Figures 4.2 and 4.3). A more prominent fault may exist west of the WWTP (Figure 4.3). Regional faulting and rift tectonics control the geometry and shape of the basin, as well as the thickness and distribution of the Santa Fe Group sediments and their major aquifers.

The Cerrillos uplift lies southwest of the study area (Figure 4.2). This north-plunging, structural high is covered by relatively thin Santa Fe Group strata and lavas of the 2 to 3 million-year-old Cerros del Rio volcanic field. Santa Fe Group sediments thicken to the northeast of this feature, as shown by Grauch et al. (2009). Thickening is pronounced north-northeastward of a structural flexure called the Rancho Viejo hinge zone (Grauch et al., 2009), which wraps around the south end of the Española Basin (Figures 4.2 and 4.3). The hinge zone deforms the Tesuque Formation and lower Tertiary and older units. Near La Cienega and Cieneguilla, thickness of Santa Fe Group sediments ranges from zero to about 2000 ft across the Rancho Viejo hinge zone.

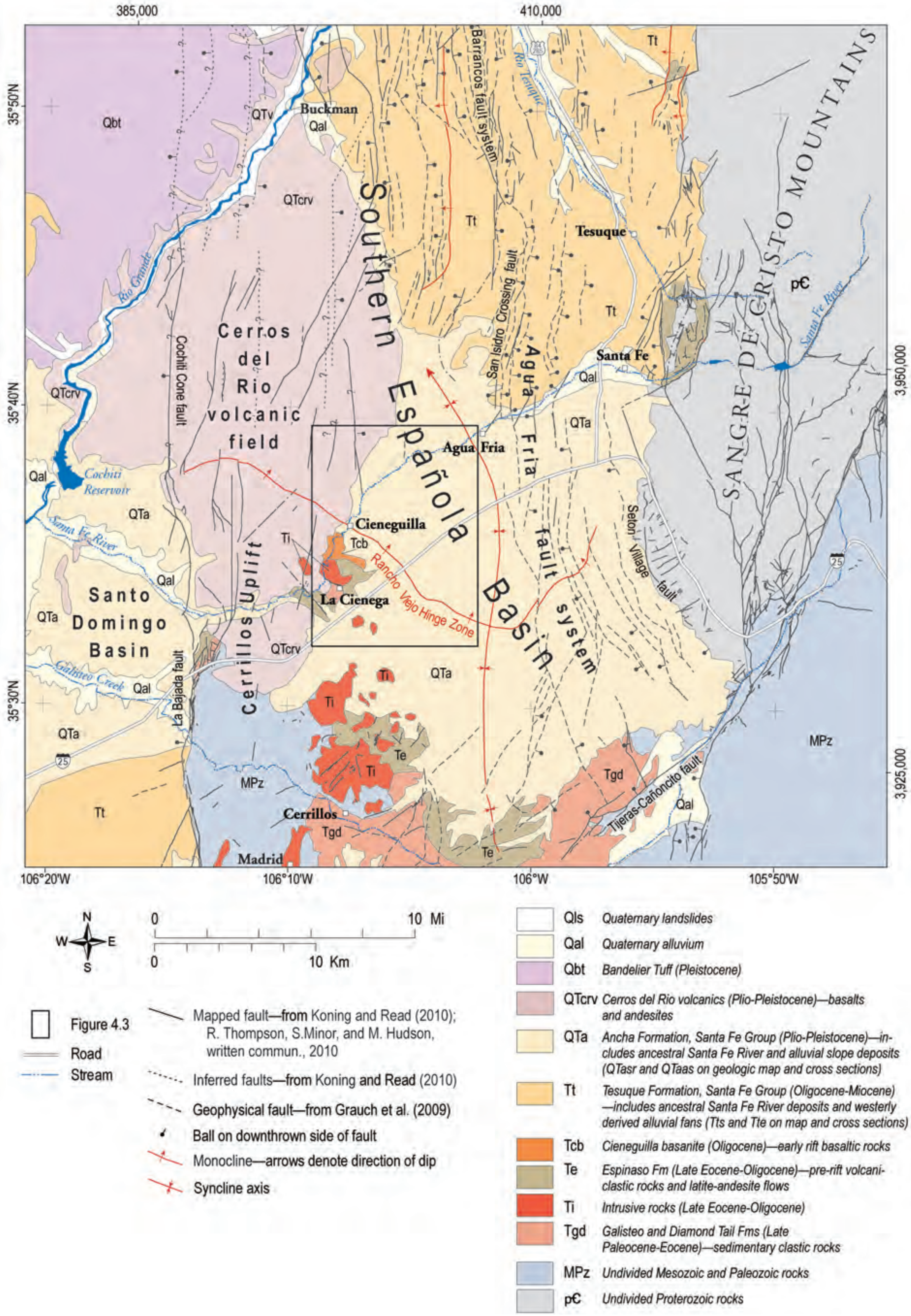

Figure 4.2: Regional geologic setting of La Cienega and Cieneguilla, southern Española Basin. Modified from Grauch et al., 2009.

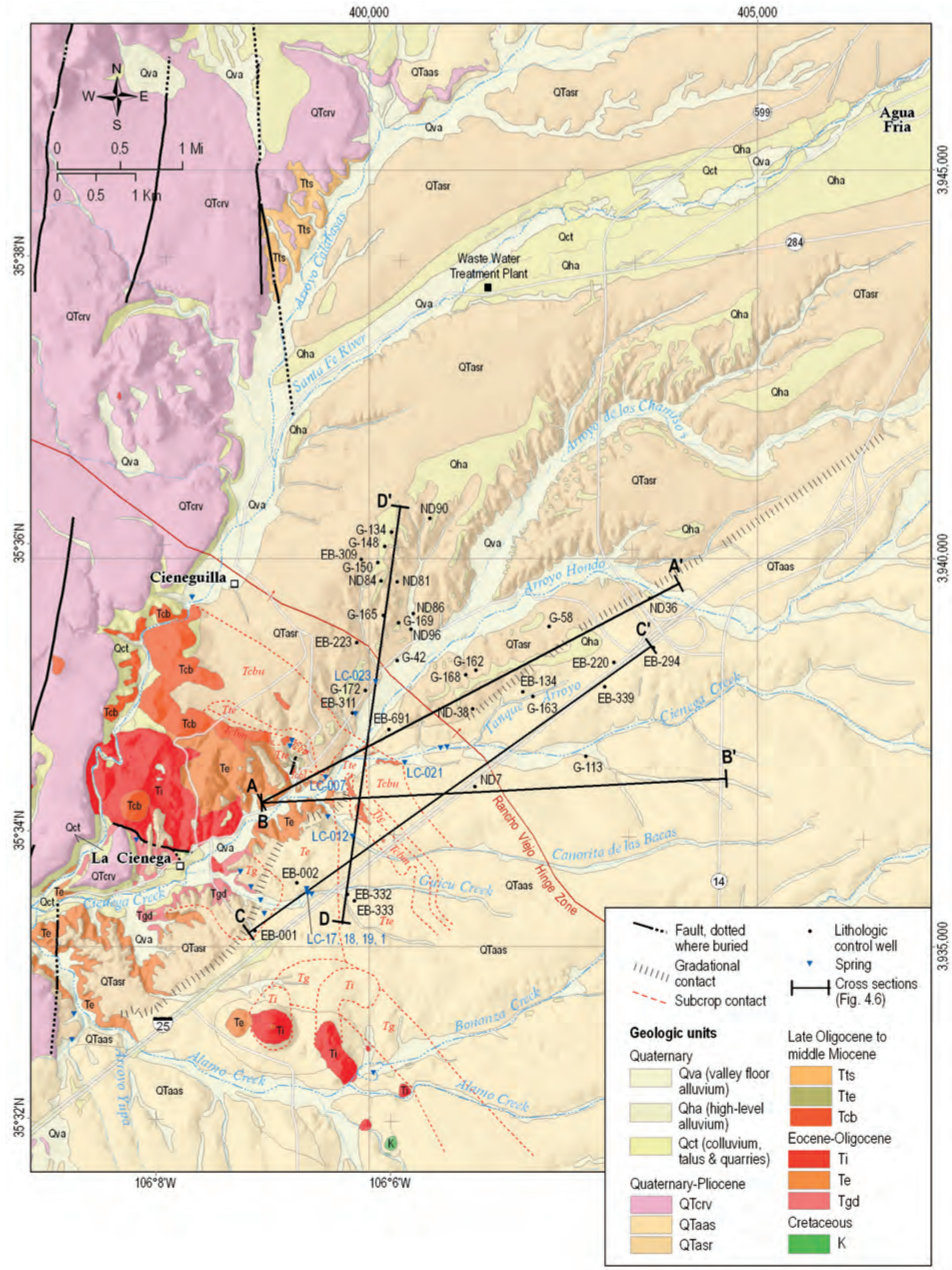

Figure 4.3: Generalized geologic map of the study area. See Figures 4.4 and 4.6 for the stratigraphic context of subsurface units.

Geologic History. For the last 30 million years, tectonic forces have slowly torn the North American continent apart along the Rio Grande rift. The Earth's crust has been uplifted, stretched, broken, and invaded by magma, and the rift's basins have filled with sediments and volcanic rocks. The geologic features now found within the complex, rift-margin setting of La Cienega shape the region's aquifers, and control how and where groundwater moves and where springs and wetlands are located. The genesis of the various rock formations that control modern hydrogeology in the La Cienega area is briefly summarized below (Figures 4.4 and 4.5).

Pre-rift volcanic activity between 36 and 28 million years ago created volcanic edifices between La Cienega and Madrid to the southeast and emplaced igneous intrusions beneath and near the volcanoes. Erosion of these volcanic highlands produced the grayish, volcanic sediment deposits of the Espinaso Formation in adjacent lowlands to the north, including in and around La Cienega.

Initiation of rifting around 26-28 million years ago was accompanied by basaltic volcanism, tectonic subsidence, and filling of the Española Basin with thick sequences of sediment and minor volcanic flows now referred to as the Santa Fe Group. Near La Cienega, volcanism was dominated by low-silica magmas called the Cieneguilla basanite. Between basanite eruptions, tectonic tilting and uplift to the west caused erosion of the Espinaso Formation from the Cerrillos uplift. Northeast-flowing streams transported sediment derived from the Espinaso Formation and Cieneguilla basanites and deposited it on alluvial fans near La Cienega (Figure 4.5; Koning and Johnson, 2006; Koning and Read, 2010). This sediment, called lithosome E of the Tesuque Formation, interfingers with lithosome S of the Tesuque Formation beneath La Cienega (Figures 4.4, 4.5, and 4.6; Koning and Read, 2010). Lithosome S was deposited on a west-sloping fluvial fan by an ancestral version of the Santa Fe River (Koning et al., 2004). Lithosome A was deposited on piedmonts to the north and south by smaller mountain-front drainages. Deposition of the Santa Fe Group continued until about 8 million years ago, after which erosion began. In the study area, this erosion removed Tesuque Formation strata younger than about 13 million years.

Sedimentation and volcanism resumed in the basin about 3 million years ago, beginning with deposition of the Ancha Formation (Koning et al., 2002). These coarse sediments were derived from the Sangre de Cristo Mountains and deposited on top of the Tesuque Formation by west-flowing piedmont streams (QTaas on Figures 4.3, 4.4, 4.5, and 4.6) and the ancestral Santa Fe River (QTasr). Because of tectonic tilting during the preceding 5 million years, an angular unconformity separates the Ancha Formation from the older Tesuque Formation (Spiegel and Baldwin, 1963; Koning et al., 2002). Cerros del Rio volcanism occurred over the former Cerrillos uplift from 2.7 to 1 million years ago, with most rocks being 2.7-2.2 million years old (Thompson et al., 2006). Depositionof the Ancha Formation ceased between 1.5 and 1.2 million years ago. Erosion has dominated the last 1.2 million years, episodically interrupted by brief periods of aggradation within river valleys. The last period of aggradation resulted in sand, clayey sand, and gravel filling the bottoms of modern valleys.

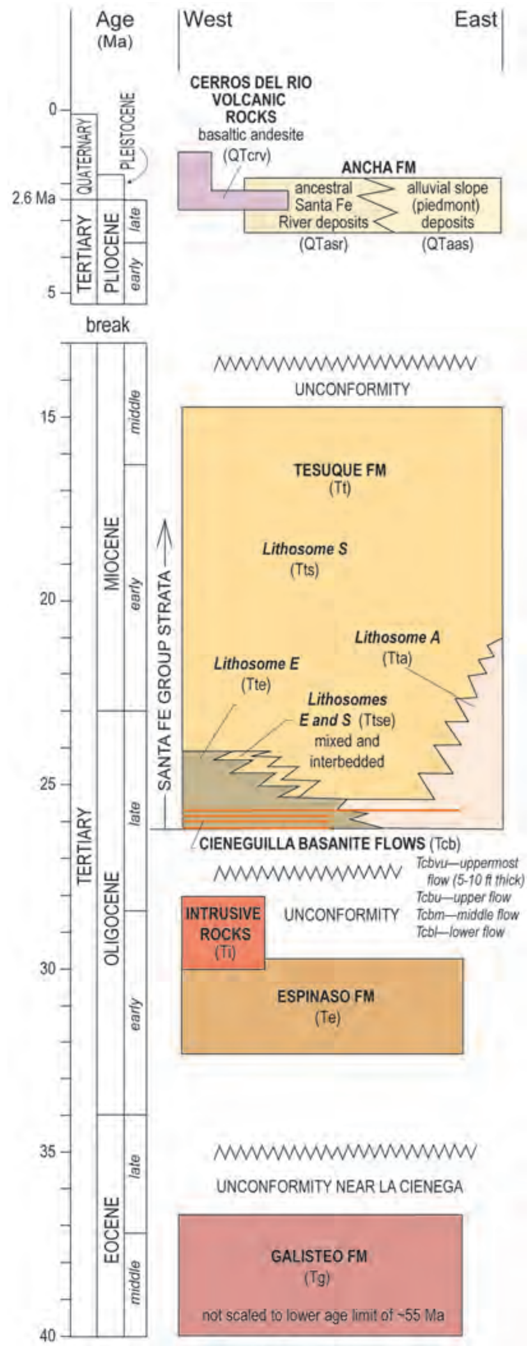

Figure 4.4: Stratigraphy of the La Cienega Area with age on the vertical axis (in millions of years [Ma]).

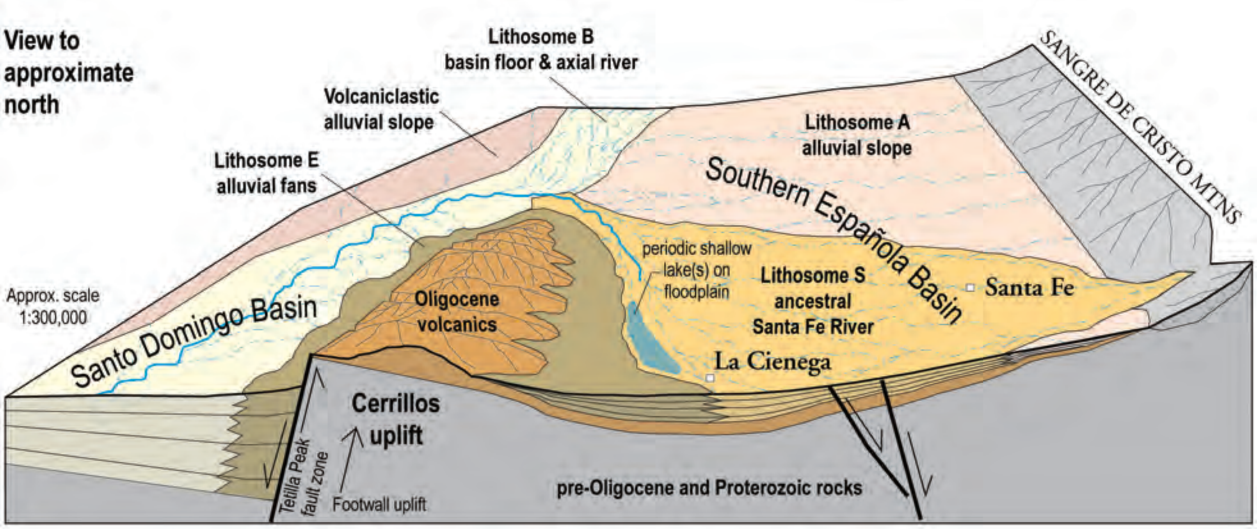

Figure 4.5: Three-dimensional conceptual block diagram illustrating stratigraphy, Tesuque Formation lithosomes, paleogeography, and depositional setting of the Española Basin 14 to 22 million years ago.

Geologic Units in the La Cienega Area and Their Hydrologic Significance. The rocks and deposits exposed in the study area consist of (from youngest to oldest): 1) surficial deposits of Quaternary age; 2) younger Tertiary volcanic rocks; 3) Ancha Formation (Pliocene to Pleistocene); 4) Tesuque Formation of the Santa Fe Group and its lithologic subdivisions (Oligocene to Miocene); and 5) bedrock strata including Cieneguilla basanite (late Oligocene), Espinaso Formation (early Oligocene) and Galisteo Formation (Eocene). These units are shown on the geologic map (Figure 4.3), the stratigraphic column (Figure 4.4), and on the series of geologic cross sections (Figure 4.6).

Surficial Deposits: Surficial sedimentary deposits (Qva, Qha, and Qct on Figure 4.3) occur throughout the study area, but most are too thin to show on the geologic map and cross sections or form significant aquifers. Some of the principal drainages contain between 5 and 50 (?) ft of alluvium consisting of sand, gravel, and silt. These young fluvial deposits are important as they form a hydraulic link between shallow groundwater in adjacent units and channel flow in streams, particularly along the perennial reaches of lower Arroyo Hondo and La Cienega Creek.

Younger Tertiary Volcanic Rocks: Pliocene to Pleistocene basalts and andesites of the Cerros del Rio volcanic field form the high plateau west of Cieneguilla and west and southwest of La Cienega (Figures 4.2 and 4.3). These basalts erupted on the surface as fluid lavas and flowed across the landscape, filling valleys and flowing around topographic obstructions. The basalts form thin, near-horizontal layers that thicken and thin over pre-eruption topography. These volcanic rocks cover both Santa Fe Group sediments and pre-rift sedimentary units, generally lie above the water table, and are unsaturated. Because they are extensively fractured by columnar joints, the basalts are porous and permeable in the vertical direction allowing recharge to underlying aquifers.

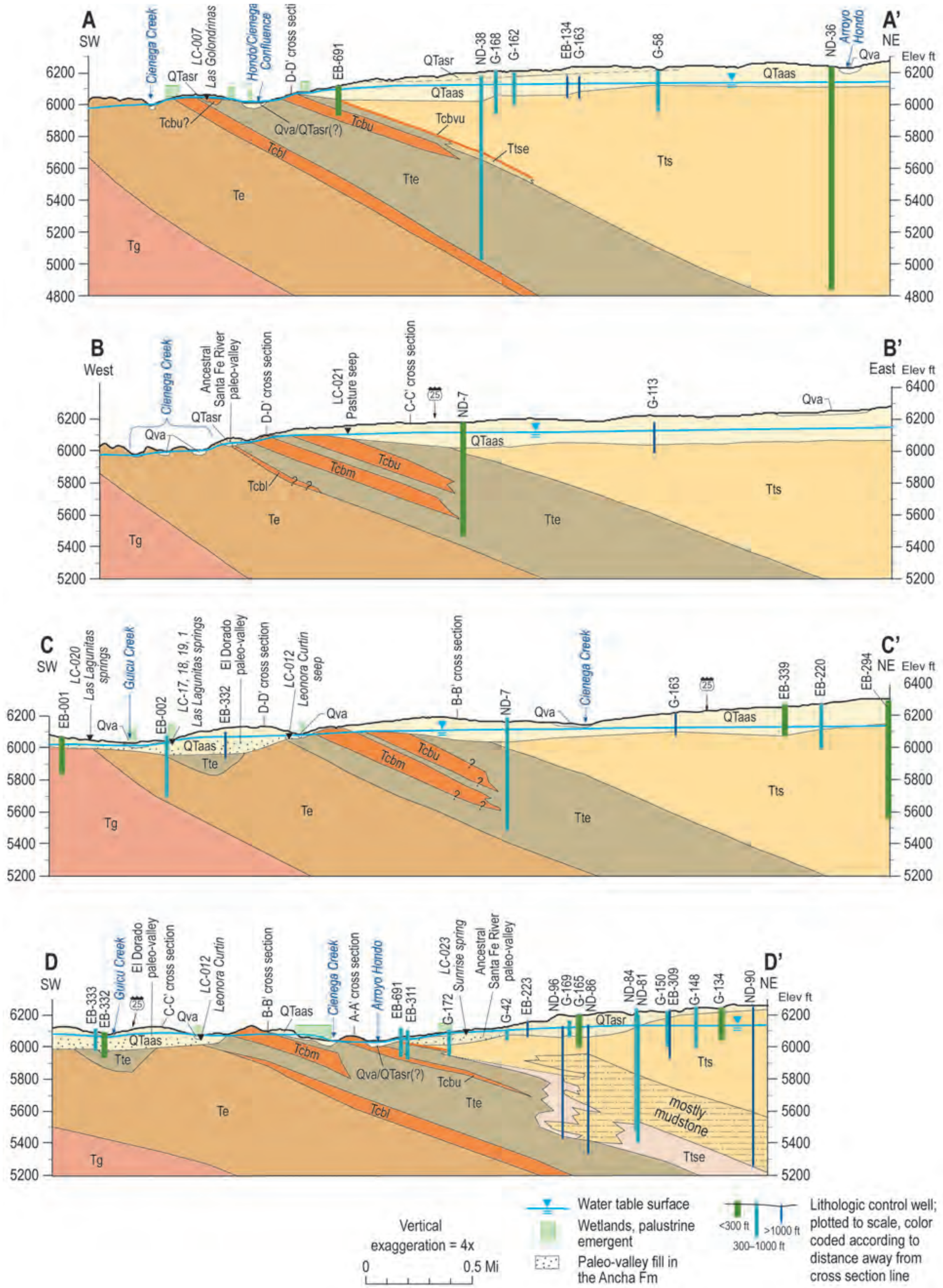

Figure 4.6: Geologic cross sections through the La Cienega Area. See Figures 4.3 and 4.4 for unit explanations.

Ancha Formation: The Pliocene to lower Pleistocene Ancha Formation is a sand, silty-clayey sand, and gravel deposit that comprises the upper portion of the Santa Fe Group basin fill and forms a locally important, shallow aquifer for the Santa Fe area. The Ancha Formation consists of two alluvial deposits: (1) sediment associated with the ancestral Santa Fe River (QTasr), and (2) alluvial slope deposits originating from the southwestern Sangre de Cristo Mountains (QTaas) (Figures 4.3 and 4.4). The ancestral Santa Fe River deposits contain abundant, laterally extensive, thick, sandy pebble-cobble channel-fills interspersed with fine-grained floodplain sediments of clayey, silty sand. In contrast, the upper alluvial slope deposits contain narrow, ribbon-like channel-fills interbedded in clayey-silty sand. Lower alluvial slope deposits are coarse grained, often containing cobbles and boulders, and locally are quite thick (up to 120 ft). In general, Ancha sediments are coarser, less consolidated, and more permeable than underlying strata, including Tesuque Formation basin fill. The base of the Ancha Formation coincides with a late Miocene to early Pliocene erosion surface that has truncated, tilted, and faulted beds of the underlying Tesuque, Espinaso, and Galisteo Formations (Figure 4.6).

Previous work has proposed that storage of groundwater and saturation of the Ancha Formation in the Santa Fe Group aquifer is controlled by three factors: (1) permeability contrasts between the Ancha and pre-Ancha formations; (2) the topography of the erosion surface at the base of the formation; and (3) sources of recharge or inflow to the formation (Spiegel and Baldwin, 1963; Johnson et al., 2008). Because of its importance as a shallow, productive zone in the upper Santa Fe Group aquifer, the Ancha Formation has recently been a focus of new studies in the Española Basin to address these hypotheses. A series of maps that depict the structural base, thickness, and extent of saturation for the Ancha Formation have been produced (Johnson and Koning, 2012) and are presented here for the La Cienega Area (Figures 4.7, 4.8, and 4.9). The characteristics of the formation's base, thickness, grain size, and permeability are significant to the understanding of how groundwater accumulates in, and flows through, the formation. Accordingly, these data are also important to our understanding of the source of water discharging from the Ancha Formation to springs and wetlands in La Cienega.

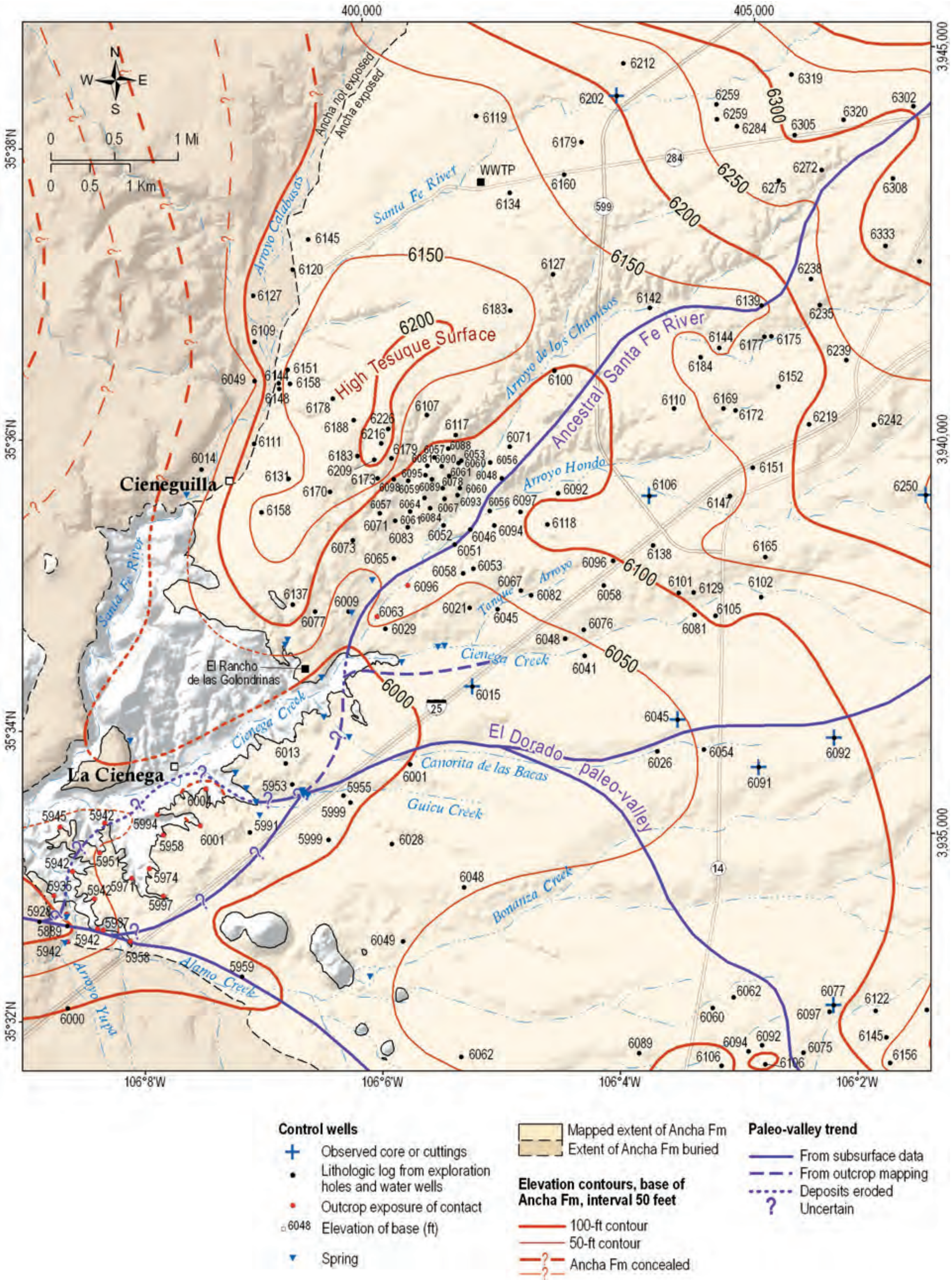

Figure 4.7: Elevation contour map of the base of the Ancha Formation near La Cienega showing paleo-topography of the pre-Ancha erosion surface (modified from Johnson and Koning, 2012).

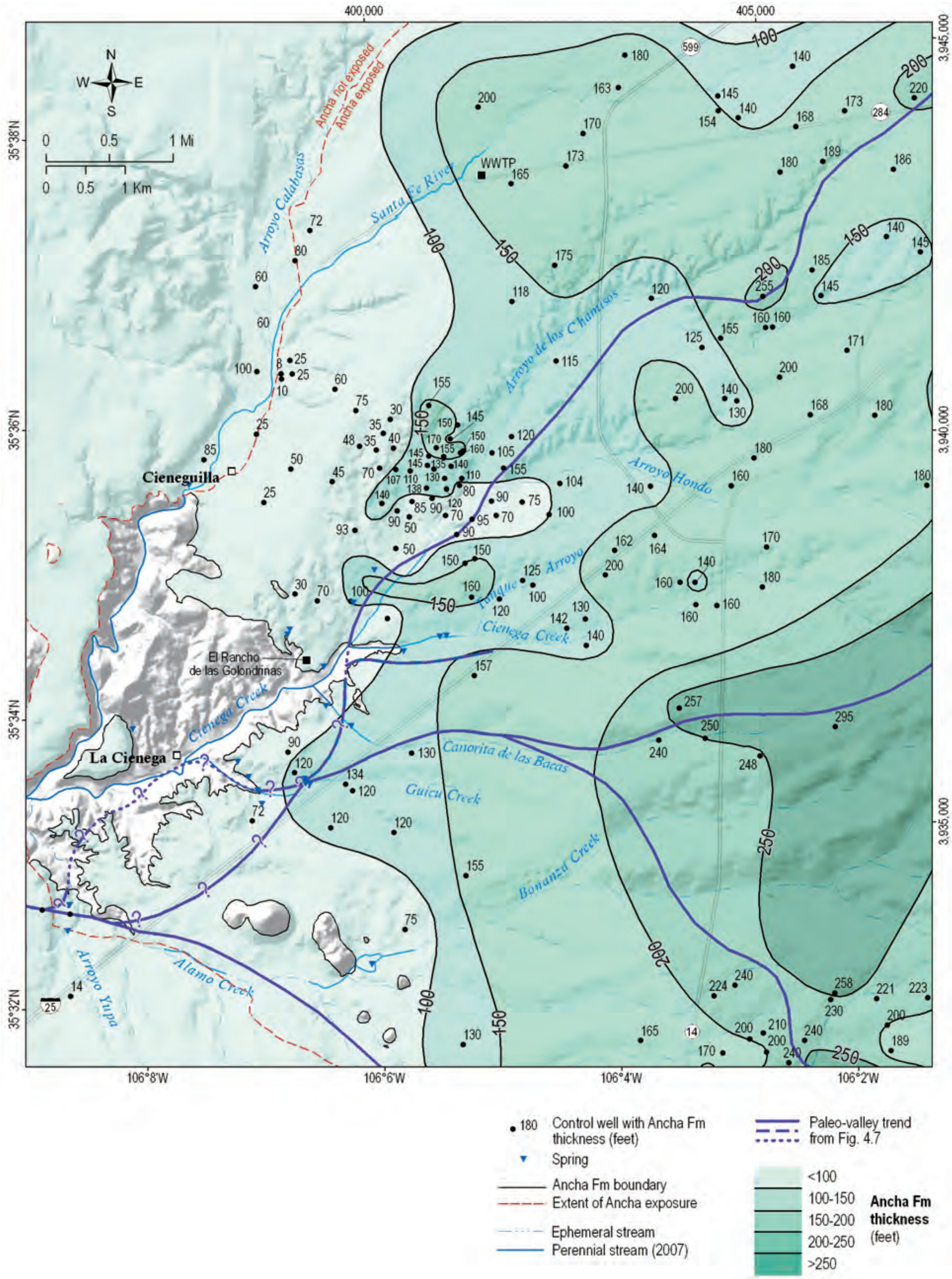

Figure 4.8: Isopach map showing thickness (in feet) of the Ancha Formation (modified from Johnson and Koning, 2012).

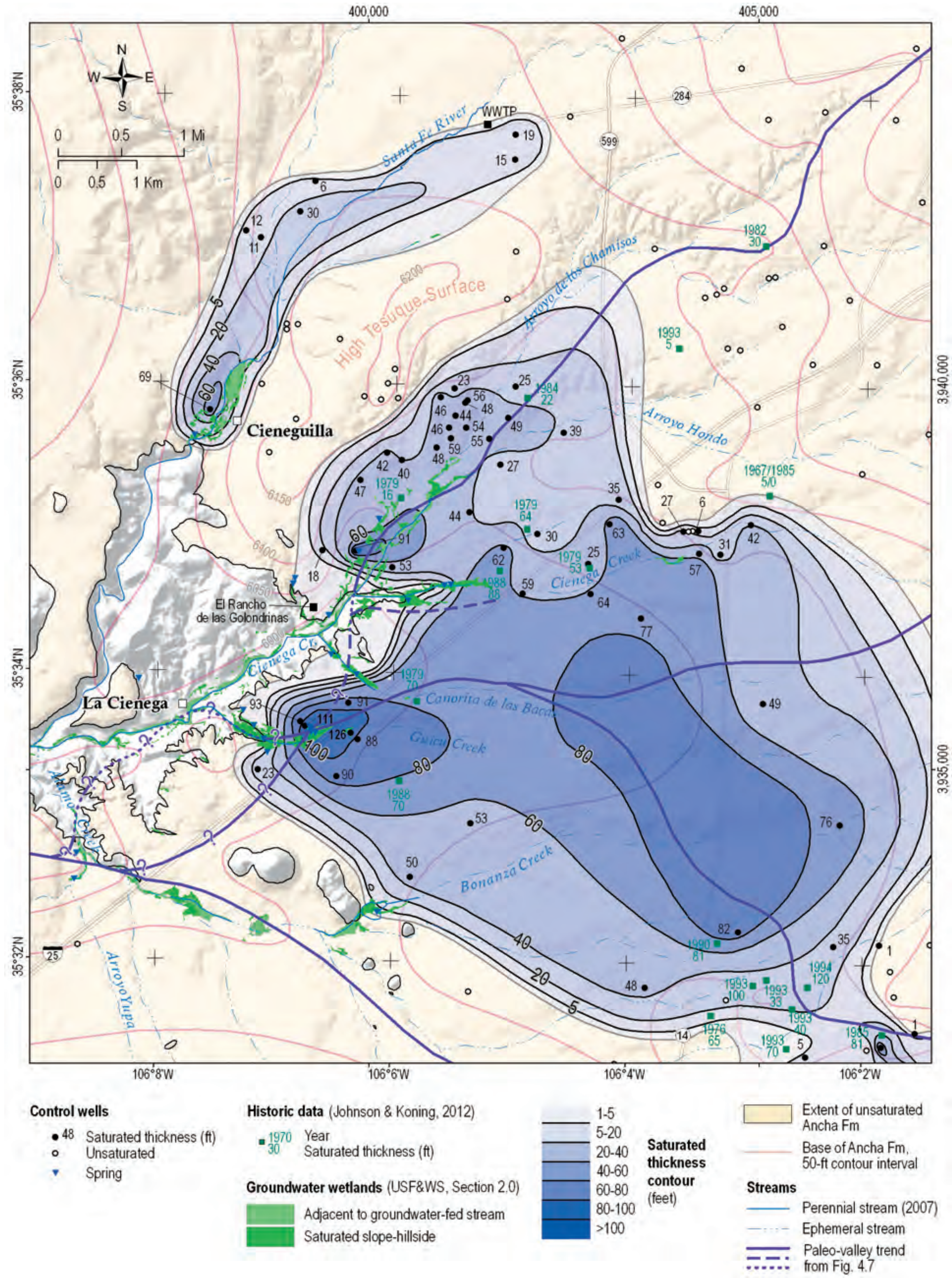

Figure 4.9: Saturated thickness (in feet) of the Ancha Formation (modified from Johnson and Koning, 2012).

A significant finding derived from mapping the base of the Ancha Formation is the delineation of paleo-valleys on the pre-Ancha erosion surface. The existence of paleo-valleys at the base of the Ancha Formation and their influence over locations of springs and wetlands has been previously studied by Spiegel (1971) and HydroScience Associates, Inc. (2004). The elevation contour map of the base of the formation (Figure 4.7) is essentially a topographic map of the pre-Ancha landscape at the time Ancha deposition began. Thus, the map illustrates general locations of valleys, ridges, and hills in the ancient, pre-Ancha land surface. From the map (Figure 4.7) two regional paleo-drainages were defined, which are believed to merge east of La Cienega (Johnson and Koning, 2012). One paleo-drainage (informally named the El Dorado paleo-valley in this report) starts in the southern Sangre de Cristo Mountains near El Dorado and enters the La Cienega Area from the east (see also Figure 4.6, cross sections C-C′ and D-D′). The second paleo-drainage – probably associated with the ancestral Santa Fe River – enters from the northeast and generally aligns with the present-day course of Arroyo Hondo and Arroyo de los Chamisos (Figure 4.6, cross section D-D′). Based on field geologic mapping, we interpret that the ancestral Santa Fe River drainage crossed present-day Cienega Creek – as demonstrated by outcropping of Santa Fe River facies (QTasr) on the east side of Cienega Creek, north of Canorita de las Bacas (Figure 4.3) – and converged with the El Dorado paleo-drainage east of the village of La Cienega (Figure 4.6, cross sections B-B′ and D-D′ Figure 4.7). The outlet of the two ancestral river systems appears to have been through the present-day location of Guicu Creek. A small, Ancha-filled paleo-valley, located east of El Rancho de las Golondrinas and parallel to Cienega Creek, was also noted during geologic mapping (Figure 4.7 and Figure 4.6, cross section D-D′). Additional Ancha-filled paleo-valleys likely exist in the study area, but would probably be of limited extent and are beyond the resolution of the current subsurface dataset.

The pre-Ancha surface (Figure 4.7) also defines a north-northeast trending paleo-topographic high on the surface of the Tesuque Formation, situated between Cieneguilla and Arroyo Hondo. The Tesuque Formation at this location consists of interbedded clay to fine sand floodplain deposits and sandy channel deposits associated with the ancestral Santa Fe River of early to mid-Miocene time. This high Tesuque surface was elevated about 150 ft above the ancestral Santa Fe River, which entered La Cienega from the northeast during late Pliocene and early Pleistocene.

In general, the lower part of the Ancha Formation contains abundant coarse sand and gravel, particularly in the eastern half of the study area. Lithologic logs from wells completed in the El Dorado paleo-valley east of La Cienega indicate the presence of cobble- and boulder-sized materials and suggest that paleo-valley deposits may be even coarser. The El Dorado paleo-valley fill is also slightly thicker, as illustrated by the Ancha Formation isopach map (Figure 4.8). Within the study area, thickness of Ancha deposits varies from over 250 ft in the El Dorado paleo-valley to less than 50 ft over the high Tesuque surface east of Cieneguilla. Geologic mapping of surface exposures near El Rancho de las Golondrinas also indicated that paleo-valley fill was locally thicker than 50 ft.

The extent and thickness of saturation zones within the Ancha Formation and the spatial relation to springs, wetlands, and mapped paleo-valleys are shown in Figure 4.9. Saturated-thickness contours were constructed from point data of water-levels and saturated thicknesses measured in Ancha wells and encompass groundwater-fed springs and wetlands emerging from Ancha Formation sediments (See Section 2.0: Wetlands). Figure 4.10 shows the distribution of pre-Ancha geologic formations, together with the 80- and 100-foot saturation contours from Figure 4.9. Figure 4-11 is a plot showing the range of hydraulic conductivity values estimated from aquifer tests for the Ancha Formation and underlying geologic units (Section 6.5 Appendix E, Johnson and Koning, 2012). The figure shows that Ancha deposits have relatively high conductivities, ranging from 4 to 252 ft/d, with a mean of 45 ft/d. These values are generally larger than for underlying strata in the Tesuque and Espinaso Formations.

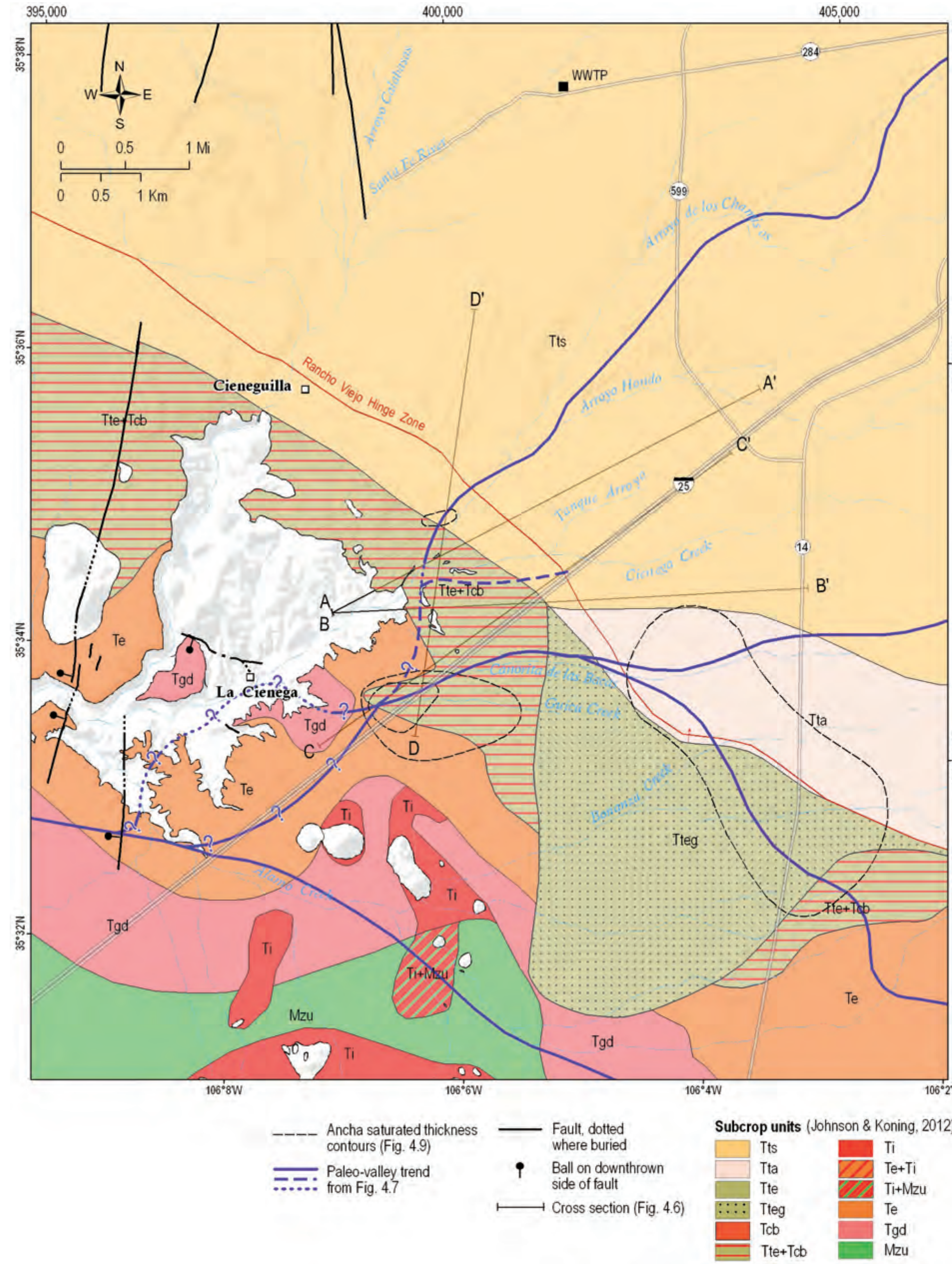

Figure 4.10: Subcrop geologic map showing distribution of strata underlying the Ancha Formation. Contours depict the 80- and 100-ft zones of saturation in the overlying Ancha Formation (Fig. 4.9). Tteg — Lithosome E (Tte) derived from Cerrillos Hills; Mzu — undivided Mesozoic strata; Tgd — Galisteo and Diamond Tail Formations.

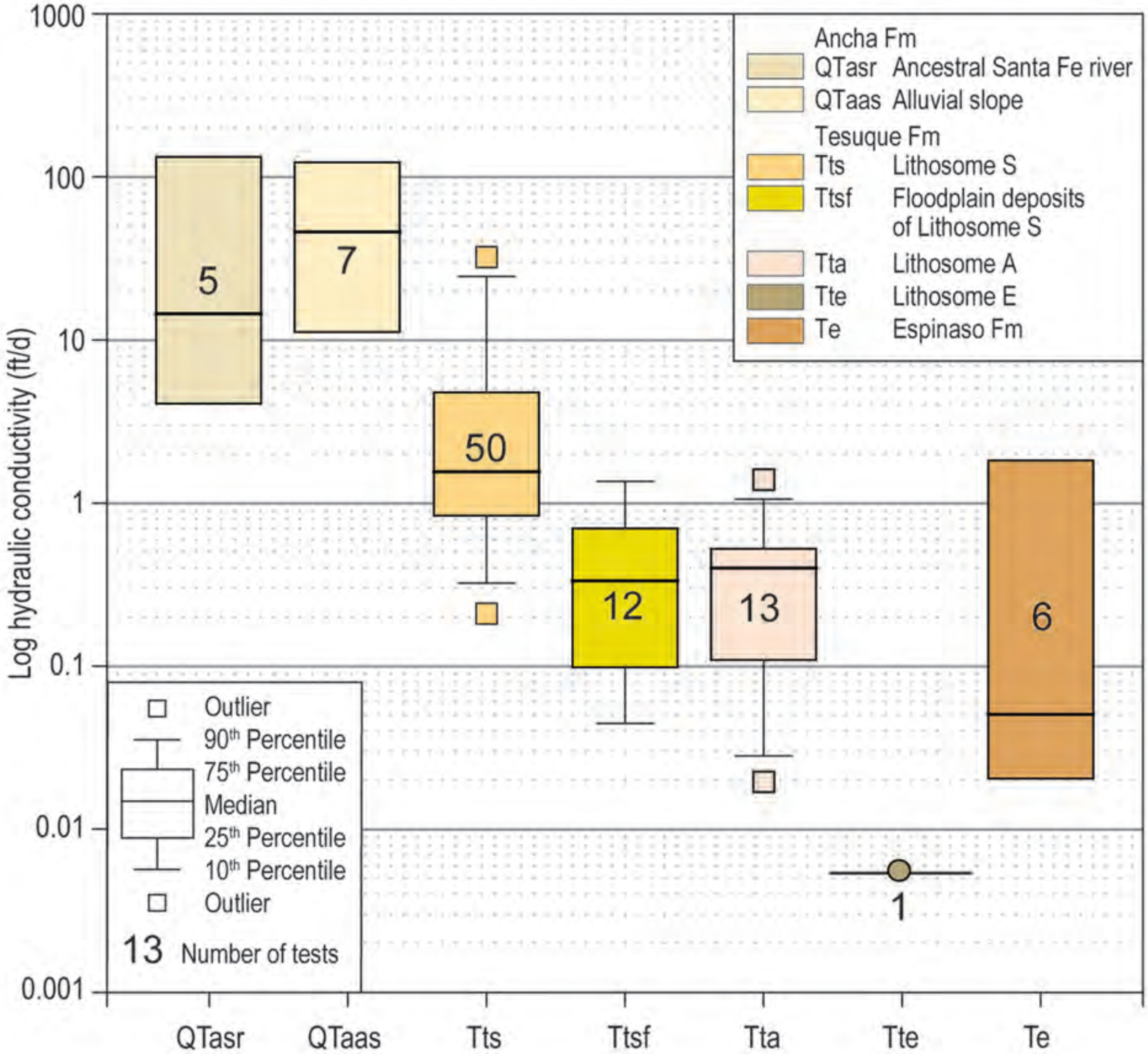

Figure 4.11: Percentile plot of hydraulic conductivity (ft/d) by geologic unit. Values of hydraulic conductivity are estimated from aquifer tests summarized in Section 6.5, Appendix E.

These figures convincingly demonstrate that:

1. The thickest zones of saturation in the Ancha Formation occur east of La Cienega and correlate directly with areas of paleo-valley fill that overlie lower permeability geologic units (Figures 4.9 and 4.10).
2. Springs that sustain wetlands discharge primarily from saturated Ancha Formation either at a contact with underlying strata (north slope of Guicu Creek for example) or in incised drainages (as in Cienega Creek and Arroyo Hondo above Cienega Creek) (Figure 4.9).
3. The thick zone of saturated Ancha Formation extending east from lower Guicu Creek sustains the extensive wetlands at Las Lagunitas (Figure 4.9), is associated with channel fill in the El Dorado paleo-valley (Figure 4.7), and is underlain by relatively low permeability geologic units of the Tesuque Formation (Tta, Tte), the Cieneguilla basanite (Tcb), and the Espinaso Formation (Te) (Figure 4.10).
4. Springs and wetlands along the Santa Fe River, at and upstream of Cieneguilla, discharge from saturated Ancha Formation beneath the river. This Ancha saturation zone is disconnected from those near La Cienega, apparently interrupted by the high Tesuque surface (Figures 4.7 and 4.9).

Tesuque Formation: In the Santa Fe area, the Tesuque Formation (upper Oligocene to upper Miocene) forms the bulk of the Santa Fe Group basin fill. The formation consists of silty-clayey sandstone and sandstone, with minor conglomerate, siltstone and claystone (Spiegel and Baldwin, 1963; Koning et al. 2007), and has been subdivided into interfingering map units called lithosomes (Koning and Read, 2010) that correspond to deposits from different regional paleo-drainage systems. In the La Cienega Area, there are three significant lithosomes with unique hydrologic properties (Figures 4.3 through 4.6 and 4.10). Lithosome S (Tts), deposited by a west-flowing, ancestral Santa Fe River (Koning et al., 2004; Koning and Read, 2010), is a coarse, pebbly sand that becomes increasingly finer-grained away from the mountain front. In the study area, it is composed of reddish sand and pebbly sand channel-fills that are interbedded with clay, silt-clay, and very fine, sandy floodplain deposits. The floodplain deposits increase to the west and can often act as aquitards, locally creating confined aquifer conditions. Lithosome A (Tta) is alluvial slope sediment originating from the Sangre de Cristo Mountains. It is composed of fine sand and clayey-silty sand interspersed with sparse, coarse-grained channel fills. The deposit is present beneath the Ancha Formation in the southeast corner of the study area, and grades laterally into lithosome S to the northwest (Figure 4.10). Lithosome E (Tte) consists of clayey-silty sand and gravel derived from volcanic rocks of the Cieneguilla basanite and Espinaso Formation. The Tesuque Formation generally overlies these volcanic rocks (Koning and Read, 2010; Myer and Smith, 2006), but lithosome E interfingers with the Cieneguilla basanite in the subsurface (Figures 4.4 and 4.6). The contact between the Tesuque and the Espinaso Formations is unconformable (Figure 4.4).

Pump test data indicate that both lithosomes A and E have significantly lower hydraulic conductivities than the Ancha Formation (Figure 4.11). The coarse river deposits of lithosome S (Tts) have hydraulic conductivities comparable to the lower ranges of Ancha Formation, but the fine floodplain deposits (Ttsf) are significantly less permeable.

Bedrock Strata: Cieneguilla Basanite, Espinaso Formation and Galisteo Formation: The Cieneguilla basanite is a dark gray basalt. The various flows of this unit followed paleo-topography and are laterally discontinuous. Near the intersection of La Cienega and Arroyo Hondo, four Cieneguilla basanite flows were identified. Only two of these flows appear to extend more than 1 km to the south. Buttress-style contacts of the lowest Cieneguilla basanite flow (Tcbl) against the older Espinaso Formation near El Rancho de las Golondrinas indicate that the flow filled an east-trending paleo-valley. Higher flows (Tcbm, Tcbu, and Tcbvu in Figure 4.6) are more laterally extensive. Near La Cienega, the Espinaso Formation mostly consists of well-cemented alluvial deposits of volcanic-derived conglomerates and sandstones. Eocene alluvial sediments of the Galisteo Formation consist of sandstone and pebbly sandstone channel fills interbedded with clayey mudstone deposits. As a whole, the pre-Santa Fe Group strata are much less permeable than either the Ancha or upper Tesuque Formations, largely due to their strong cementation.

Geologic Control of Groundwater Flow and Discharge to Springs and Wetlands: The La Cienega area is situated at the edge of the Española Basin where the Santa Fe Group aquifer becomes thin and pinches out over underlying strata that have a lower hydraulic conductivity. The Ancha Formation forms the upper and most permeable portion of Santa Fe Group aquifer. The lower 50 to 100 ft of alluvial slope deposits in the Ancha Formation (QTaas) are generally coarse grained and contain paleo-valley deposits with boulder, cobble and coarse sand channel fills. These coarse deposits store groundwater originating from both surface recharge and groundwater inflow from adjoining Tesuque Formation strata. The regional hydraulic gradient drives groundwater flow west and southwest toward the lowest elevation outlets at La Cienega. Groundwater preferentially moves through the coarsest deposits, including paleo-valley fill in the Ancha Formation. Thinning of the aquifer forces groundwater to the surface where it emerges from the Ancha Formation in numerous seeps and springs along the modern valleys of Cienega Creek, Guicu Creek and Arroyo Hondo.

The Santa Fe Group Aquifer. Regional Groundwater Conditions: Groundwater flow in the Santa Fe Group aquifer, which consists of basin fill sediments of the Tesuque and Ancha Formations, has been discussed generally by Spiegel and Baldwin (1963), Mourant (1980), McAda and Wasiolek (1988), and Johnson et al. *(in press)*. Under natural conditions, groundwater moves along flow paths from areas of recharge to areas of discharge at springs, streams, ponds, and wetlands. Historic water-level maps for the Española Basin (Spiegel and Baldwin, 1963; Mourant, 1980; Johnson, 2009) have shown that groundwater flows westward through Santa Fe Group sediments from the mountains on the east towards discharge areas on the west side of the basin (Figure 4.12). Depth to groundwater in the Santa Fe Group aquifer system varies from less than 20 ft to more than 500 ft. Shallow groundwater occurs in the discharge areas along the Santa Fe River below Cieneguilla, in lower Cienega and Guicu Creeks, and Bonanza Creek. Geochemical characterization and flow-path modeling north of the Santa Fe River by Johnson et al. *(in press)* demonstrates that the western portion of the basin, west of Agua Fria, is a discharge zone for the regional aquifer, which is characterized by upward movement of warm, sodium-rich groundwater from deep circulation pathways in the Tesuque Formation.

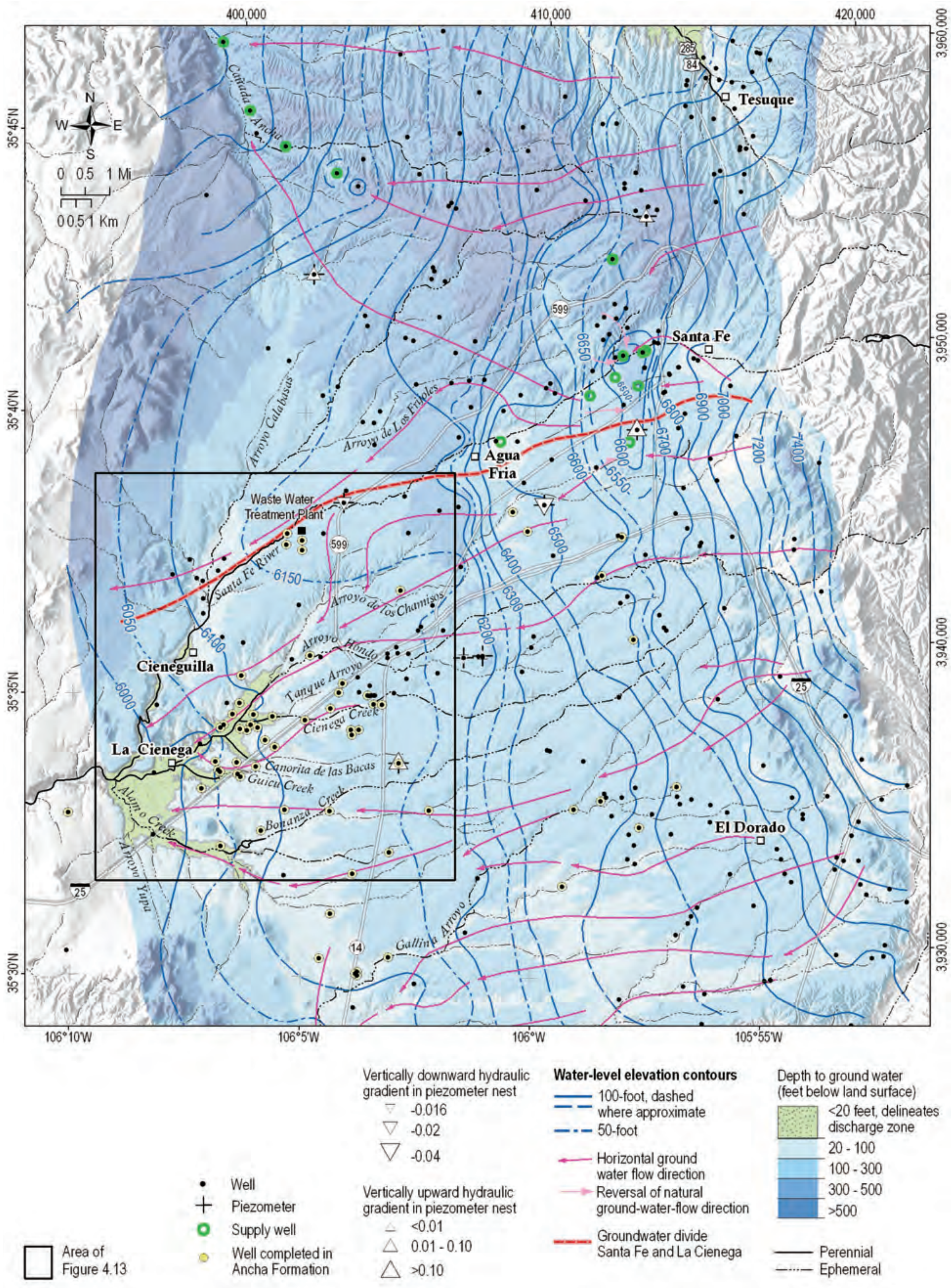

Figure 4.12: Regional groundwater flow conditions for 2000 to 2005, in the Santa Fe area (Johnson, 2009).

Early work by Spiegel and Baldwin (1963) also defined three groundwater units in the Santa Fe area —a northern unit, the Cienega unit, and a southern unit—and hypothesized that groundwater in each unit contributes, respectively, to discharge areas along the Rio Grande, the Santa Fe River, and Galisteo Creek. The 2000-2005 regional map (Johnson, 2009) also estimated flow-line boundaries separating the Cienega unit and its discharge to the Santa Fe River, from the Rio Grande unit to the north (Figure 4.12). The objective behind defining such groundwater units has been to evaluate recharge zones and flow paths in the Santa Fe Group aquifer that discharge groundwater to streams, springs and wetlands. In the La Cienega Area, the boundaries of these units are generally not defined by bedrock divides and are transient features affected by both pumping and recharge.

Recharge to the Santa Fe Group aquifer via streambed infiltration of surface flow along ephemeral channels of the Santa Fe River, Arroyo Hondo, and Cañada Ancha has been demonstrated by a variety of methods (Johnson et al., *(in press)*; Manning, 2009; Moore, 2007). A groundwater mound (a water- table high) over the Santa Fe River that extends west from Agua Fria towards the WWTP has been a consistent feature in historic groundwater maps representing 1952 conditions (Spiegel and Baldwin, 1963), 1977 conditions (Mourant, 1980), and 2000- 2005 conditions (Johnson, 2009). This groundwater mound demonstrates recharge to the Santa Fe Group aquifer from streambed infiltration along the Santa Fe River channel. The source of recharge water most likely includes natural channel flow, but the modern shape and extent of the recharge mound may also be affected by downstream discharge from the WWTP, which has been functioning since the early 1960s. Spiegel and Baldwin (1963) noted that the Santa Fe River crossed into the Cienega unit and proposed that drainage from the river probably provides some recharge to the La Cienega Area. The groundwater map of Johnson (2009) supports a similar interpretation.

Groundwater Conditions in La Cienega and Cieneguilla: To improve resolution of the groundwater surface in the vicinity of the La Cienega and Cieneguilla wetlands, and better assess sources of water to springs and wetlands, a local water table map (Figure 4.13) was constructed with 20-foot potentiometric contours. Water-level control included measurements in 45 shallow wells made primarily in winter 2012, and 22 spring elevations (Table 4.3). Existing water-level data from 29 wells measured between 1997 and 2007 (Johnson, 2009; NMBGMR Española Basin Water Database) filled data gaps and provided control around study-area boundaries. The groundwater map represents a significant improvement to our understanding of the shallow Santa Fe Group aquifer and its connection to springs and wetlands.

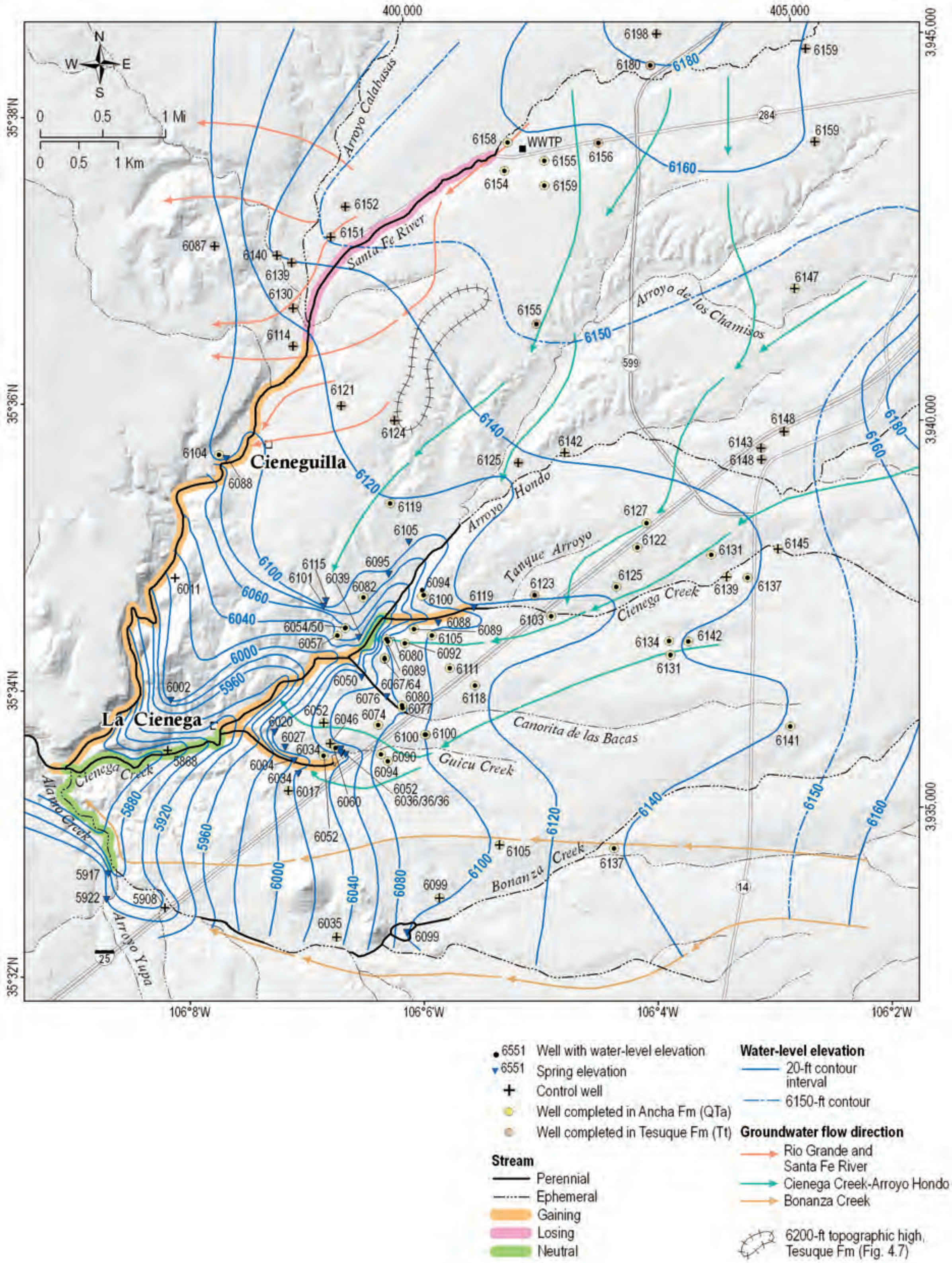

Figure 4.13: Groundwater map of 2012 water-table conditions in the La Cienega Area illustrating the water-table surface, groundwater flow directions, and interconnections between the water table and gaining and losing stream reaches. Control for potentiometric contours include 46 wells measured between March 2011 and May 2012, surface elevations at 22 springs, and existing data from 29 wells measured between 1997 and 2007 (Table 4.3). Designated gaining, neutral, and losing stream reaches reflect results of NM Hydrologic, LLC and NMOSE (2012a, 2012b).

The map (Figure 4.13), which represents 2012 conditions, shows groundwater entering the study area from the east and flowing westward toward the Santa Fe River and the Rio Grande. Water elevation contours range from 6,180 ft at the eastern study-area boundary to less than 5,860 ft at the confluence of Cienega Creek and the Santa Fe River. Horizontal flow direction is approximately represented by flow lines constructed perpendicular to potentiometric contours. Local flow directions vary from those indicated by the regional gradient (Figure 4.12), sometimes significantly, where the water-table surface is affected by recharge from or discharge to stream channels, local topography, or variations in aquifer permeability. Where potentiometric contours are deflected upstream, groundwater discharge to a gaining stream reach is indicated. Downstream deflection of contours indicates groundwater recharge from a losing stream or streambed infiltration.

Colored arrows in Figure 4.13 generally illustrate flow pathways for groundwater movement with discharge to Cienega Creek, Arroyo Hondo, Guicu Creek (green arrows), Bonanza Creek (tan arrows) and the Rio Grande and Santa Fe River (orange arrows). Groundwater discharge along lower reaches of streams and arroyos is indicated, including Cienega Creek from SR 14 to its confluence with the Santa Fe River, Arroyo Hondo above its confluence with La Cienega Creek, Guicu Creek and Canorita de las Bacas west of I-25, and the Santa Fe River at and below Cieneguilla. The aquifer recharge and discharge areas associated with the surface water system and interpreted from the groundwater map are generally consistent with measurements of stream losses and gains by NM Hydrologic LLC and the NMOSE (2012).

Potentiometric contours delineate a sizeable recharge mound beneath the Santa Fe River that extends from its confluence with Arroyo Calabasas, upstream past the WWTP, and beyond SR 599. Potentiometric contours and flow lines also indicate that groundwater flows from the recharge mound southward toward La Cienega and westward toward the Rio Grande. Southerly groundwater flow appears to diverge at the paleo-topographic high on the Tesuque Formation east of Cieneguilla (Figures 4.13 and 4.7), where it either flows southward toward seeps and springs along Arroyo Hondo or westward towards the Rio Grande or the Santa Fe River canyon. Low permeability floodplain sediments in the Tesuque Formation may impede groundwater movement and deflect flow around the paleo-topographic high. Where it overlies the topographic high in the Tesuque Formation, the Ancha Formation lies entirely above the water table and is unsaturated (Figure 4.9).

Regional Groundwater Flow, Discharge, Springs, and Wetlands: Most wetlands are groundwater discharge areas, as is the case with wetlands at La Cienega and Cieneguilla. The persistence, size, and function of wetlands are controlled by hydrologic processes (Carter, 1996). The persistence of wetlands fed by groundwater requires a relatively stable influx of groundwater throughout changing seasonal and annual climatic cycles. Characterizing groundwater discharge to wetlands and its relation to environmental factors is both critical and difficult (Hunt et al., 1999).

Springs occur where the water table intersects the land surface and provide important sources of water to streams and wetlands. Springs typically represent points on the landscape where groundwater flow paths from different sources and different depths converge. Groundwater development can affect the amount of flow from different sources to varying extents, thus affecting the resultant chemical composition of the spring water. Groundwater development can lead to reduction in springflow, a change of springs from perennial to ephemeral, or elimination of springs altogether.

Stable groundwater levels are important in maintaining the physical and chemical conditions in the root zone that promote healthy and stable growth of wetland plants (Hunt et al., 1999). Because of the complex interaction between surface and groundwater in wetlands, groundwater discharge and storage commonly are difficult components of the wetland hydrologic system to characterize. Wetland restoration requires knowledge of groundwater flow gradients and the natural range in seasonal fluctuations of the water table.

Seasonal and Long-Term Water-Level Fluctuations: Groundwater levels are controlled by the balance among recharge to, storage in, and discharge from an aquifer. Physical properties such as the porosity, permeability, and thickness of aquifer materials affect this balance, as do climatic and hydrologic factors, including the timing and amount of recharge from precipitation, groundwater discharge to surface water, and evapotranspiration (ET). When the rate of recharge to an aquifer exceeds the rate of discharge, water levels or hydraulic heads will rise. And when the rate of groundwater withdrawal or discharge is greater than the rate of recharge, the water stored in the aquifer becomes depleted and water levels will decline.

Water levels in most shallow, unconfined aquifers follow a natural cyclic pattern of seasonal fluctuation, typically rising during the winter and spring due to greater precipitation and recharge and lower ET, then declining during the summer and fall when there is less recharge and greater ET. This seasonal fluctuation pattern, driven by changes in precipitation and ET, is generally true for wetland areas as well (Carter, 1996). The magnitude of seasonal fluctuations in water levels can vary from year to year in response to varying climatic conditions. Changes in regional groundwater recharge and storage caused by climate variability commonly occur over decades. Water levels in aquifers generally have a delayed response to the cumulative effects of long-term drought.

Wetlands can be quite sensitive to the effects of groundwater pumping, both from progressive lowering of the water table and by increased seasonal changes in the elevation of the water table. The amplitude and frequency of seasonal water-level fluctuations affect wetland characteristics such as the type of vegetation, fish, and bird species present. The effects of pumping on seasonal fluctuations in groundwater levels near wetlands can complicate water-level changes and discharge patterns and perturb the natural annual cycle. In the La Cienega Area, both seasonal and long-term changes in water levels were studied in the shallow aquifer surrounding the wetlands.

Seasonal Water-Level Changes: Seasonal water-level changes in the study area were evaluated between two measurement periods in 38 shallow wells. The first measurements were taken in summer-fall of 2011 and the second in winter 2012. Results are shown in Figure 4.14A. Four of these wells were also equipped with continuous recorders of water level and water temperature from October 2011 to October 2012. An increase in water levels between summer or fall of 2011 and winter (February) of 2012 was observed in 84 percent (32 of 38) of the wells. Winter increases varied between 0.04 and 6.60 ft and occurred in wells located within or adjacent to the wetlands or in drainage valleys upstream of wetlands. The average water-level rise was 0.77 ft. Six wells showed a small water-level decline ranging from -0.13 to -0.50 ft. All wells with declining water levels are located up-gradient of wetlands, in desert uplands with scrub or juniper/scrub vegetation, and with depths to water greater than 100 ft. A summer-to-winter increase in water levels is consistent with seasonal fluctuations driven by changes in ET and/or precipitation between the growing and dormant seasons (Carter, 1996). A similar fluctuation pattern, common for wetlands, is illustrated by a continuous record from a wetland monitor well in the Leonora Curtin Wetland Preserve.

Water level and temperature in LC-025, the Leonora Curtin Wetland Preserve kiosk well, were measured continuously from October 5, 2011 to October 2, 2012. The hydrograph (Figure 4.15) shows that water levels are lowest (~12 ft below land surface or 6073 ft elevation) during the growing season, between June and late September. In October, water levels rise slowly and then increase abruptly on November 20, concurrent with a steady temperature decline. During the winter, when plants are dormant and ET is low, the water table remains elevated. Beginning April 25, an abrupt water-level decline is recorded, which corresponds with a steady temperature rise. The abrupt, synchronized and inverse changes in water level and temperature in November and April correspond to transitions between growing and dormant vegetation phases and illustrate the hydrologic response of the shallow groundwater system to changes in plant transpiration in the wetlands.

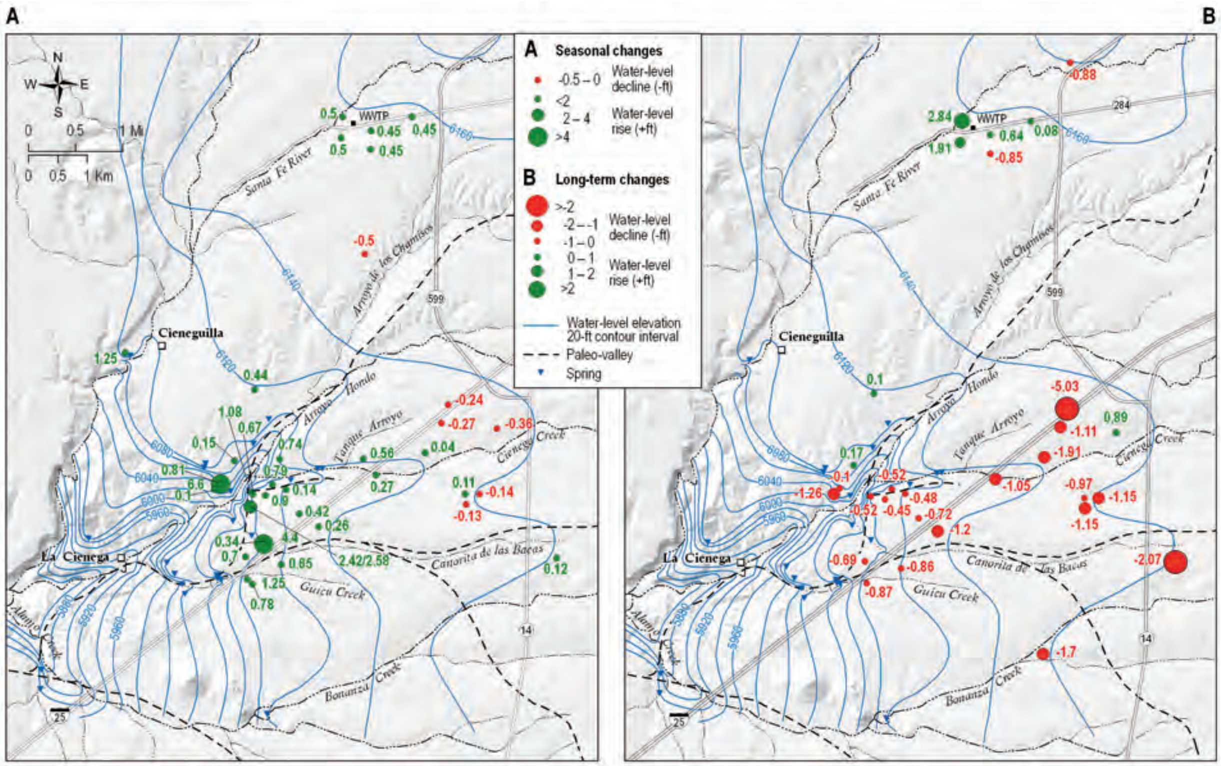

Figure 4.14: Water-level changes over time in La Cienega wells. A. Seasonal changes between summer-fall 2011 and winter 2012. B. Long-term changes 2004 to 2012. The La Cienega groundwater surface (from Figure 4.13) is shown in the background.

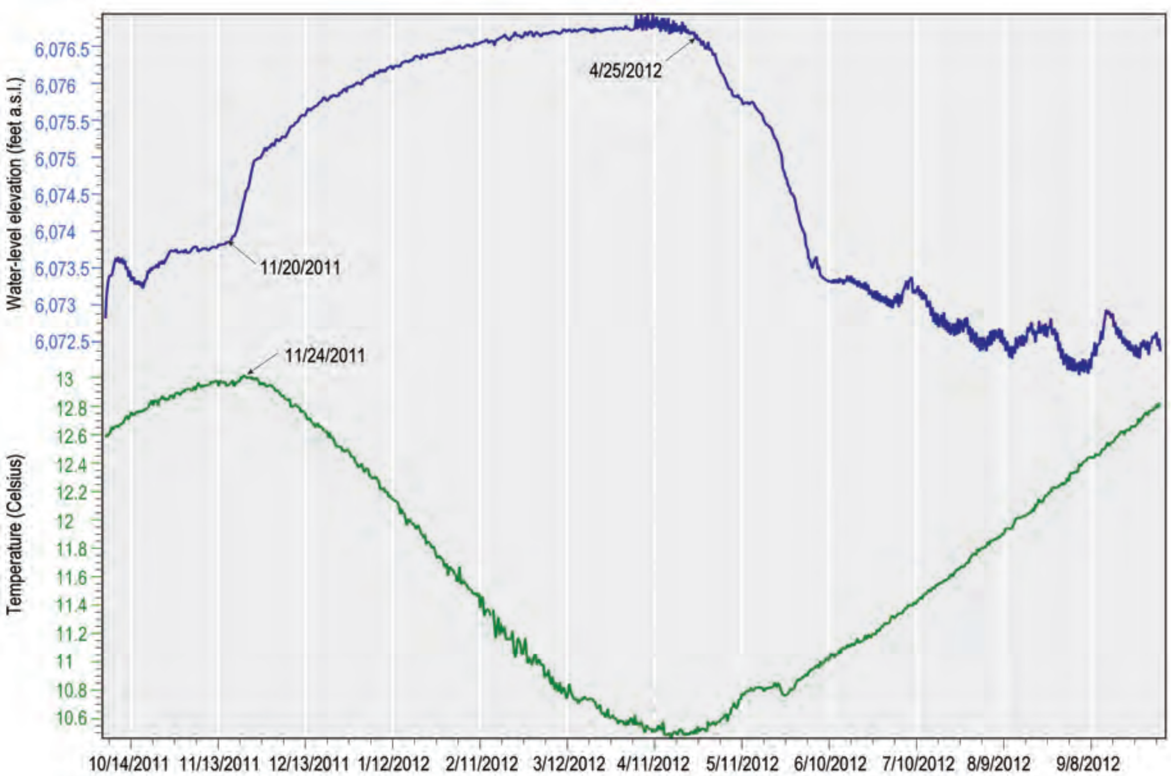

Figure 4.15: Hydrograph and thermograph from Leonora Curtin kiosk well (LC-025), La Cienega Area, showing seasonal water-level and water temperature changes October 2011 to October 2012. Land surface elevation is 6085 feet (above sea level), water level varies seasonally by 4.4 ft, and temperature varies inversely with water level by 2.45 ˚C. See map on Figure 4.16 for site location.

Long-term Water Level Changes: Long-term water level changes were evaluated using historic water level data from 29 wells measured in 2004 compared to repeat measurements of the same wells in winter 2012 (Figure 4.14B). Water-level declines were observed in 76% (22 of 29) of the measured wells and most occurred in and east of the La Cienega wetlands. Declines ranged from -5.03 to -0.10 ft, and averaged -1.16 ft for the 8-year period 2004 to 2012. A rise in water level of 0.08 to 2.84 ft was noted in seven wells, four of which are near the WWTP, two are in the Ancha Formation near the Arroyo Hondo spring zone, north of El Rancho de las Golondrinas, and one is near upper Cienega Creek. Water-level rises in WWTP monitor wells average 0.95 ft and may possibly link to small rises of 0.1 and 0.17 ft in down-gradient wells near Arroyo Hondo. Small fluctuations of a few tenths of a foot are usually considered to be within a normal seasonal or year-to-year fluctuation.

Hydrographs for five wells with data records prior to 2000, and two shallow piezometers with high frequency measurements by USGS (EB-338 and EB-607), illustrate water-level trends over time (Figure 4.16). All wells show a persistent trend of declining water levels between 1973 and 2005. In wells EB-338 and EB-607, the measurement frequency is sufficient to show the cumulative effects of seasonal water-level variations (winter highs and summer lows) and exceptionally wet seasons (a 1.21-ft water level rise in EB-338 near the Santa Fe River in spring 2005), superimposed on the effects of pumping and long-term withdrawals.

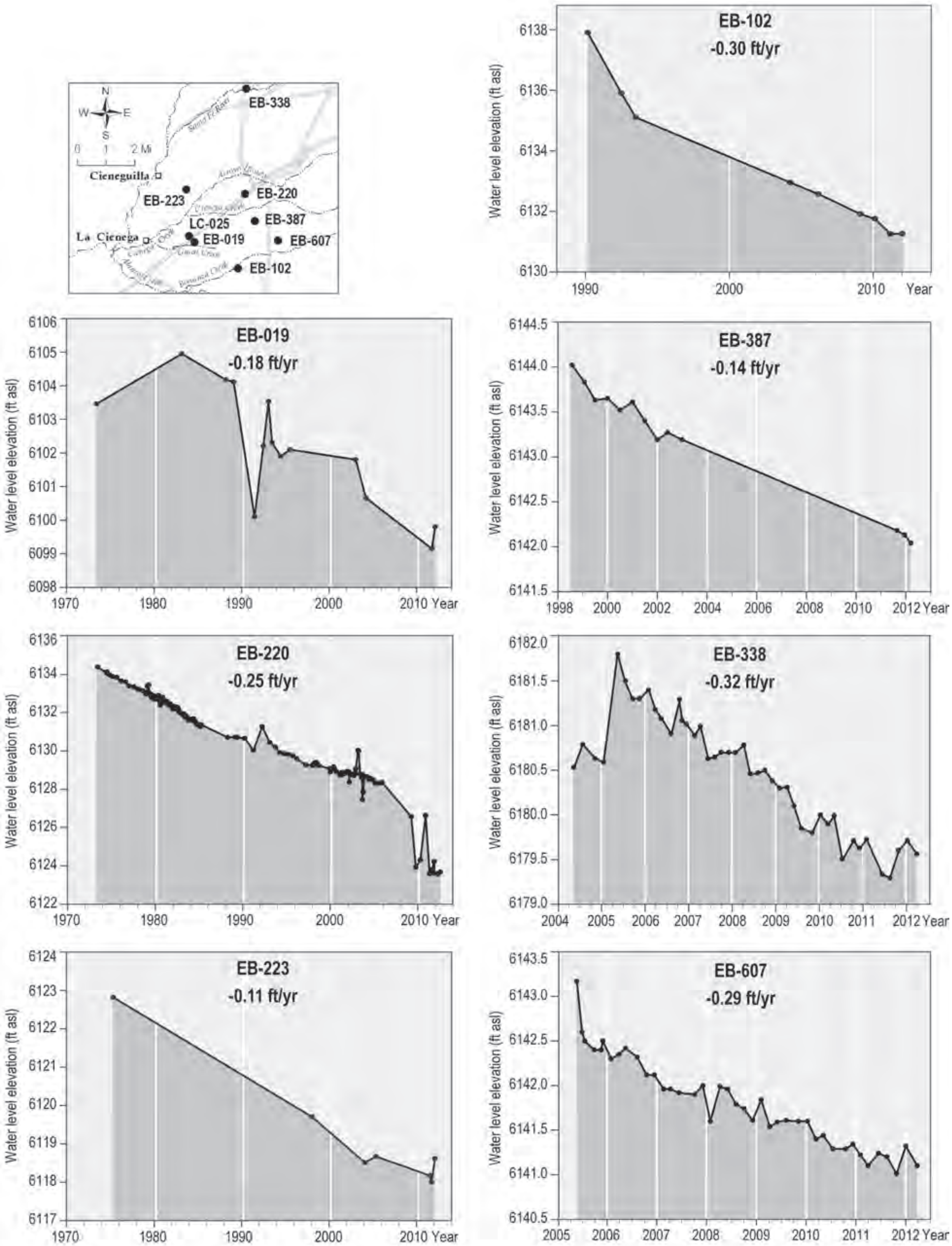

Figure 4.16: Hydrographs of La Cienega Area wells showing water-level trends over time and rates of water-level declines (ft/yr).

Chemical Characteristics and Age of Groundwater. Chemical and isotopic data for groundwater from the La Cienega Area were examined using analytical and spatial methods useful for determining source, flow paths, recharge, mixing, and residence time. Parameters evaluated include total dissolved solids (TDS), calcium (Ca^{2+}), sodium (Na^{+}), magnesium (Mg^{2+}), sulfate (SO_4^{2-}), chloride (Cl^{-}), bromide (Br^{-}), deuterium (δ^2H) and oxygen-18 ($\delta^{18}O$). Groundwater residence time was evaluated using a combination of methods, including radiocarbon (^{14}C) dating of dissolved inorganic carbon (DIC), tritium (^3H) content and chlorofluorocarbons (CFCs). Contours of chemical data were constructed by interpolation of concentration values using inverse distance weighting in ArcGIS, followed by manual smoothing. Surface water sites are not used as control for contours of chemical and isotopic data from groundwater; they appear on figures to provide a comparison. Concentrations of chemical, isotopic, and age dating parameters measured in wells and springs are presented in Tables 4.4, 4.5, and 4.6.

Major Ion Chemistry and Water Type: The contoured distribution of dissolved solids and ratios of calcium-to-sodium concentration are shown in Figure 4.17. Groundwater from the Santa Fe Group aquifer is relatively dilute in dissolved minerals, with values for TDS ranging from 92 to 391 mg/L (Figure 4.17A) (Table 4.4). Dissolved solids are highest (>250 mg/L) in wells and springs located southwest of the hinge zone at the edge of the basin, in the Cienega Creek valley. Groundwater in the Galisteo Formation is also high in TDS (≥350 mg/L). Wells with the lowest TDS values are located near the Santa Fe River (108 to 152 mg/L), and Arroyo Hondo and Tanque Arroyo (92 to 144 mg/L). A TDS concentration of 454 mg /L was measured in discharge from the WWTP.

Most groundwater (80% of samples) in the Santa Fe Group aquifer near La Cienega is calcium rich with lesser amounts of sodium and magnesium. Calcium concentrations range from 2 to 86 mg/L with a median value of 31 mg/L. Sodium concentrations range from 7 to 125 mg/L with a median of 24 mg/L. The distribution of calcium and sodium is illustrated as a calcium-to-sodium ratio (Figure 4.17B), where values greater than 1 indicate calcium dominance and values less than 1 indicate sodium dominance. Calcium-rich groundwater (Ca/Na ratio > 2.0) occurs primarily adjacent to the Santa Fe River and the upper valleys of Arroyo Hondo and Tanque Arroyo, which indicates recharge to shallow groundwater from channel infiltration. A stream sample from the Santa Fe River is also Ca-rich, with a Ca/Na ratio of 3.7. The occurrence of sodium-rich groundwater (Ca/Na ratio < 1.0) in the Santa Fe Group aquifer is discontinuous. It occurs in deep basin wells drawing water from the Tesuque Formation, a bedrock well completed in the Galisteo Formation, springs west of Arroyo Hondo, and in discharge from the WWTP. Many of the groundwater samples near La Cienega have an intermediate calcium-sodium signature (Ca/Na ratio between 2.0 and 1.0) that reflects a combination of different sources. Water-type designations for spring and well waters are included in Table 4.4.

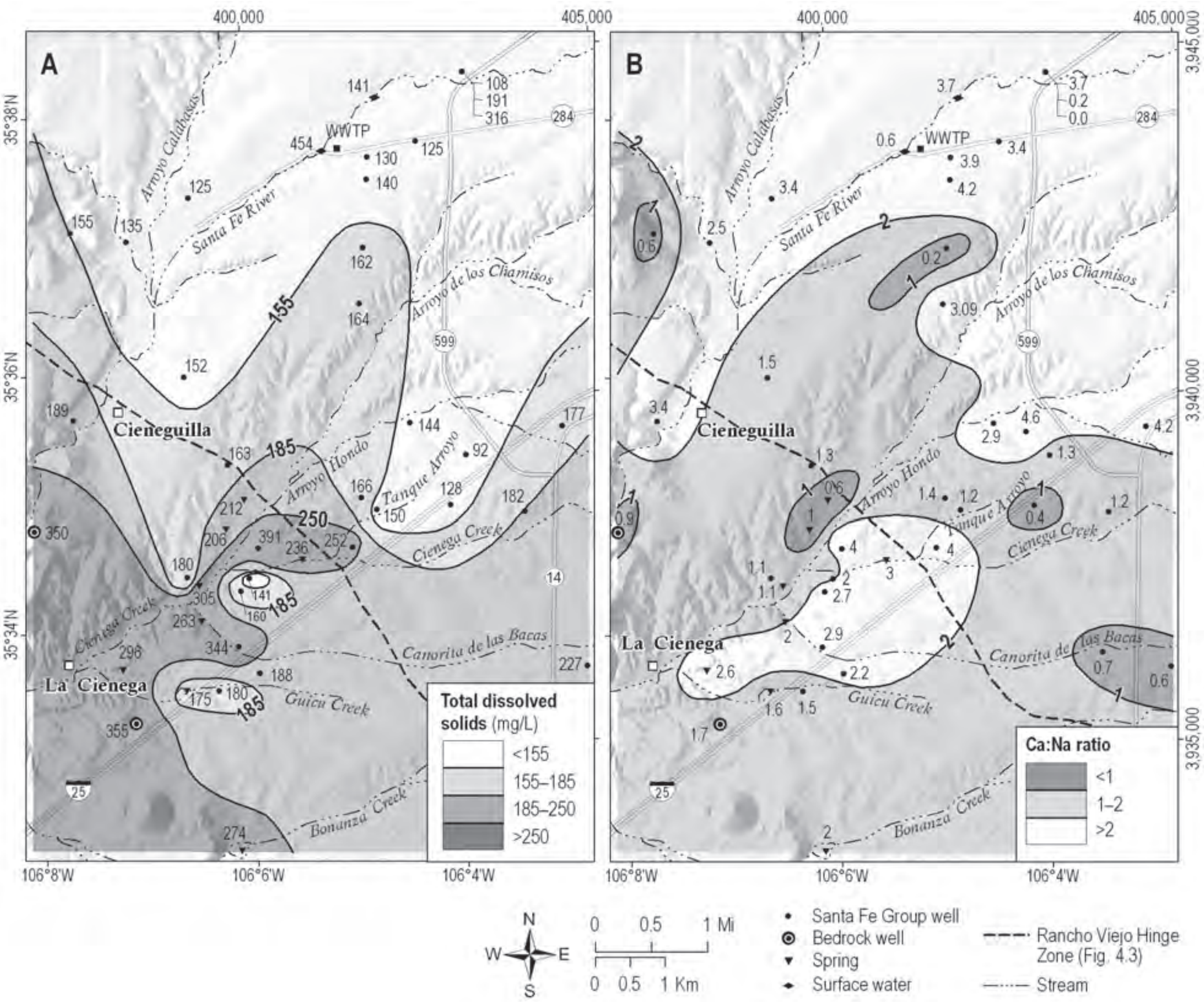

Figure 4.17: Maps showing distribution of: A. total dissolved solids (TDS, mg/L), and B. calcium to sodium ratio (meq/L).

A plot of the proportions of the major cations (calcium [Ca], magnesium [Mg], sodium [Na], potassium [K]) and anions (bicarbonate-carbonate [HCO_3 and CO_3], sulfate [SO_4], chloride [Cl]) for all samples is shown on a Piper diagram in Figure 4.18. The Piper plot provides an illustration of water type and ion chemistry for groundwater and surface water from the La Cienega Area. Trends in ion chemistry observed on the Piper diagram and the Ca/Na distribution figure (Figure 4.17) support hydrologic interpretations of groundwater sources, recharge and flow paths for the La Cienega springs and wetlands.

Mixing of Deep and Shallow Groundwater Sources: Elevated Na in deep-basin groundwater in the southern Española Basin and increasing Na concentrations along flow paths results from cation exchange, wherein dissolved Ca and Mg are exchanged for Na on montmorillonite clay (Johnson et al., *in press*). The prominent cation trend in the Piper diagram for La Cienega (Figure 4.18) shows a similar evolution of Ca- and Ca-Mg-HCO_3 water to Na-HCO_3 water. This trend, which indicates cation exchange, is primarily expressed through two well-sample groups: (1) wells near streams and arroyos (the Santa Fe River, Arroyo Calabasas, Arroyo Hondo and Tanque Arroyo that plot near the Ca-HCO_3 apex; and (2) wells drawing groundwater from deep in the Tesuque Formation that contain Na-HCO_3 or mixed Na-Ca-HCO_3 water. Cation compositions of springs and shallow wells near the wetlands of La Cienega primarily plot between these two well sample groups, indicating that spring and wetland discharge is a mixture of shallow, recent recharge and older, deeply circulating groundwater from the Tesuque Formation. Well and spring water discharging in the upper valley of La Cienega Creek have the highest calcium content, and thus the highest proportion of recently recharged groundwater. Guicu Creek wells and springs have a slightly lower calcium content and higher sodium. Arroyo Hondo well waters contain about 40% sodium, and the two springs contain up to 60% sodium, similar to the cation chemistry of deep wells in the Tesuque Formation.

Mixing of Wastewater Discharge and Shallow Groundwater: It is also important to consider possible mixing of treated wastewater from the WWTP with the groundwater system in the La Cienega Area. When two chemically different waters mix, the composition of the mixture will be intermediate between the two end members, and the effects are visible on a Piper diagram. If a water is strictly the result of mixing, without the addition or removal of any phase, then the mixture will exhibit exactly the same proportions between the end members on both cation and anion triangles as well as the diamond (Hounslow, 1995).

Discharge water collected near the outlet of the WWTP in August 2012 has an ion signature unique from other well and spring waters in the La Cienega Area (Figure 4.18). Its water-type is Na-Ca-HCO_3-Cl, and the sample is the only chloride-rich Na-Ca-HCO_3 water observed in the area (Table 4.4). Elevated Cl in treated wastewater typically comes from evaporative enrichment during the treatment process. The only natural sources of chloride in the environment are salt deposits such as halite (NaCl), brines and hot springs, and there are no common sinks for chloride except salt precipitation. Thus, chloride is considered to be a conservative tracer of water movement in many environments, including alluvial groundwater systems such as the Santa Fe Group aquifer. Where simple mixing between chloride-rich waters and other bicarbonate or sulfate waters occurs, the mixing proportions can be easily observed on a Piper plot by applying the criteria described above. There is no evidence in Figure 4.18 that well or spring waters in La Cienega are chemically influenced by treated wastewater, or are mixtures of treated wastewater and groundwater from the Santa Fe Group aquifer.

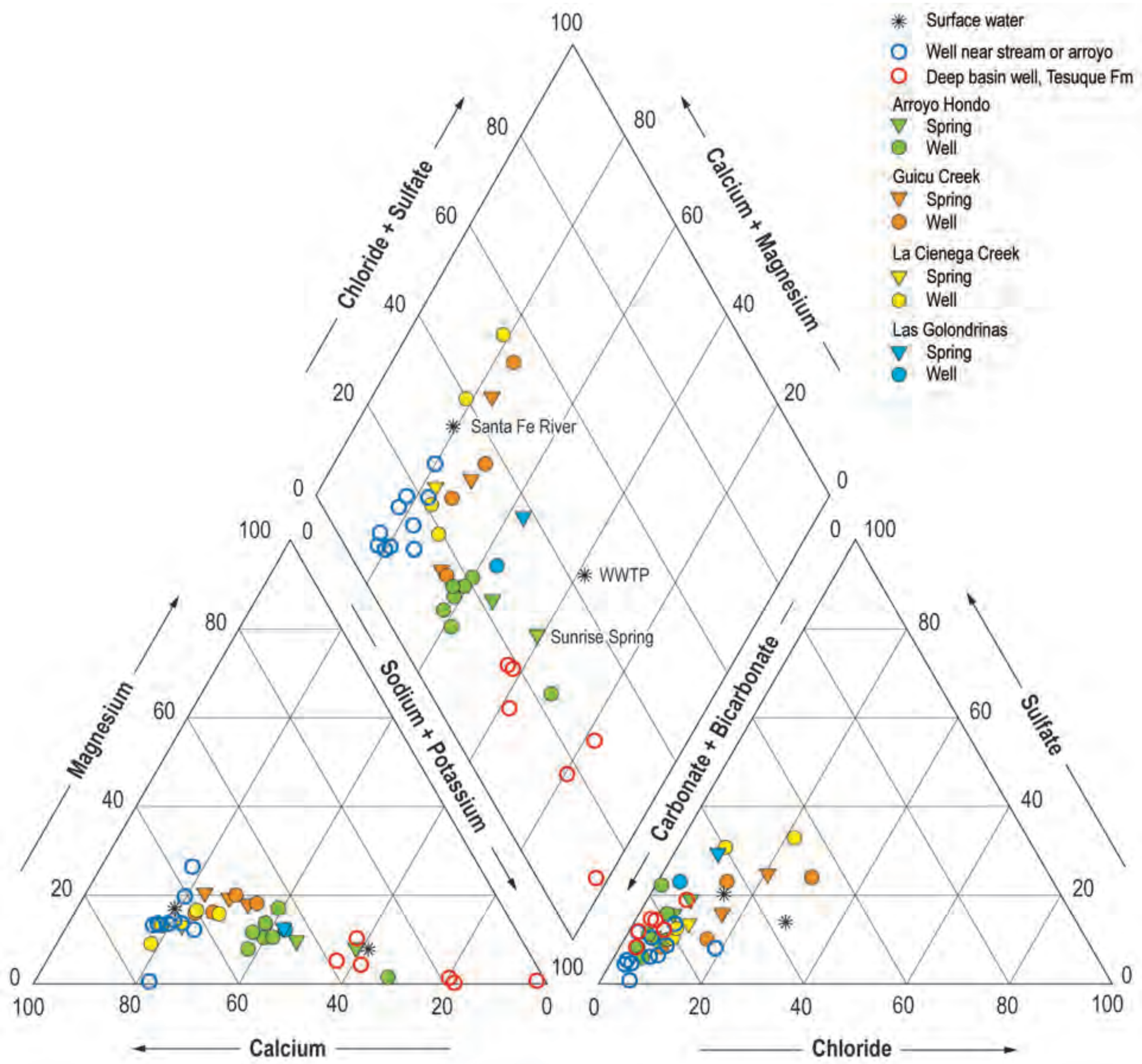

Figure 4.18: Piper diagram displaying percentages of major ions (meq/L) in well, spring, and surface water near La Cienega. Samples are symbolized to indicate locations adjacent to streams or arroyos, groundwater sourced from the Tesuque Formation, or a spring-wetland zone.

Isotopic Characteristics and Groundwater Residence Time: Hydrogen-2 (δ^2H) and Oxygen-18 ($\delta^{18}O$) Isotopes: Stable isotope values (Table 4.5) of groundwater from wells and springs in the La Cienega Area and wastewater discharge to the Santa Fe River are plotted with a local meteoric water line (LMWL) for the Santa Fe area (Anderholm, 1994) in Figure 4.19. Values for these waters vary from -74.7 to -113.3 ‰ ^{2}H and -10.3 to -15.6 ‰ δ^{18}O. The isotopic composition of spring and shallow well samples varies over a small range, -86.5 to -74.7 ‰ δ^2H and -12.1 to -10.3 ‰ δ^{18}O, that mimics the composition of flow in the Santa Fe River and Arroyo Hondo reported by Anderholm (1994) (-92 to -68 ‰ δ^2H and -13.2 to -10 ‰ δ^{18}O). The similarity in isotopic composition between surface water and shallow groundwater is consistent with the general view that groundwater discharging at La Cienega is recharged by runoff from the southern Sangre de Cristo Mountains, and specifically these two major drainages.

Groundwater from deep wells in the Tesuque Formation (EB-336, EB-337, and EB-386, Table 4.5) is significantly depleted in deuterium (< -95 ‰ δ^2H) relative to both modern surface water and groundwater from shallow wells and springs in La Cienega. Johnson et al. *(in press)* have demonstrated that a deuterium composition of less than -95 ‰ in the Española Basin indicates fossil groundwater with a residence time of ≥13,000 years and up to 30,000 years. Groundwater with an intermediate composition—for example EB-328, -94‰ δ^2H—is interpreted to be a mixture of old and young waters.

A notable trend in the isotopic composition of shallow well and spring waters in La Cienega (Figure 4.19) is that most well water lies above the LMWL, whereas all spring water lies below the LMWL. The spring samples from La Cienega, Guicu Creek, and Cieneguilla, which form a linear trend with a slope lower than the LMWL, have undergone minor evaporation typical of surface water and very shallow groundwater. A similar enrichment of Cl and SO4 observed in some of the same shallow well and spring samples in the Piper diagram (Figure 4.18) may also reflect evaporative concentration of these ions in shallow groundwater in the discharge zone.

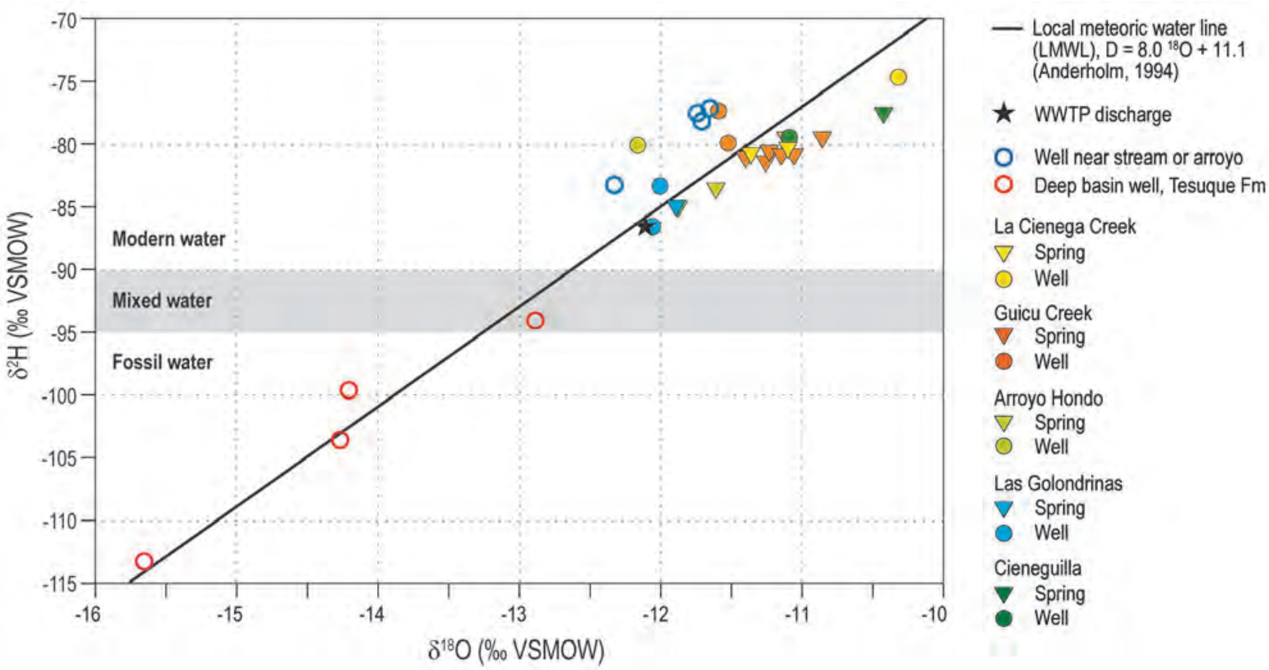

Figure 4.19: Isotopic data (hydrogen-2 (δ^2H, ‰) versus oxygen-18 (δ^{18}O ‰)) for groundwater from wells and springs in the La Cienega Area and the WWTP. Data (Table 4.5) are shown in relation to a local meteoric water line (LMWL) for the Santa Fe area from Anderholm (1994).

It is also significant that, with few exceptions, springs and wells from the same watershed or hydrologic flow path have similar and unique compositions. This is particularly true in the case of the Guicu Creek and La Cienega Creek springs, which discharge along the eastern slopes of the La Cienega Creek valley. These samples have similar isotopic compositions that lie along a line with a slope of 3 (Figure 4.19), indicating a common water source undergoing progressive evaporation. Springs and wells located along the western slopes of the La Cienega Creek valley, in Las Golondrinas and lower Arroyo Hondo, have a depleted isotopic composition relative to eastern spring and wells. Although the isotopic variation amongst different hydrologic zones is small, it is consistent, and reflects the small compositional differences in groundwater that originates from slightly different source areas and follows unique flow paths.

Groundwater Residence Time: The residence time of groundwater that discharges to springs and wells in La Cienega was evaluated using multiple isotopic and chemical methods, including radiocarbon (^{14}C) dating of the dissolved inorganic carbon (DIC) content of groundwater, tritium (^{3}H) content, and chlorofluorocarbon (CFC) composition. Results of these methods are shown in Tables 4.5 and 4.6 and discussed below.

The radioisotopes of ^{14}C and ^{3}H are produced in the atmosphere by natural and anthropogenic processes, become entrained in the hydrologic cycle, enter the groundwater system with recharge, and slowly decay as groundwater flows through the aquifer. Carbon-14 has a relatively long half-life (5730 years) and is used to detect groundwater with residence times of several 100s to many 1000s of years. Results are reported as radiocarbon years before present, RCYBP, where "before present" means prior to 1950. Tritium has a relatively short half-life (12.43 years) and its presence in groundwater provides evidence of active recharge within the last 50 years. By measuring ^{3}H content or ^{14}C activity in groundwater or the DIC content of groundwater, relative to modern levels, we can estimate how long groundwater has resided in the aquifer and whether the water represents a mixture of different aged sources. Depending on the geochemical setting, chemical interactions between dissolved carbonate and the sediment or rocks making up the aquifer can dilute the amount of ^{14}C measured in a water sample, and provide an anomalously old age.

Chlorofluorocarbons (CFCs) are atmospheric contaminants that are resistant to degradation and soluble in water, making them a useful marker for modern groundwater recharge. Because CFC concentrations have increased in the atmosphere since the 1940s, and their input function is known, they can provide a precise age for young groundwater. However, point-source contamination of shallow groundwater with CFCs derived from discarded automobiles and refrigerators can render the method useless for groundwater dating. This is the case for nearly all samples collected and analyzed in 2011 in the La Cienega Area.

Apparent radiocarbon ages for samples from the La Cienega Area range from 10,780 to 1550 RCYBP (Figure 4.20, Table 4.5). The oldest groundwater (>6,500 RCYBP) occurs in Tesuque and Ancha wells situated furthest from major streams and arroyos, specifically between the Santa Fe River and Arroyo Hondo. Well water east of the interstate in the Guicu Creek drainage is similarly aged. The youngest groundwater (1550 RCYBP) was observed in a spring adjacent to the Santa Fe River in Cieneguilla. Groundwater from springs and shallow wells discharging along the slopes, hillsides, and drainages east of La Cienega Creek and Arroyo Hondo also have relatively young apparent ^{14}C ages (2480 to 4280 RCYBP). Spring waters discharging along slopes west of Arroyo Hondo and La Cienega Creek are notably older – 4860 to 7240 RCYBP – than eastern springs.

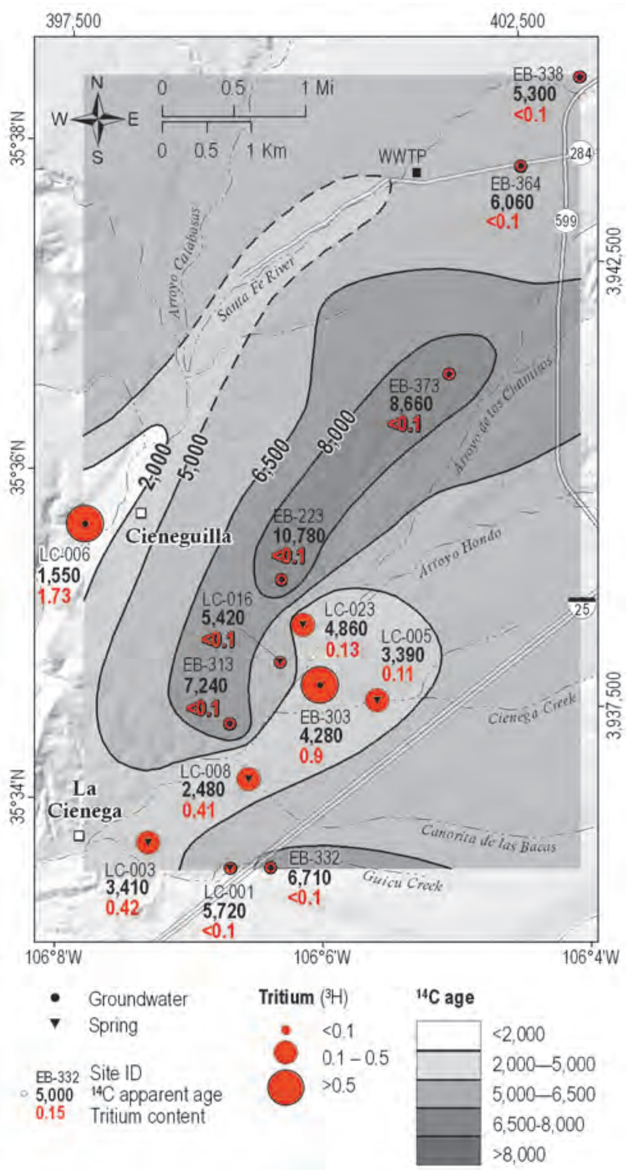

Figure 4.20: Contoured distribution of apparent ^{14}C age of groundwater (RCYBP), shown with tritium (^3H) content (tritium units, TU), from La Cienega wells and springs. Isotopic and age data are shown in Table 4.5.

The ^{14}C age distribution pattern of the youngest groundwater occurring near stream and arroyo channels is repeated in the ^{3}H data. Tritium contents greater than 0.1 TU, which indicate groundwater recharge during the last 50 years, are only observed in springs and wells located in stream and arroyo channels, specifically those at Sunrise Springs, Cieneguilla, and east of Cienega Creek. These samples, which have ^{14}C ages of several thousand years and ^{3}H contents indicating modern recharge, demonstrate that mixing of water masses with distinctively different ages occurs in the wetland discharge zones. Because mixing scenarios for various combinations of old and young waters are non-unique, identifying an exact age for groundwater discharging to a spring is neither possible nor relevant. The importance of the result is to verify mixing of groundwater with dramatically different ages in wetland discharge. A conceptual illustration of mixing different ages of groundwater along flow paths is illustrated in Figure 4.21.

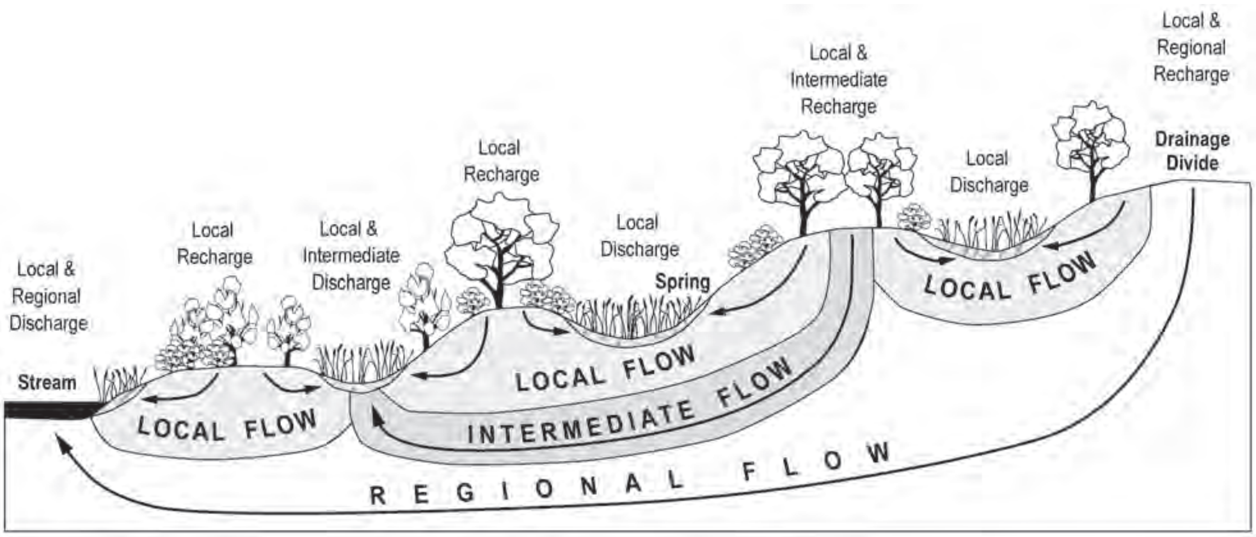

Figure 4.21: Groundwater flow paths vary greatly in length, depth, and travel time between recharge and discharge areas. Local, intermediate and regional flow paths converge at a regional discharge area, resulting in mixing of groundwater of different ages (modified from Winter, 1976).

Age distribution patterns of groundwater in the La Cienega Area have some important implications concerning the sustainability of springs and wetlands.

- Groundwater discharging to springs and groundwater-saturated wetlands east of Cienega Creek and Arroyo Hondo represents a mixture of young groundwater (<50 years) recharged locally and older groundwater discharging from deeper in the Santa Fe Group aquifer.
- Groundwater discharging to springs and groundwater-saturated wetlands on the western slopes of Cienega Creek and Arroyo Hondo also represents a mixture of different aged groundwater, but clearly includes a larger fraction of older groundwater discharging from deep circulation pathways in the Tesuque Formation.
- The pattern wherein the oldest groundwater occurs furthest from Cienega Creek and young groundwater with measurable tritium is detected within the drainage and at the terminus of tributary channels (Arroyo Hondo, Guicu Creek and Canorita de las Bacas) indicates that the wetland zones and stream valleys are areas of both discharging and recharging groundwater. This pattern is probably linked to the hydrologic responses of bank storage during storm events and local recycling of discharged groundwater back into the groundwater system. A good example is observed east-to-west along Guicu Creek, where the oldest discharging groundwater is observed in well EB-332 east of I-25 (a ^{14}C age of 6,710 RCYBP) and groundwater ages become younger west along the flow path.
- Groundwater in the recharge mound beneath the Santa Fe River near SR 599 contains no detectable tritium, possibly because the volume of recharge is negligible relative to the volume of water in aquifer storage.

Summary and Conceptual Model of Groundwater Flow and Discharge to Springs and Wetlands. The exploration of springs and wetlands in La Cienega reveals a complex, three-dimensional groundwater system wherein groundwater discharge from multiple flow pathways in the Santa Fe Group regional aquifer sustains the wetland environment. The location of the wetlands is controlled by the geologic setting. Their sustenance depends on an adequate and stable water supply. The La Cienega wetlands water budget is dominated by groundwater inflow and surface water outflow, with seasonal water level and water storage fluctuations controlled by changes in evapotranspiration between growing and dormant periods.

A conceptual model of the local hydrogeology of the wetlands is portrayed through geologic maps (Figures 4.3, 4.5 and 4.10), four detailed geologic cross sections (Figure 4.6), and detailed structural and hydrologic maps of the Ancha Formation (Figures 4.7, 4.8, and 4.9). The Ancha Formation is the geologic stratum that concentrates groundwater discharge to the springs and wetlands. The hydrologic conditions surrounding the wetlands are presented through: (1) a regional water table map (Figure 4.12); (2) a local water table map (Figure 4.13) depicting 2012 conditions, well and spring locations, horizontal groundwater flow direction, and gaining, losing, and neutral stream reaches; (3) seasonal and long-term water-level fluctuations (Figures 4.14A and B); (4) an annual hydrograph and thermograph from a wetland well at Leonora Curtin Wetland Preserve (Figure 4.15); and (5) a series of seven hydrographs from local and regional wells (Figure 4.16) showing a persistent, long-term trend of declining water levels. Chemical characteristics are presented through maps and diagrams that delineate groundwater source and residence time for springs and wetlands (Figures 4.17 through 4.20). The important elements of the hydrogeologic conceptual model are merged in three-dimensional block diagrams (Figures 4.21 and 4.22) and the most salient conclusions regarding regional and local hydrogeology and wetland hydrology are summarized below.

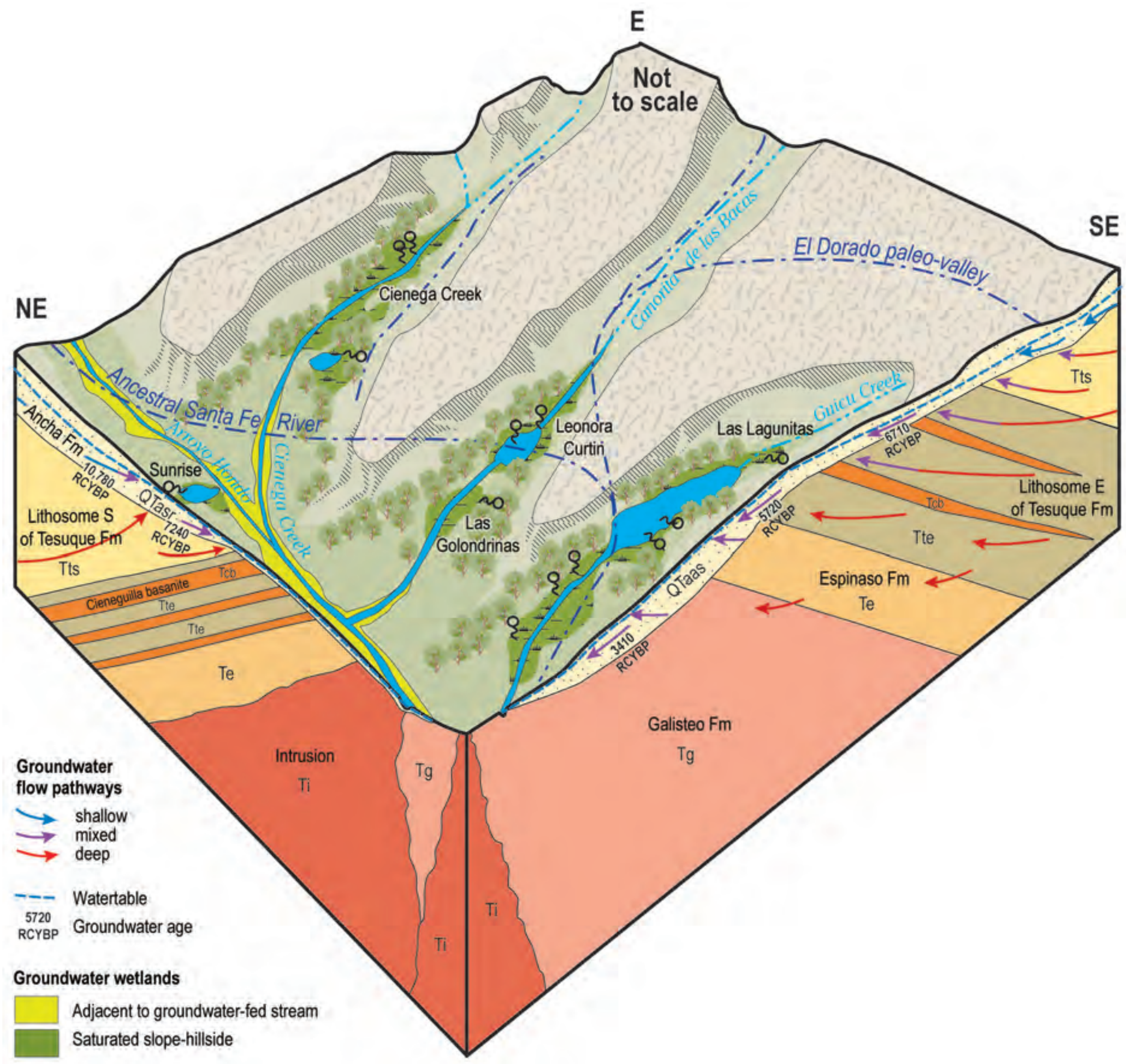

Figure 4.22: Hydrogeologic conceptual block diagram of spring zones in the La Cienega Area illustrating the geologic controls for groundwater discharge and source of waters for springs and wetlands.

1. Groundwater sustaining springs and wetlands originates from the Santa Fe Group regional aquifer system, which consists of the deeper sandy strata of the Tesuque Formation and the shallow, sand and gravel deposits of the Ancha Formation. The base of the Ancha Formation coincides with a late Miocene to early Pliocene erosion surface that has truncated tilted and faulted beds of the underlying Tesuque Formation, Oligocene volcanics, and Galisteo Formation. As the Santa Fe Group aquifer becomes thin and pinches out over underlying low-permeability strata, groundwater is forced to the surface to discharge in spring and wetland zones and associated drainages.
2. The Ancha Formation directly feeds most spring and wetland zones. Storage of groundwater and saturation of the Ancha Formation is controlled by three factors: (1) permeability contrasts between the Ancha and pre-Ancha Formations; (2) the topography of the erosion surface at the base of the formation; and (3) sources of recharge or inflow to the formation. Paleo-valleys incised at the structural base of the Ancha Formation provide elevation-dependent drains that gather groundwater and concentrate groundwater flow and discharge to wetland and spring zones.
3. Two paleo-valleys — the El Dorado paleo-valley and the ancestral Santa Fe River — at the base of the Ancha Formation provide hydrogeologic and elevation control over locations of spring and wetland zones. The El Dorado paleo-valley controls the discharge locations for spring-wetland zones at Las Lagunitas in Guicu Creek and the Leonora Curtin Wetland Preserve in Canorita de las Bacas. The Cienega Creek spring-wetland zone is strongly aligned with paleo-channel fill identified during geologic mapping that may be associated with another channel of the El Dorado paleo-valley. Sunrise Springs and other springs along the western slopes of Arroyo Hondo, above its confluence with Cienega Creek, are controlled by the paleo-valley of the ancestral Santa Fe River.
4. A water-table map of 2012 groundwater conditions shows groundwater entering the study area from the east and flowing westward toward the Santa Fe River and the Rio Grande. Flow-path analysis demonstrates groundwater discharge to wetland areas in Cienega Creek, Arroyo Hondo, Guicu Creek, the Santa Fe River, and Canorita de las Bacas. Aquifer recharge and discharge areas interpreted from the groundwater map are generally consistent with the stream losses and gains measured by NM Hydrologic LLC and the NMOSE in 2012.
5. The 2012 water-table map delineates a recharge mound beneath the Santa Fe River that extends from its confluence with Arroyo Calabasas, upstream past the WWTP, and beyond SR 599. Flow-path analysis indicates that groundwater flows from the recharge mound southward toward La Cienega and westward toward the Rio Grande. Southerly groundwater flow diverges at a paleo-topographic high on the Tesuque Formation east of Cieneguilla (delineated in mapping of the structural base of the Ancha Formation), where it either flows southward toward seeps and springs along Arroyo Hondo or westward towards the Rio Grande or the Santa Fe River canyon.
6. Seasonal water-level changes evaluated in 38 shallow wells between summer–fall of 2011 and winter 2012 showed a consistent increase in winter water levels of an average 0.77 ft in wetland zones. Declining water levels (-0.13 to -0.50 ft) occurred in wells located in desert uplands with a depth to water greater than 100 ft. A hydrograph and thermograph of continuous measurements from October 5, 2011 to October 2, 2012 in a well at Leonora Curtin Wetland Preserve show that wetland water levels are lowest during the growing season (June to late September) and highest in the winter dormant season (December to mid-April). Abrupt, synchronized and inverse changes in water level and temperature in November and April correspond to transitions between growing and dormant vegetation phases and illustrate the hydrologic response of the shallow groundwater system to changes in plant transpiration in the wetlands.
7. Long-term water level changes evaluated in 29 area wells with repeat measurements in 2004 and 2012 show persistent water-level declines in 76% of the measured wells, most of which occurred in and east of the La Cienega wetlands. Declines ranged from -5.03 to -0.10 ft, and averaged -1.16 ft for the 8- year period. Water-level rises (0.08 to 2.84 ft) occurred in wells near the WWTP, in the Ancha Formation near the Arroyo Hondo spring zone, north of El Rancho de las Golondrinas, and near upper Cienega Creek. Small fluctuations of a few tenths of a foot are within a normal seasonal or year-to-year fluctuation. Hydrographs for area wells show a persistent trend of declining water levels between 1973 and 2012, and where the measurement frequency is sufficient, also show the cumulative effects of seasonal water-level variations (winter highs and summer lows) and recharge events (spring 2005), superimposed on the effects of pumping and long-term withdrawals.
8. Chemistry, isotope, and age (^{14}C and tritium) characteristics of groundwater verify that mixtures of multiple groundwater sources with distinct chemistries and residence times feed wetland zones east and west of Cienega Creek. Mixing occurs in various proportions between groundwater from deep

regional flow paths through the Tesuque Formation and groundwater from local to intermediate flow paths within the Ancha Formation and uppermost Tesuque Formation. Wetlands east of Cienega Creek have notably younger ages, with greater amounts of modern recharge, than do springs and wetlands west of Cienega Creek and Arroyo Hondo. Wetland zones and stream valleys are areas of both discharging and recharging groundwater, which indicate that local hydrologic processes, such as bank storage during storm events and local recycling of discharged groundwater and surface flows, play an important role in wetland function.